



Progress and challenges on the thermal management of electrochemical energy conversion and storage technologies: Fuel cells, electrolyzers, and supercapacitors

Saman Rashidi^b, Nader Karimi^{c,d}, Bengt Sundén^{e,*}, Kyung Chun Kim^f, Abdul Ghani Olabi^g, Omid Mahian^a

^a School of Chemical Engineering and Technology, Xi'an Jiaotong University, Xi'an, 710049, China

^b Department of Energy, Faculty of New Science and Technologies, Semnan University, Semnan, Iran

^c School of Engineering and Materials Science, Queen Mary University of London, London, E1 4NS, UK

^d James Watt School of Engineering, University of Glasgow, Glasgow, G12 8QQ, UK

^e Department of Energy Sciences, Lund University, P.O. Box 118, Lund SE-22100, Sweden

^f School of Mechanical Engineering, Pusan National University, Busan 46241, Republic of Korea

^g Sustainable and Renewable Energy Engineering, University of Sharjah, Sharjah, United Arab Emirates

ARTICLE INFO

Keywords:

Thermal management
Electrochemical heat generation
Fuel cells
Electrolyzers
Supercapacitors
Green hydrogen
Electrified transport

ABSTRACT

It is now well established that electrochemical systems can optimally perform only within a narrow range of temperature. Exposure to temperatures outside this range adversely affects the performance and lifetime of these systems. As a result, thermal management is an essential consideration during the design and operation of electrochemical equipment and, can heavily influence the success of electrochemical energy technologies. Recently, significant attempts have been placed on the maturity of cooling technologies for electrochemical devices. Nonetheless, the existing reviews on the subject have been primarily focused on battery cooling. Conversely, heat transfer in other electrochemical systems commonly used for energy conversion and storage has not been subjected to critical reviews. To address this issue, the current study gives an overview of the progress and challenges on the thermal management of different electrochemical energy devices including fuel cells, electrolyzers and supercapacitors. The physicochemical mechanisms of heat generation in these electrochemical devices are discussed in-depth. Physics of the heat transfer techniques, currently employed for temperature control, are then exposed and some directions for future studies are provided.

1. Introduction

A shift from fossil fuel-based energy technologies to those based on renewable resources is a crucial prerequisite to sustainability [218]. Energy conversion and storage have proven to be the key requirements for such a transition to be possible. This is particularly due to the intermittency of renewable power generation, which has in turn spiked major interest in development of carbon-free energy vectors such as hydrogen. They are also a key requirement because of the major difficulties encountered in the large-scale storage of electricity [314] and the possibility of generation of electricity from hydrogen by employing fuel cells or combustion engines [268]. Currently, there are extensive activities on production of hydrogen from the surplus of renewable power (the so-called 'power-to-gas' technology) [180]. This is part of the

ambitious plans to replace natural gas with hydrogen as a future carbon-free fuel for generation of electricity and heat [277]. Production and conversion of hydrogen by using electrolyzers and fuel cells are the essential elements for such plans. Robustness of these electrochemical technologies directly influences the speed of transition to hydrogen [252]. Aside from exploring hydrogen as a renewable energy carrier, there are also vast, ongoing efforts being put into the storage of electricity. Batteries are the primary directives for this to be made possible [189]. Alternative technologies, such as super-capacitors, are also gaining increasing attention [256].

There exist a large number of studies concerned with different technologies of fuel cells ([238, 270, 313],b), electrolyzers [83,194], and supercapacitors [318, 339]. A common issue with all these technologies, however, is their high sensitivity to temperature, emphasizing

* Corresponding author.

E-mail address: bengt.sunden@energy.lth.se (B. Sundén).

<https://doi.org/10.1016/j.pecs.2021.100966>

Received 7 December 2020; Received in revised form 3 August 2021; Accepted 21 September 2021

Available online 4 October 2021

0360-1285/© 2021 The Author(s). Published by Elsevier Ltd. This is an open access article under the CC BY license (<http://creativecommons.org/licenses/by/4.0/>).

the need for them to all be operating within a narrow temperature range. This is particularly well known for batteries [155] but can also be applied to fuel cells, electrolyzers and super-capacitors. Generation and transfer of heat in electrochemical systems cover a wide range of physical and electrochemical processes at nano, micro and macro scales [271, 320]. These include interfacial phenomena on the surface of electrodes, electrochemical kinetics, conduction, and single and multi-phase convection of heat. Immense efforts have already been placed on the development of cooling technologies for electrochemical devices. Several passive and active cooling techniques have been implemented on electrochemical systems, all of which have resulted in varying degrees of success. Nevertheless, temperature control in electrochemical energy devices continues to be a major challenge, and calls for further research. This paper delivers a comprehensive and critical review concerning temperature control in electrochemical energy devices. It emphasizes the less explored but imperative areas of temperature control, such as: the fundamentals of heat generation in electrochemical devices, the alternation between cooling and heat generation and the recent progresses made on the design of cooling systems for electrochemical devices. Batteries are excluded from this work, as there are already extensive reviews on their temperature control [14, 15, 51, 58, 139, 155, 162, 253, 258, 276, 335, 340]. The focus of this review is on fuel cells, electrolyzers and super-capacitors.

2. Fuel cells

Fuel cells are an alternative to the conventional combustion technologies for power generation that often have low efficiencies [26]. Fuel cells offer several benefits over combustion engines such as no toxic combustion products (e.g. CO or NO_x), good efficiencies and small emissions of greenhouse gases. Further, due to having no moving part, they operate almost silently. Fuel cells find applications in vehicles, power generation systems, and aerospace systems [118, 294]. Further, they have potentials for integration with other energy technologies leading to improved efficiencies [74, 206]. As an energy conversion technology, fuel cells feature certain advantages in comparison with wind and photovoltaic technologies. Their capacity factor is about 95%, while those of wind and solar systems are 17.5% and 25.8%, respectively [69]. In addition, they have relatively short payback periods [69]. The efficiency of the fuel cells is directly related to different factors such

as type of fuel and electrode, and the operating conditions. The latter is the route through which the working temperature can influence fuel cells.

Usually, different criteria are considered for classifying the fuel cells such as type of fuel, electrolyte, temperature, and applications. Proton Exchange Membrane Fuel Cell (PEMFC), Molten-Carbonate Fuel Cell (MCFC), Phosphoric Acid Fuel Cell (PAFC), Alkaline Fuel Cell (AFC), and Solid Oxide Fuel Cell (SOFC) are the common types of fuel cells. In this review, PEMFCs and SOFCs receive the most attention. This is because, as Fig. 1 shows, the market is currently dominated by these two types of fuel cell [93]. PEMFCs and SOFCs are widely useable in both stationary and moving applications covering a broad spectrum from small devices (micro-cogeneration modules) to large power and propulsion units [93]. Further, PEMFC has the greatest share of the total FC capacity installed in recent years [93]. Furthermore, recently, there has been a major increase in the practical use of SOFC units. For example, in 2014 installation of about 2700 SOFC units was reported, while in 2018 this reached 27,800 units [87; 93]. Other types of fuel cells, such as DMFC, MCFC and PAFC have received comparatively much less attention lately, while the work on them is ongoing [93].

2.1. Thermal management of fuel cells

In fuel cells a considerable part of the fuel energy is transformed to heat. Removal of this heat is essential for smooth operation of fuel cells. In addition, each type of fuel cell operates within a certain range of temperature, which further reflects the importance of an effective thermal management. A variety of cooling techniques are employed for the cooling of fuel cells. These include heat pipes, cooling channels and fins with large values of thermal conductivity. The working temperatures of different types of fuel cell are compared in Fig. 2. This figure also shows the relationship between the working temperature, efficiency, system complexity, fabricating costs, and materials costs of different fuel cells. According to Fig. 2, as the working temperature increases, the efficiency enhances, while the materials cost drops [293]. The high operating temperature of molten-carbonate fuel cells and SOFCs boosts the quality of waste heat and allows for the improvement of thermodynamic efficiencies by utilizing combined heat and power systems [207]. Further details of the heat recovery process from SOFCs will be provided in section 2.2.9.

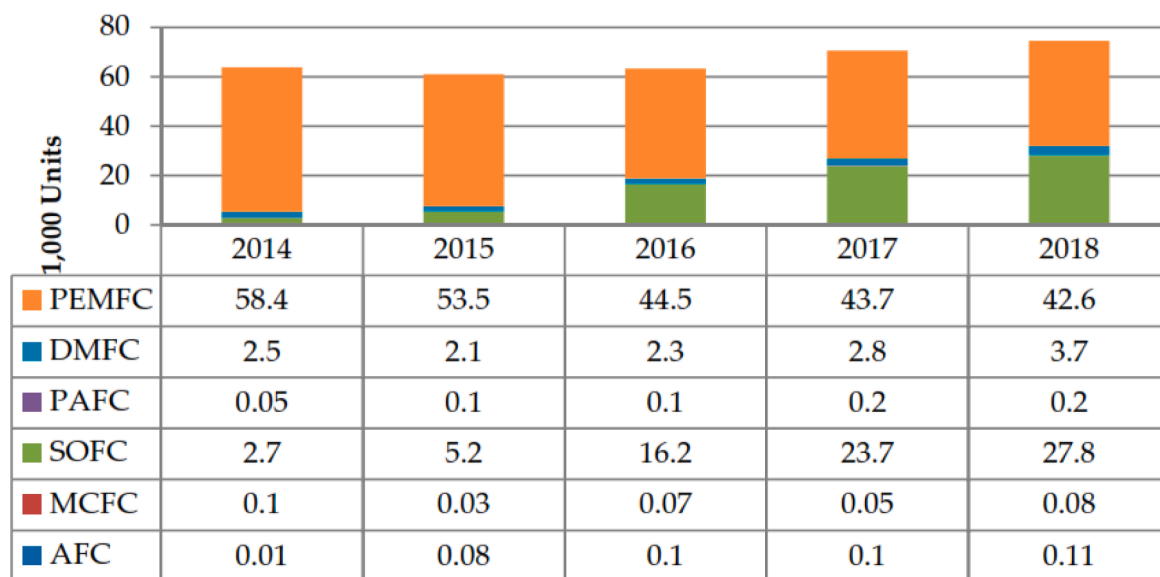


Fig. 1. Shipments of different types of fuel cell [93].

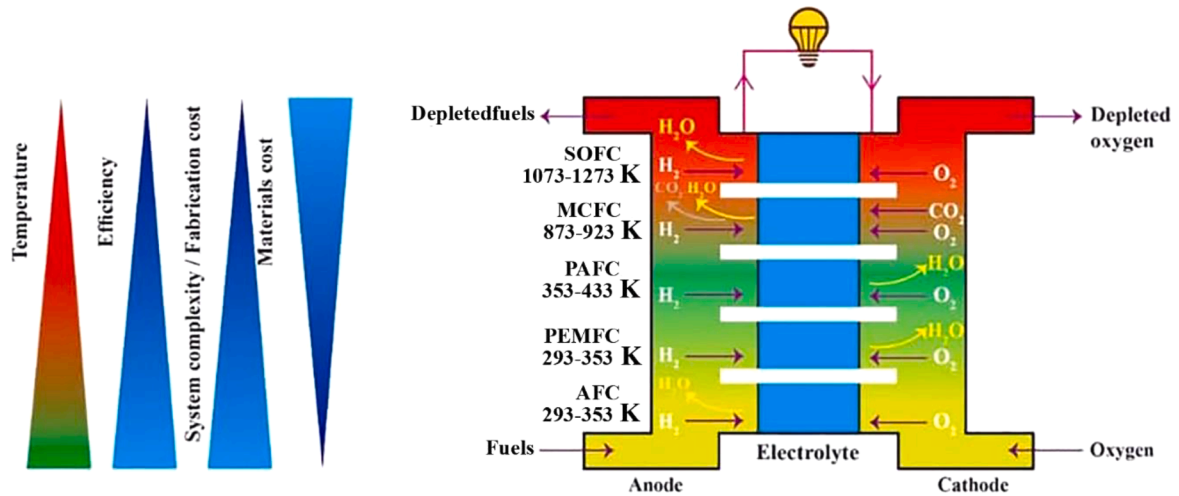


Fig. 2. Comparison between the working temperatures of various types of fuel cells [293].

2.1.1. Heat generation mechanism in fuel cells

2.1.1.1. Heat generation mechanisms in proton exchange membrane fuel cells. Heat generation and removal from the stacks is amongst the most important issues in PEMFCs. This is because fuel cells can generate an amount of heat comparable to their electrical power output [143,147]. In PEMFCs (see Fig. 3) heat is generated by the following mechanisms [329]:

- Reversible heat generated by electrochemical reactions, known as entropic heat

Thermodynamics of fuel cell assert that even in an ideal case, generation of some waste heat is unavoidable [232]. The reversible heat can be determined as the difference between the total chemical energy of the reactants and the highest useful energy based on the second law of thermodynamics. To maintain a constant temperature when electrical current flows, thermal energy should be removed from the electrode chamber. The reversible heat caused by the global reaction of hydrogen oxidation can be obtained by [232]:

$$Q_{\text{reac}}^{\text{tot}} = \Delta G^{\text{tot}}(T, P) - \Delta H^{\text{tot}}(T, P) = -T\Delta S_{\text{rev}}^{\text{tot}}(T, P) \quad (1)$$

where ΔG , ΔS , and ΔH are changes in Gibbs free energy, entropy, and enthalpy, respectively. The corresponding heat flux can be calculated by:

$$\dot{Q}_{\text{reac}}^{\text{tot}} = \frac{i}{2F} Q_{\text{reac}}^{\text{tot}} \quad (2)$$

in which i and F are the current density and Faraday's constant, respectively.

- Heat generated due to irreversibilities in reactions

The irreversible heat is generated by the irreversible electrochemical reactions in the fuel cell. Based on the activated complex theory [2], the electrochemical reactions occurring in the fuel cell lead to heat dissipation. These irreversibilities can be calculated at the anode and cathode by [2]:

$$Q_{\text{act}}^a = -T\Delta S_{\text{irr}}^a(T, P), \quad (3)$$

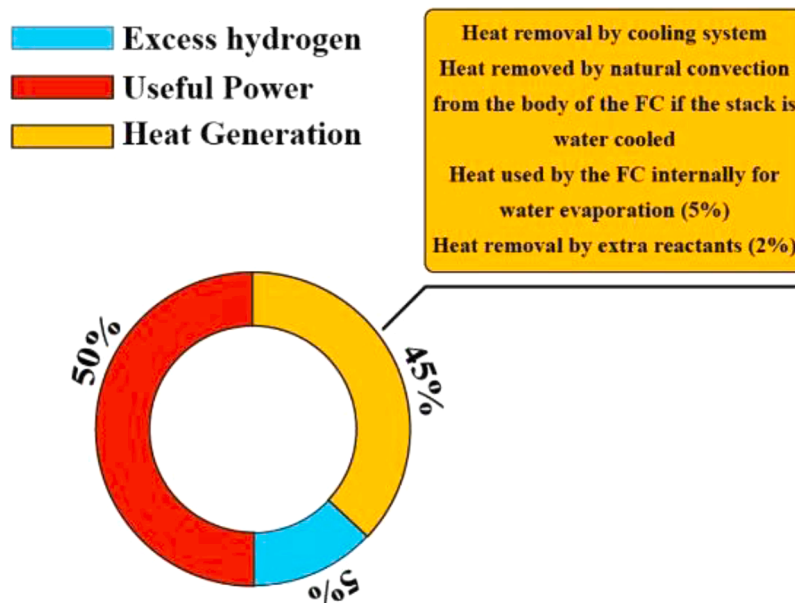


Fig. 3. The outputs of proton exchange membrane fuel cells [134].

$$Q_{act}^c = -T\Delta S_{irr}^c(T, P). \quad (4)$$

They cause the over-potentials at the electrodes, which are related to geometrical parameters, current density, and reactants properties such as pressure, temperature, and concentration [232]. The generated heat fluxes due to irreversibilities of reactions at the anode and cathode are determined by:

$$\dot{Q}_{act}^a = Q_{act}^a \frac{i}{2F}, \quad (5)$$

$$\dot{Q}_{act}^c = Q_{act}^c \frac{i}{2F}. \quad (6)$$

In general, source of irreversibilities in fuel cells are the followings.

Activation overpotential: This irreversibility is due to the transfer of charge, which occurs in the course of the electrochemical reaction on the surface of electrode. The loss is caused by the slowness of the reaction taking place on the electrode surface [5].

Mass transport overpotential: This irreversibility occurs because of the reduction in the concentration of the reactant at the interface between electrodes and electrolyte. As a result of diffusion and convection of the electrolyte, the reactants concentration change. Accumulation of the reaction products further dilutes the reactants. The resultant concentration gradient can reduce the electrode activities and hence the terminal voltage drops [152].

Fuel crossover overpotential: Fuel crossover commonly occurs in an alcohol fuel cell [82]. Although the electrolytes do not conduct electricity and are practically impermeable to reactant gases, a part of fuel diffuses from the anode towards the cathode to react with oxygen, leading to fewer electrons in the created electron current, which move via the external circuit [63]. Because of this motion, the cathode potential decreases leading to degradation of the overall conversion efficiency of the fuel cell. This can occur when the concentration of the intermediate species produced by the fuel oxidation exceeds that of oxygen at the cathode. The rise in temperature intensifies the crossover influence [230].

Ohmic overpotential: Electrolytes in fuel cells often contribute to ohmic resistance, due to the ionic nature of their conductivity. Also, an electrode involves resistance to the current of electrons and there is a contact resistance at the cell terminals [152]. As expected, large values of electrical conductivity of fuel cell components are favorable in decreasing the ohmic heat that is produced by resistance of electrons to flow through the system. Proton transport between the anode and cathode through the membrane leads to enthalpy variations because of the membrane conductivity. The heat released during this process is calculated by [232]:

$$Q_J = 2\Delta H_{H^+}^c - 2\Delta H_{H^+}^a \quad (7)$$

- Heat generated by condensation of the produced water vapor

In fuel cells, water vapor can be condensed as its partial pressure reaches the saturation pressure. Hence, an extra heat source associated with water evaporation/condensation in the gas diffusion layers should be considered. In practice, low gas stoichiometry results in water condensation inside the channels or/and in the gas diffusion layers [232]. The heat generated by water evaporation/condensation can be easily calculated from the latent heat $L_v(T)$ at temperature T:

$$l_v(T) = \Delta H_{H_2O_{liq}}^f - \Delta H_{H_2O_{vap}}^f \quad (8)$$

During condensation (or evaporation) of water in the system, a specific amount of heat is released (or consumed), which is not directly linked to the cell voltage [232]. However, accumulation of large amount of water in the gas diffusion layer leads to flooding of the electrode and a subsequent drop of voltage [232]. It is worthy to note that the generated heat due to water vapor condensation is significantly lower as compared

with the heat generated by other sources [101]. Irreversible, ohmic and entropic heats account for 35%, 10%, and 55% of the total heat generated [108, 146]. The total heat generation is directly related to the efficiency and output power of PEMFCs [108, 146].

Fig. 4 shows the variations of heat and power generation with the current densities. Clearly, heat generation rates increase at higher current densities or lower cell voltage. Here, current density is defined as the amount of current supplied by a fuel cell divided by the total area of the fuel cell electrode. For a single cell, the overall heat generation rate ($W \cdot cm^{-2}$) is estimated by [171, 192]:

$$q'' = (E_m - E_{cell}) \times i \quad (9)$$

where E_{tn} indicates the thermoneutral voltage or the thermal voltage that shows the hypothetical voltage of the fuel cell with the unrealistic assumption that all change in the enthalpy of reactions is converted to electricity. i and E_{cell} indicate the current density and the cell working voltage, respectively. E_{tn} can be calculated based on the higher heating value of the fuel with the assumption that the generated water is in liquid phase or according to the lower heating value when the generated water is in the gaseous phase. As indicated in Eq. (9), the rate of heat generation can increase as the current density rises or the cell voltage drops. Consequently, at larger values of the current density, the rates of heat generation in PEMFCs exceed those of electricity generation. This poses major challenges in the thermal management of stacks, particularly for automotive applications that need to operate at larger current densities. In addition, Fig. 3 shows that the cell voltage drops as the current density increases [192]. As for all generators, fuel cells have their internal resistances and therefore the voltage drops as the current increases.

Fig. 5 represents a typical temperature profile across a PEMFC where the mechanisms of heat transfer between different components are indicated. The thermal properties vary considerably with materials, polytetrafluoroethylene content in gas diffusion substrate, compression, and water content. In PEMFC, the heat transfer in the cells includes conduction in the solid matrix and convection in the pores under the local thermodynamic equilibrium between the two phases [146]. The influences of heat adsorption/generation during the phase change of water should be also considered [319].

2.1.1.2. Heat generation mechanisms in solid oxide fuel cells. The mechanisms of heat generation in SOFC are somehow similar to those of PEMFC. Fig. 6 shows the energy generation in a typical SOFC. The major source of heat in a SOFC system is the cells. Certain portion of the heat is released due to the electrochemical reactions at the electrodes while the overpotential losses further boost the cells temperature. Since not all the supplied fuel is consumed in SOFCs, combustion of the unreacted fuel exhausted from the cells. Fuel usage factor, or the fuel consumption rate, is usually about 0.8 or less and the remaining fuel is fulminated downstream of the cells, generating extra heat [317].

As displayed in Fig. 7, there are three overpotentials in the SOFCs. Overpotentials are oriented from the nature of the fuel cell voltages in response to the loading conditions. The electrochemical reactions in the SOFC can cause the fall in potential owing to the activation resistance or activation polarization. The second drop in potential is due to the ohmic resistances in the components of the fuel cell when the electrons and ions are conducted in the electrodes and electrolyte, respectively. Finally, the third drop, which is considerable for larger values of current density, is attributed to the mass transport resistances or concentration polarizations in the flow of the fuel and oxidant [170]. Joule heating or ohmic loss is assigned by the internal resistances of the cells consisting of electrode overpotential and electrical resistance. The ohmic loss is due to the ionic conduction resistance of the electrolyte layer and the electric resistances of the electrodes and the current collection components. Accordingly, the current collecting pathway and conductivity of cell materials are two parameters affecting the overall ohmic loss of SOFCs

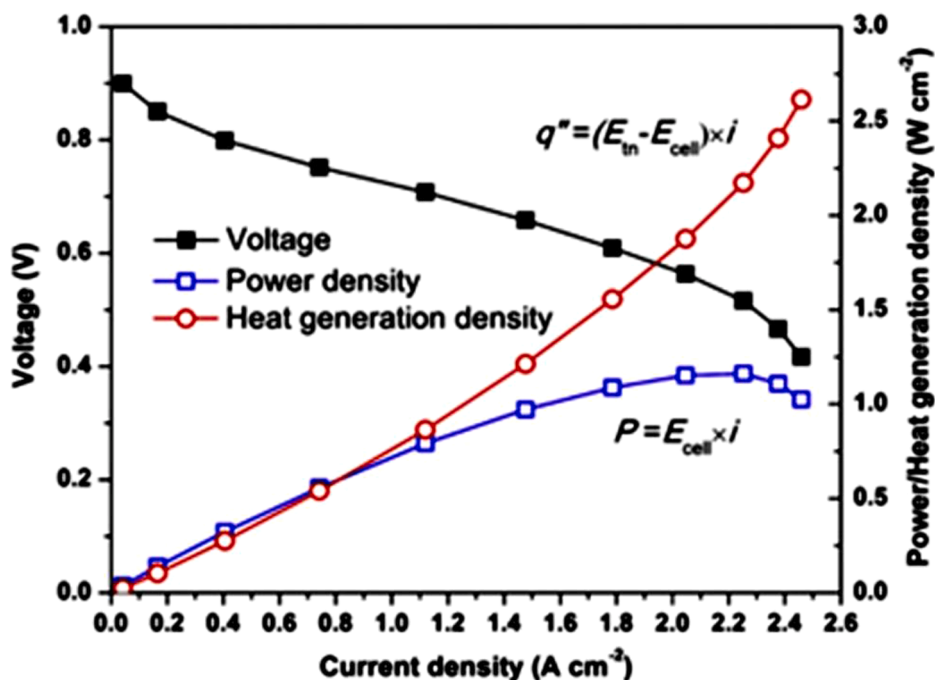


Fig. 4. The variations of heat generation and power generation with current densities for a PEMFC [217].

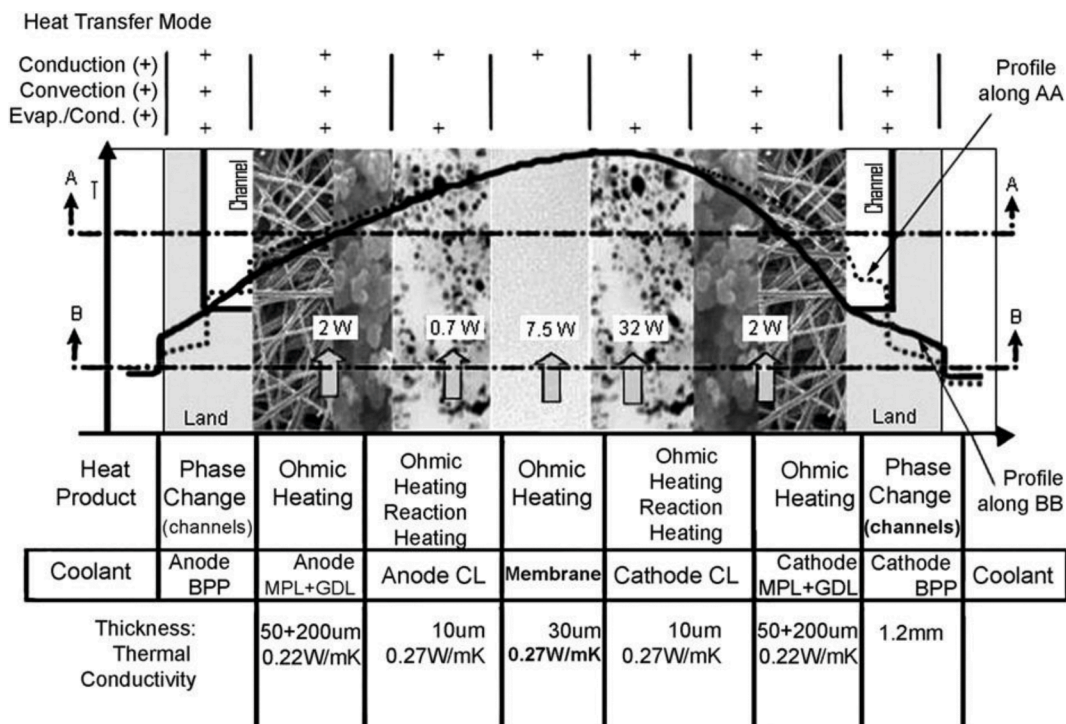


Fig. 5. The mechanisms of heat transfer between different components of a PEMFC [146].

[170].

Recently, Guk et al. [113] investigated the effects of different parameters on the thermal characteristics of SOFCs. They concluded that the temperature increase is more noticeable near the air/fuel inlet and it gradually declines towards the fuel outlet. Due to its relatively larger partial pressure, hydrogen leakages are more likely near the inlet, causing more direct oxidation and thus higher heat release. Increases in the temperature make the gas components more active and increases the pressure. Both of these lead to leakage of gas and, consequently, direct

oxidation happens and the corresponding temperature increases. The increase in the temperature also occurs as the flow rate increases under the same operating temperature. This is, again, due to the undesired fuel crossover through the electrolyte leading to direct hydrogen oxidation. Oxygen ions, decreased at the cathode by free electrons or the electron crossover, travel from cathode to anode or hydrogen from anode to cathode and lead to the exothermic reactions between oxygen and hydrogen. In addition, electrochemical cell reactions can increase the temperature of the cell electrode. Guk et al. [113] found that the direct

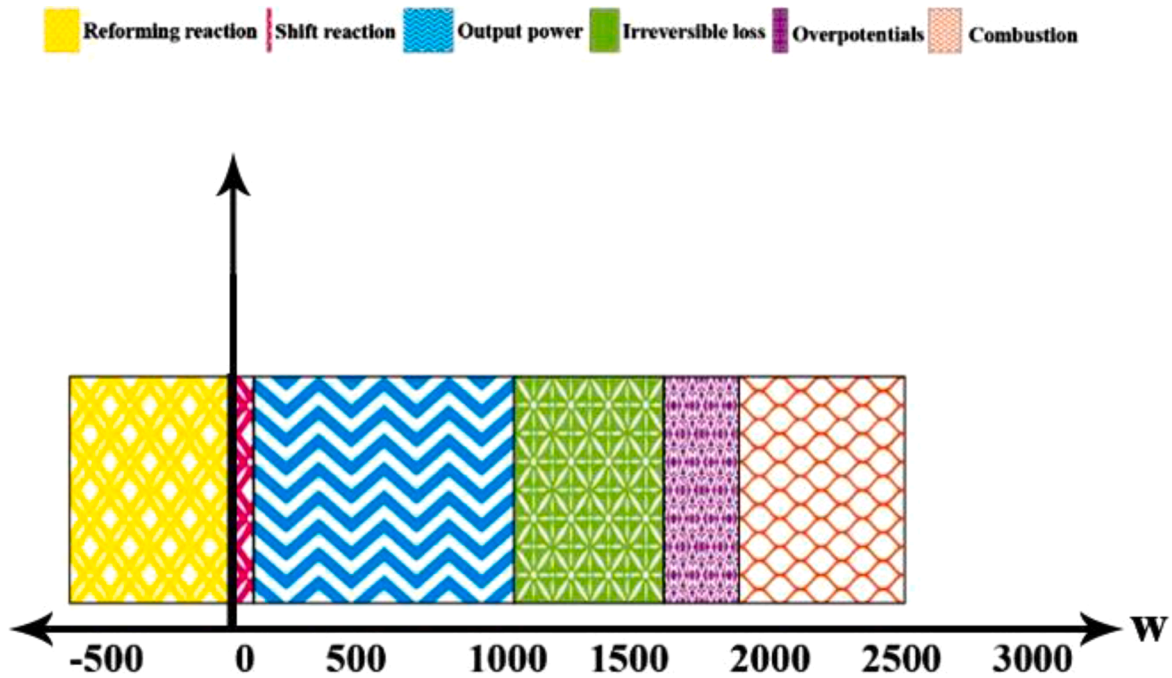


Fig. 6. The heat generation in a typical SOFC [317].

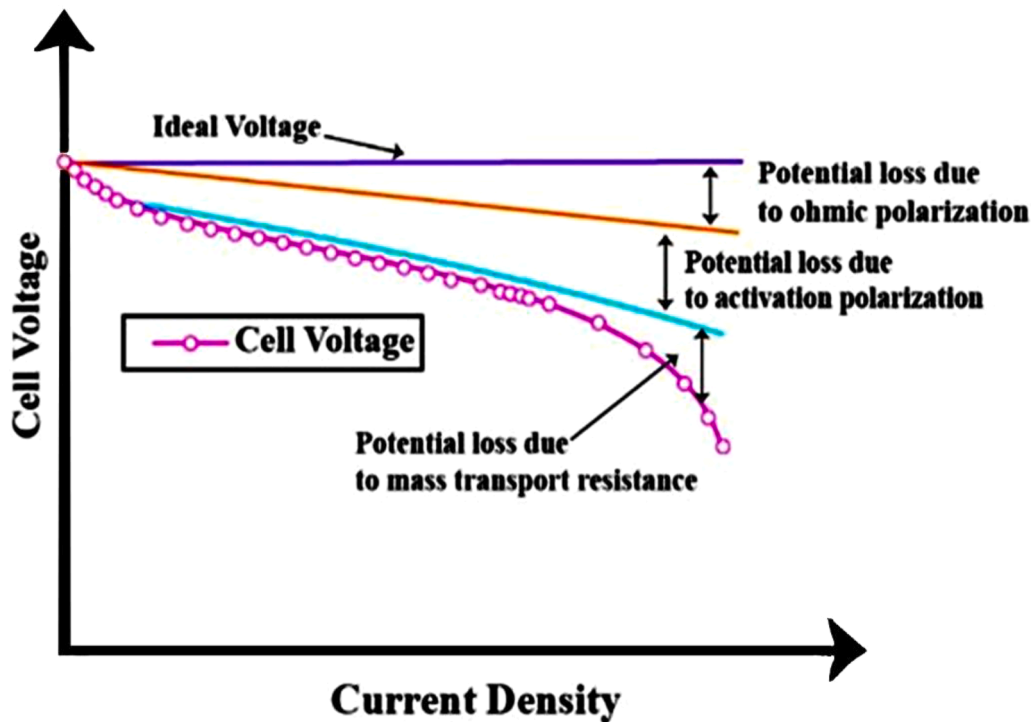


Fig. 7. Conjectured description of the overpotentials in an SOFC [170].

oxidation of hydrogen by fuel crossover is the main reason for increasing the cell mean temperature during open circuit and loading condition. Yet, under loading, electrochemical oxidation of hydrogen is responsible for the cell temperature gradient.

Fig. 8 depicts the mechanisms of heat transfer between the main components of a SOFC, including heat transfer by species transportation, conduction between two solid structures, convection between the solid and gas structures, and radiation between two solid surfaces [55].

Finally, it is noted that the operation principles of the fuel cells

involve thermodynamics, hydrodynamics, mass transfer and electrochemistry. Any comprehensive model should consider the transport of electron, proton, oxygen, and water together with the temperature influences and electrochemical reactions [270]. These establish a complex nonlinear system with multi-input and multi-output for which development of mathematical models and control strategies are difficult [275]. This implies that the temperature considerations should be included at the design stage and provides yet another reason for understanding the mechanisms of heat generation and transfer in fuel cells.

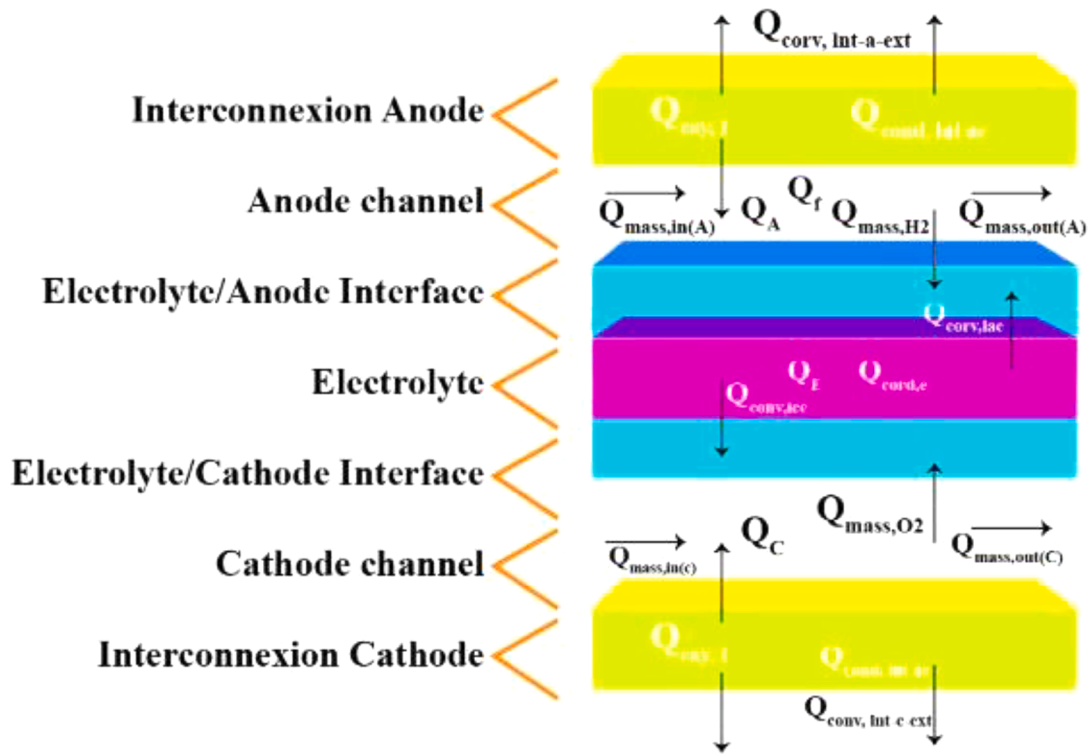


Fig. 8. The mechanisms of heat transfer between different components of an SOFC [55].

It is known that the cell temperature features a nonlinear relationship with gas fluxes, the gas temperatures, and the environmental temperature [173].

2.1.2. Governing equations

Many physical phenomena occurring in fuel cells can be represented by the equations for the conservation of mass and momentum as well those for the transport of energy, chemical species and current. These equations are presented in Table 1.

It should be noted that the source term in the transport of energy can include heat of reaction, ohmic heat, and/or heat of condensation and evaporation for the phase change processes. This source term is different in the various components of fuel cells [24]:

- In the ducts with gas flow, phase change is the only feasible heat source or sink. This includes condensation of water vapor in the gas streams as a source of heat or evaporation of liquid water in the ducts, as a sink of heat. Indeed, evaporation takes place only if the liquid water in the gas stream is in contact with unsaturated vapor. Conversely, existence of saturated water vapor is essential for the condensation to happen. Condensation can also occur when gaseous reactants or their constituents, i.e., oxygen or hydrogen, disappear in the electrochemical reactions over a catalyst substrate.
- In substrates for gas diffusion, the ohmic resistance of solid and phase change within the pores are the sources of heat.
- In catalyst substrates, the sources of heat include the heat release by the electrochemical reactions, heat provided by the electronic and ionic resistances and the enthalpy of evaporation.

The only source of heat, in membranes, is the ohmic resistance. It is further noted that radiation heat transfer within the electrode and electrolyte substrates and also surface-to-surface radiation within the fuel and oxygen flow channels can considerably affect the temperature fields and the overall operational condition of SOFCs [67].

2.1.3. Importance of thermal management of fuel cells

2.1.3.1. Importance of thermal management of proton exchange membrane fuel cells. As discussed earlier, an effective thermal management is central to optimal performance in PEMFCs [20]. Thermal management aims to maintain the working temperature of the stack within the favorable range and setting uniform temperature distributions across the stacks and their individual components [8]. It should be noted that the stack efficiency diminishes when fuel cells work under high temperatures due to the degradation of the catalyst and membrane [240, 328]. On the other hand, it is expected that at low temperatures the reaction kinetics occur slowly which may result in flooding of water with low saturation pressure. This is a critical issue from the water management viewpoint in fuel cells [66, 140]. PEMFCs have received significant attention as the ideal automotive power sources due to their high efficiency and zero emissions [238]. At high powers under typical automotive operating conditions, some hot spots may form on the bipolar plates and the cathode. These accelerate thermal aging of the membrane and catalyst sintering in the cathode [238] reflecting the importance of thermal management for this type of fuel cells.

2.1.3.2. Importance of thermal management of solid oxide fuel cells. The thermal management of SOFCs is an essential requirement for the operation and maintenance of the device. The local reaction rates in SOFCs are highly related to the local temperature distribution [326]. Temperature non-uniformity damages SOFCs. When the temperature in SOFCs exceeds the critical value, it leads to electrode sintering and unwanted reactions happen between electrodes and electrolytes [124, 201]. The SOFC efficiency lessens by reducing the reactive sites caused by the sintering of the electrode pore structures [312]. In addition, the thermal stresses produced by the temperature gradients and sintering lead to thermal cracking and delamination in the system [202, 310]. Meanwhile, the high local temperatures and gradients can also cause sealing failure. To ensure adequate electrochemical activities without excessive degradations, the temperature ranges for SOFCs should be kept within particular limits [92]. The SOFC temperature range is

Table 1.

The conservation equations to represent physical phenomena in the fuel cells [157].

Name	Equation	Component
Conservation of mass	$\frac{\partial \rho}{\partial t} + \nabla \cdot (\rho v) = 0$ ρ : Density v : Velocity	Gas flow duct, gas diffusion substrate, catalyst substrate
Conservation of momentum	$\frac{\partial (\rho v)}{\partial t} + \nabla \cdot (\rho v v) = -\nabla p + \nabla \cdot (\mu^{eff} \nabla v) + S_m$ p : Fluid pressure μ^{eff} : Mixture average viscosity S_m : Momentum source term	Gas flow duct, gas diffusion substrate, catalyst substrate
Conservation of energy	$(\rho c_p)_{eff} \frac{\partial T}{\partial t} + (\rho c_p)_{eff} v \cdot \nabla \cdot (T) = \nabla \cdot (k_{eff} \nabla T) + S_e$ c_p : Mixture-averaged specific heat capacity T : Temperature k : Thermal conductivity S_e : Energy source term eff : Effective properties in the porous media	All components
Conservation of species	$\frac{\partial (\epsilon \rho x_i)}{\partial t} + \nabla \cdot (v \epsilon \rho x_i) = \nabla \cdot (\rho D_i^{eff} \nabla x_i) + S_{s,i}$ x_i : Mass fraction of gas species $S_{s,i}$: Source or sink terms for the species D_i^{eff} : Fickian diffusion of species in a porous medium ϵ : Porosity eff : Effective properties for the porous media	Gas flow duct, gas diffusion substrate, catalyst substrate
Conservation of electric charge	$\nabla \cdot (k_s^{eff} \nabla \phi_s) = S_{\phi_s}$ k_s^{eff} : Electrical conductivity of the solid ϕ_s : Solid phase potential S_{ϕ_s} : Source term, which represents the volumetric transfer of current at the anode and cathode catalyst substrates	Electrodes and external electric circuit
Conservation of ionic charge	$\nabla \cdot (k_m^{eff} \nabla \phi_m) = S_{\phi_m}$ k_m^{eff} : Ionic conductivity in the ionomer phase ϕ_m : Electrolyte phase potential S_{ϕ_m} : Any volumetric source term in either of anode or cathode $S_{\phi_m} = S_{\phi_s}$	Catalyst substrate and membrane

mainly dominated by the oxygen ion conductivity across the electrolyte material. Different electrolyte materials have different optimal temperature range allowing for efficient ion transport. Typical SOFCs have 8% mol yttria-stabilized zirconia electrolyte for which the optimal conductivity is in the range of 1023 K to 1123 K. Currently, there is active research on new electrolyte materials operating at lower temperatures to lower the cost of the cell, whilst maintaining the good performance achieved at high temperatures ([187] and [188]). During the starting-up and operation of SOFCs, it is essential to have a uniform temperature distribution across the unit [12, 237]. For instance, the temperature difference along the axis direction of a typical 1.5-m-long tubular SOFC by Siemens-Westinghouse was about 200 K [245]. The reasons for avoiding high temperature gradients in SOFCs include decreasing thermal stress and the resultant brittle failures, homogenizing current distributions, decreasing the maximum temperature to hinder decay of the cells and the interconnected materials and, simplifying the operational models and control techniques [282]. It is further noted that thermal management of SOFCs could increase the electro-chemical activities that in turn enhances the efficiency [89]. It follows that the thermal management of fuel cells is a critical and

intricate task.

2.1.4. Different techniques used for thermal management of fuel cells

The techniques used for the control of temperature across fuel cell components are directly related to the size and power capacity of the fuel cell. Edge cooling [248], cooling with separate airflow [99], air cooling [175], liquid cooling [219], cooling with phase change [57] and cooling employing the cathode air supply [49] are the main methods used for fuel cells thermal management. In general, for fuel cells that work with a power larger than 10 kW, the cooling of the system is performed by using a liquid while for powers less than 2 kW the cooling can be done by air. The benefits and restrictions of cooling methods used for thermal management of fuel cells are summarized in Table 2. Most broadly, the cooling methods of fuel cells are classified into two groups of passive and active. Passive cooling methods refer to those technologies that do not require power consuming devices such as pump or fan. Hence, passive cooling technology are often simple [329]. Edge cooling and cooling with heat pipe are two examples of passive cooling methods. Unlike passive methods, active cooling methods consume power by employing pumps or fans to provide forced convection of liquids or air.

2.1.4.1. Thermal management of proton exchange membrane fuel cells.

Shah [254] reported that the flow of reactants is sufficient to cool down

Table 2.

The advantages and restrictions of cooling methods used for thermal management of fuel cells [329].

Cooling method	Fuel cell power	Advantages	Challenges/limitations
Cathode air	Less than 0.1 kW	Simple structure Without coolant loop Inexpensive	Needing stacks with big size and high weight Without controlling temperature stack Natural convection cannot be employed to remove heat
Separate airflow	0.2 to 2 kW	Simple structure Without coolant loop Small parasitic powers	Impractical method Trade-off between cooling efficiency and parasitic powers
Edge cooling	About 1 kW	Simple structure Good overall system reliability Small parasitic powers Without coolant scaling issues	Limitation in heat transfer length Lack of affordable materials with great mechanical attributes and very large value of thermal conductivity
Phase change with boiling process	About 1 kW	Eliminating coolant pump Decreasing coolant flow rates Providing uniform working temperature Employing refrigeration fields and electronic equipment and components	Two-phase flow instabilities Coolant boiling temperatures should be lower stack working temperature (particular coolant) Incompatible with automotive powertrains
Phase change with evaporation process	0.5 to 75 kW	Simple structure Cold starting abilities Internal humidifying process	Needing a particular design Dynamic controlling for water evaporation rates Thermal mass of liquid water on cold startup
Single phase liquid cooling	More than 10 kW	Great cooling capacity Flexible control of cooling capacity Cooling improvement capacity employing various techniques Employing in automotive usages	Radiator size and weight High parasitic powers Requiring extra equipment

the PEMFCs with power less than 0.1 kW. The separate air channels along with reactant streams are suitable for cooling down the PEMFC with the power in the range of 0.2–2 kW while, PEMFCs with powers larger than 10 kW need liquid coolant. The schematic view of the various cooling techniques applied to PEMFCs is displayed in Fig. 9. The suitable power levels for cooling techniques of PEMFCs are displayed in Fig. 10.

2.1.4.1.1. Active cooling methods. Active or forced cooling methods include the following sub-categories.

Forced cooling by cathode air flow

For PEMFCs with small sizes, the stacks can be cooled down only by using the cathode air flow. Normally, this cooling method is not employed for fuel cells with electrical power larger than 5 kW [164]. Fig. 11 shows a schematic view of this cooling method. With their many advantages over ordinary lead-acid batteries and diesel generators, air-cooled fuel cells are commonly used in portable and backup energy generation. These include extended runtime, higher reliability, higher performance, and reduced environmental impact [255]. In these fuel cells, the external surface area of the stack is much larger than the active surface area, e.g., air breathing PEMFC stacks. This enables the stacks to dissipate thermal energy at the rates comparable to those of heat generation. This method features the drawback of requiring relatively large channel size for cathode side of the stack in comparison with the anode side that can eventually lead to larger volume of the stacks. De las Heras et al. [70] designed three configurations for an air-cooled fuel cell. These configurations and their features are presented in Table 3. Four fans are used in configuration 1, which are divided into two groups. The first group is always in use when fuel cell is operating, while the second group is switched on only when the stack temperatures exceed the optimal value. It should be noted that such an optimal value varies with the operational condition [306]. In configuration 2, both groups of fans are monitored by measuring the difference between the actual stack temperature and the ideal temperature provided by the company. In configuration 3, a flow adapter and adjustable fan speed are used. In this case, only one fan is used, which operates with a variable speed by a control procedure. This makes configuration 3 the most effective of all configurations listed in Table 3.

Qiu et al. [228] performed a numerical study to investigate a PEMFC

cooled with cathode air flow. They considered two cathode flow ducts, as disclosed in Fig. 12. Two designs were assessed for the cathode duct, including those with opening at the side and curved features. Qiu et al. concluded that using wavy surfaces at the bottom of the flow ducts results in the efficiency enhancement of the fuel cell. This is because it could increase the mass transfer between the duct and catalytic layer by inducing a vertical velocity component of the air flow. The contact area between the air and gas diffusion layer is increased by using the open cathode flow duct. Although more surface of gas diffusion layer is exposed to air flow in the duct, this configuration may not provide higher efficiency as compared with the fuel cell with an unmodified duct. It is important to note that the smaller contact between the bipolar plates (will be described in detail in section 2.2.6) and gas diffusion layer intensifies the contact resistance, which can then offset the efficiency enhancement caused by the higher mass transfer rates.

Cooling with separate air flow

For a stack with power larger than a few hundred watts, separate cooling ducts are required in which air blows to dissipate the heat generated by the exothermic reactions occurring in the fuel cells as discussed in section 2.2.1 [120]. A schematic view of this cooling method is shown in Fig. 13. It should be noted that the membrane might be dried as the supply of cooling air to the cathode increases. Accordingly, it is required to design separate ducts for the cooling air [163]. This method is usually suitable for PEMFC stacks with powers between 0.1 kW and 2 kW [163]. It offers the possibility of extracting more thermal energy from the stack without affecting the airflow.

Liquid cooling

It is well known that generally liquids have higher specific heat and thermal conductivity than gases. As a result, it is reasonable to use liquids instead of air for cooling the stacks with higher heat generation rates (greater than 2 kW). In large scale applications such as automotive in which high powers are needed (~100 kW), for cooling of PEMFC stacks it is recommended to use separate channels with a liquid as the coolant ([100]). Deionized water would be a suitable choice due to its high specific heat, i.e., $4181.8 \text{ J.kg}^{-1}.\text{K}^{-1}$. For operation in cold climates, an antifreeze coolant such as a mixture of water and ethylene glycol can be used [272]. The coolant should also have low electrical conductivity to avoid current leakage through the cooling loop and

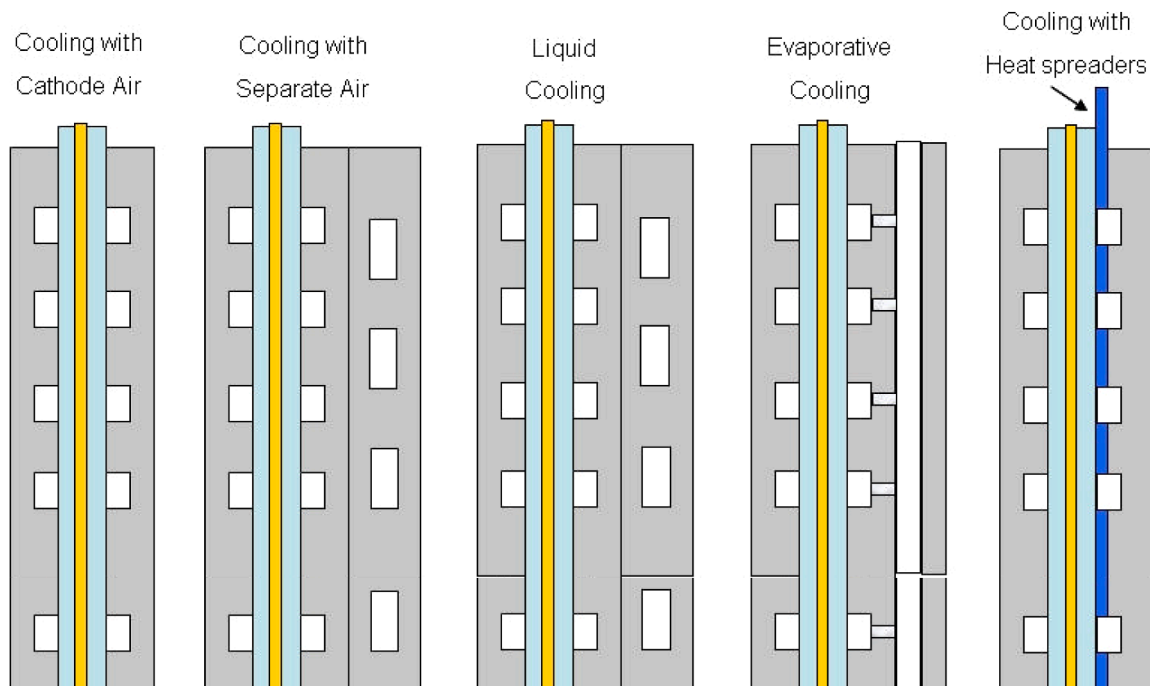


Fig. 9. The various cooling techniques employed for PEMFCs [120].

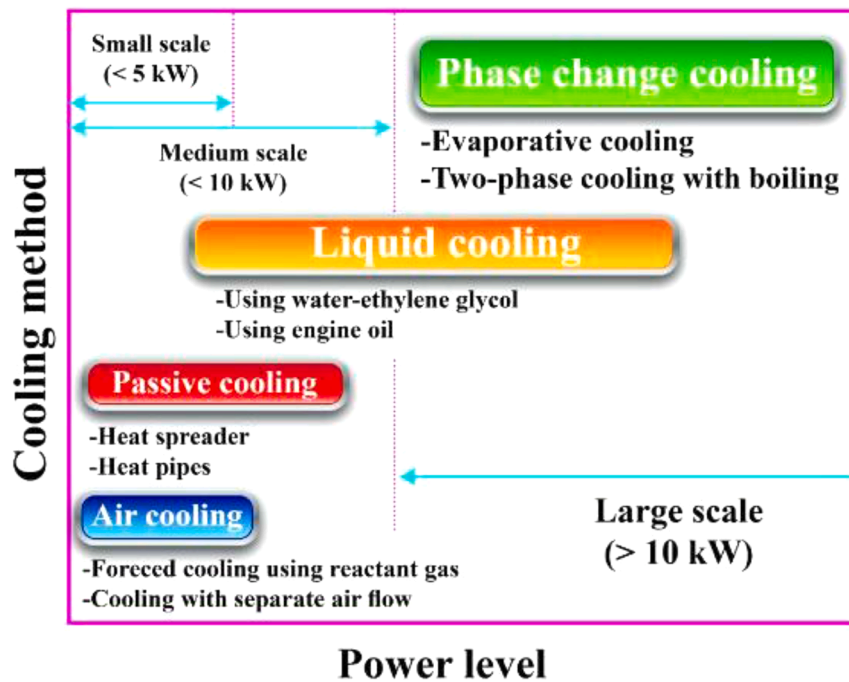


Fig. 10. The suitable power levels for cooling techniques of PEMFCs [57].

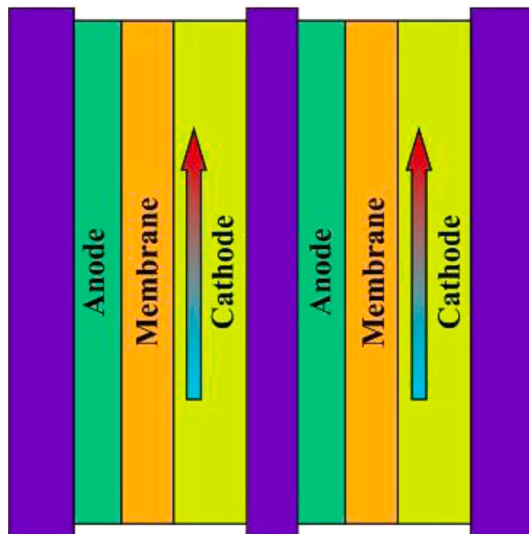


Fig. 11. Cooling with cathode air flow [95].

decay of the bipolar plates [247]. However, incompatibility with the aluminum heat exchangers is an important issue associated with the usage of deionized water as coolant [102].

Generally, the costs and weights of this cooling technique are higher than those of air cooling, as extra components including coolant loop, heat exchangers, pumps, flow regulation valves, and deionizing filters are required [267]. Lin et al. [176] designed a liquid cooling for PEMFC stacks, as shown in Fig. 14. They considered various configurations of coolant and hydrogen channels. The authors indicated that for a better management of water, a counter-flow configuration for the hydrogen channels could be used. Further, to improve temperature control of the system, the counter-flow arrangement was recommended for the coolant channels. In addition, both counter-flow configurations of the coolant and hydrogen channels could further enhance the temperature uniformity of the stack.

Fig. 15 shows a liquid cooled module designed for PEMFCs. In this

module, heat is removed from the stack by forced convection of liquid water through circular ducts inside the bi-polar plates. A conventional liquid to air cross-flow louvered fin radiator was also employed for rejection of waste heat to the environment. The stack temperature can be controlled by feedback control of the radiator by a bypass valve. The temperature rise of the coolant across the stack was kept at the maximum value of 5 K employing a variable flow rate pump. The inlet cathode gas is wetted by employing a vapor exchange module from the cathode exhaust while the anode is dead ended.

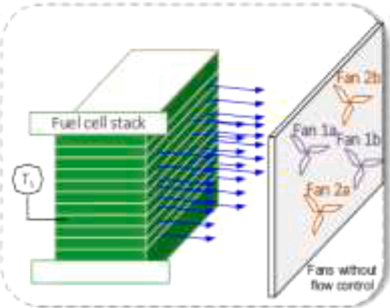
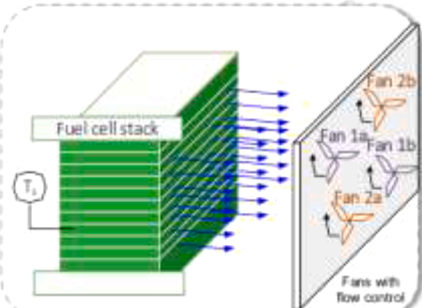
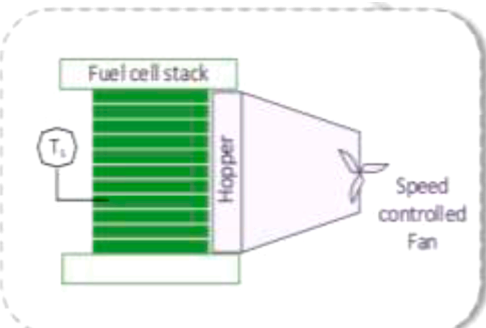
Nanofluid cooling

Water as a conventional liquid for cooling PEMFCs has some disadvantages, including its low thermal conductivity [134]. Thus, nanofluids containing uniformly distributed nanoparticles could serve as an alternative to water in cooling applications. High ratio of contact surface area to volume of nanoparticles that are added to the base coolant leads to significant improvement of thermal conductivity and diffusivity of nanofluids [11,114]. Nonetheless, nanoparticles also boost the viscosity of the liquid. In order to enhance the heat transfer rate in ordinary liquids by a factor of two, the pump power should be boosted about tenfold. However, if the thermal conductivity of liquids is doubled by employing nanoparticles, the pumping power often does not increase beyond three times. As a result, a large boost in thermal conductivities of coolants by employing nanoparticles leads to saving a large amount of pumping power [56, 134]. Nanofluids can make the cooling system smaller, for example, the frontal area of the radiators can be reduced by about 10% [134]. They can further decrease the freezing point in comparison with the base coolant, which is desirable in automotive applications [263].

The electrical conductivity of water with ions is much larger than that of pure water, which leads to interruption of the electrical current throughout the fuel cell stack [17]. When water is passed through the closed loop, it is in contact with the material and might be contaminated by a large number of ions. As a result, it is important to employ de-ionizing filters when employing water or mixture of water/ethylene glycol as coolants [17]. Deionization process removes cations, including calcium, sodium, copper, iron and also anions, including chloride, nitrate, sulfate. Deionization faces some important challenges, most notably the high capital and operational costs [295]. By the usage of a nanofluid in the cooling loop, there is no need to use de-ionizing filter.

Table 3.

The configurations and their features discussed by De las Heras et al. [70]. The cooling system was designed for a PEMFC with the power of 3.4 kW and operating temperature in the range of 299 K to 339 K.

Structures	Costs (€)	Auxiliary power consumption (kW)	Air-flow control	Homogenous temperature distribution	Performance (Ratio of Electrical power to hydrogen consumption)
Four fans without controlling system: 	~800	0.3648	No	No	30%
Four fans with controlling system: 	~800	0.3648	Yes	No	42%
One fan with speed controlling system: 	~200	0.091	Yes	Yes	50%

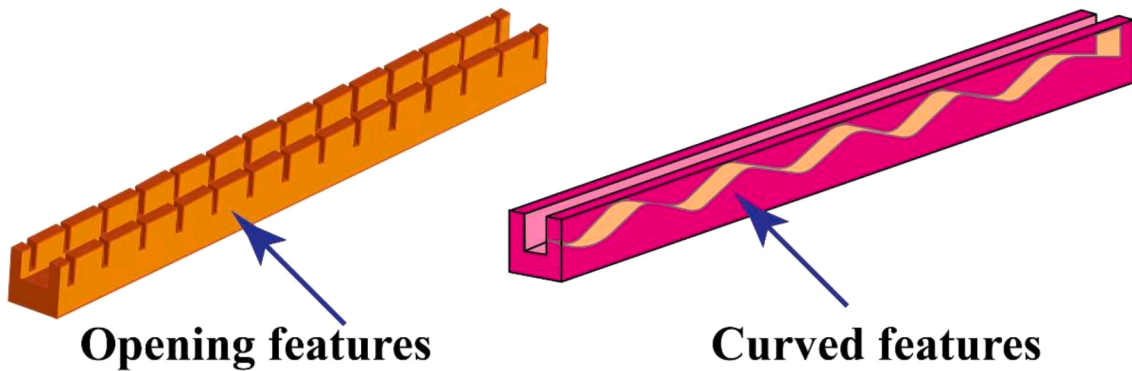


Fig. 12. The cathode flow ducts considered by Qiu et al. [228], the cooling system was designed for a PEMFC with the operating temperature of 333 K.

Free ions will be neutralized after reacting with nanoparticles dispersed in the coolant, and, hence, have no effect on the electrical conductivity (See Fig. 16). Nanoparticles are designed for immobilization of both

negative and positive ions in the fluid but remain active until they are saturated with the ions [79].

To employ nanofluids for cooling of PEMFCs, they should meet the

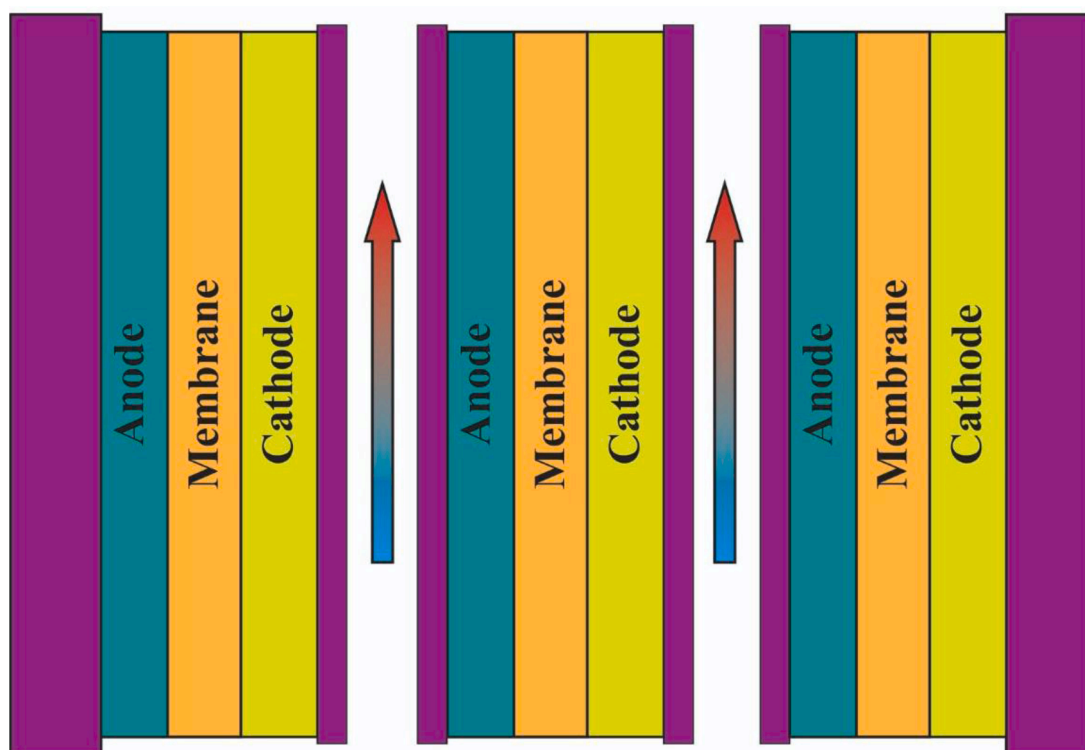


Fig. 13. Cooling with separate air flow [95].

following requirements [267]:

- Having smaller values of dielectric since an external electrical field can polarize them, this may lead to electricity leakage through the coolant flow.
- Having low freezing point to be useable in all climates.
- Having saturation temperature by about 10 K to 20 K lower than the optimized operating temperature of the stack [107].
- Adding nanoparticles to the base coolant generally ameliorates the heat transfer rate; however, to neutralize the negative effect of nanoparticles on pumping power, an optimal concentration for nanoparticles should be selected.
- The nanofluids should be non-explosive, non-flammable, and have no toxicity for humans and the environment.

Although nanofluids could enhance the performance of the cooling system in PEMFCs, sedimentation of nanoparticles (instability of nanofluid) and clogging the channels can affect the efficiency of PEMFCs. Adding surfactants to the base fluid or functionalizing nanoparticles can improve the stability of nanofluids. Nanofluids with lower ionic strength offer improvements in electrical conductivity, while this declines at higher ionic strength [134]. Al_2O_3 -water [158], CuO-water [243], Al_2O_3 -water ethylene glycol mixture [324], SiO_2 -ethylene glycol and SiO_2 -glycerol [9] et al., 2018) are examples of the nanofluids used for thermal management of fuel cells.

Finally, it should be noted that nanofluids are yet to be commercially used in PEMFCs. Before commercialization of nanofluids for use in PEMFCs, the following issues should be addressed [126, 234, 244]:

- A high-quantity nanofluid with excellent long-term and high-temperature stability should be provided.
- Effective methods should be employed to retain the stability of nanofluids in real time as sedimentation of nanoparticles is unavoidable after a long-term running. *Re*-dispersion of the aggregation of nanoparticles through using dispersion devices in the cooling

system with functions of agitation or of ultrasound could be a proper choice.

- Although surfactants can be employed to enhance the dispersion and adhesion efficiency of nanoparticles in fluid, the effects of surfactant on the physical properties and efficiency of cooling system should be considered.
- The environmental issues associated with nanofluids containing heavy metals, toxic substances, and other hazardous materials, have limited their applications as coolants in fuel cells.

Evaporative cooling

The heat of vaporization can become the basis of a cooling process by injection of water to the reactant flow of PEMFCs. Water absorbs the heat generated by the electrodes and evaporates while the temperature remains constant. This cooling technique features some superiorities to liquid cooling, including decreasing the coolant flow rate, simplification of module layout, and omitting coolant pump [107, 266]. It also takes advantage of the latent heat of phase change, which is generally very large. As a result, application of this method reduces the coolant flow rate, which in turn, makes the cooling system more compact and less expensive. The coolant circulation can be provided by a pressure difference, density difference or hydrophilic wicking. In some cases, for example, circulation provided by density difference or hydrophilic wicking, there is no need to use a coolant pump. This cooling technique can also help preventing drying of the membrane through a constant supply of water.

In general, phase-change cooling processes include boiling and evaporating [235, 236]. In the evaporation, the stack temperature is less than the boiling temperature of the coolant. However, in the boiling, the boiling temperature of the coolant should be lower than the temperature of stack. Fig. 17 shows an evaporatively cooled stack with the usage of liquid water at the cathode.

In their study of evaporative stack cooling, Barbir [24] analyzed the effects of water injection at the cathode. Fig. 18 displays the water injection rates needed at various working conditions for the evaporative cooling of the stacks. They reported that at higher loads the required

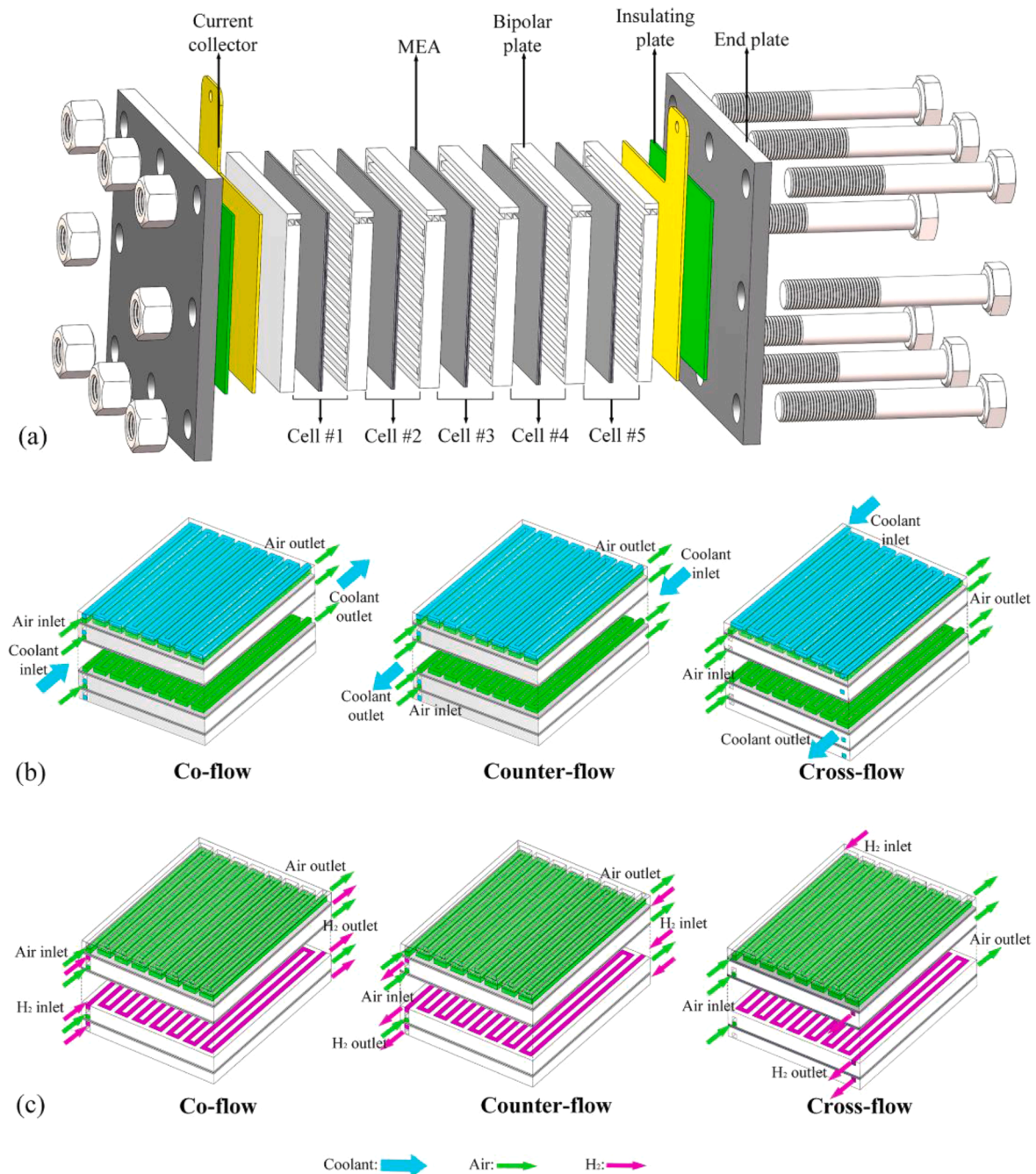


Fig. 14. a) The PEMFC considered by Lin et al. [176]; b) various configurations of the coolant channel; c) various configurations of the hydrogen channel. The cooling system was designed for a PEMFC with the power density in the range of 2.23 kW.L^{-1} to 2.39 kW.L^{-1} .

water injection to achieve saturation conditions at the outlet increased.

An evaporatively cooled thermal management system designed for PEMFCs is displayed in Fig. 19. In this design, the liquid water is added into the cathode flow ducts. The water evaporates and humidifies the cells and removes the waste heat. The cathode exhaust is then cooled and the evaporated water condenses along with some of the product water. Then, the condensed water is separated in the cyclone and stored in a water reservoir for reusing. The system further employs a louvered fin radiator for removing heat from the cathode exhaust.

Fly and Thring [96, 97] compared the evaporative and liquid cooling techniques for fuel cell vehicles. They concluded that the radiator frontal area needed to provide thermal and water balance for an evaporatively cooled module is about 27% less than that with a liquid cooling module. This is due to larger values of the heat transfer coefficient in the

condensing radiator. For the boiling approach, HFE-7100 with boiling temperature of 334 K at 1 atm was identified as a good option [46]. Choi et al. [57] investigated experimentally the boiling heat transfer of HFE-7100 in a mini-channel and its cooling efficiency for fuel cells. These authors found that the boiling heat transfer coefficient of HFE-7100 in the mini-channel is mostly related to the heat flux and vapor quality. However, it has a lower sensitivity to the mass flux. It was also observed that the dominant boiling mechanism of this coolant, in the mini-channel, is nucleate boiling. For the usual heat generation rates in fuel cells, the boiling-based cooling technique can maintain the wall temperatures below 336 K with a spatial variation of less than 0.5 K. Nonetheless, this is provided that the system does not reach the critical heat flux conditions. At the critical heat flux, the wall temperature increases above 364.5 K at the pressure of 1 bar.

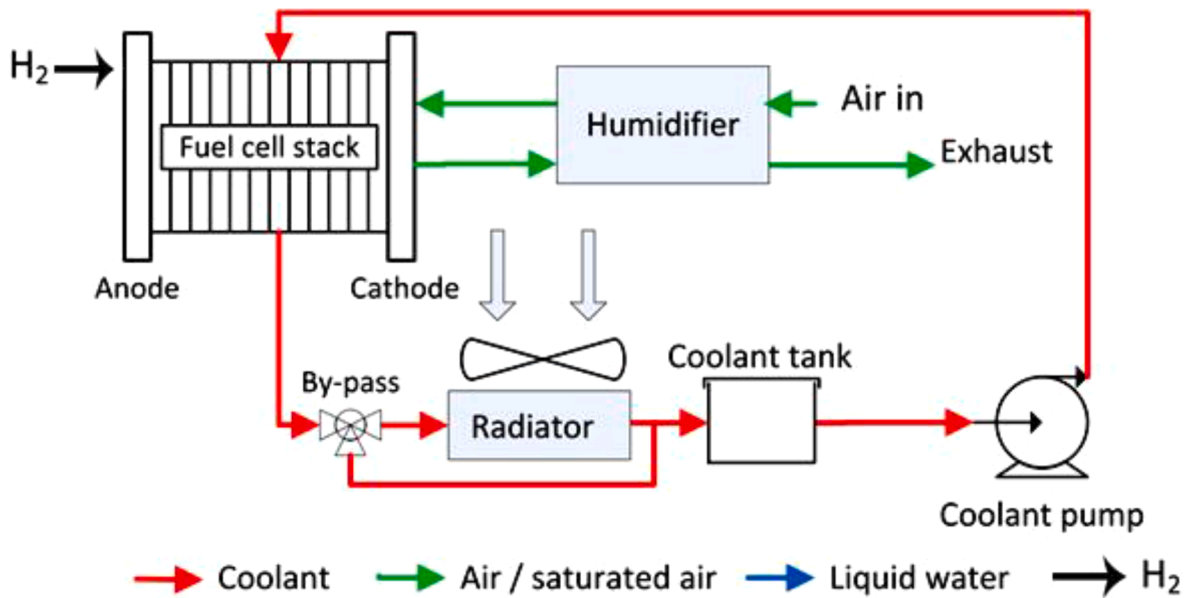


Fig. 15. A liquid cooled module designed for PEMFCs [97], the cooling system was designed for a PEMFC with the power of 60 kW.

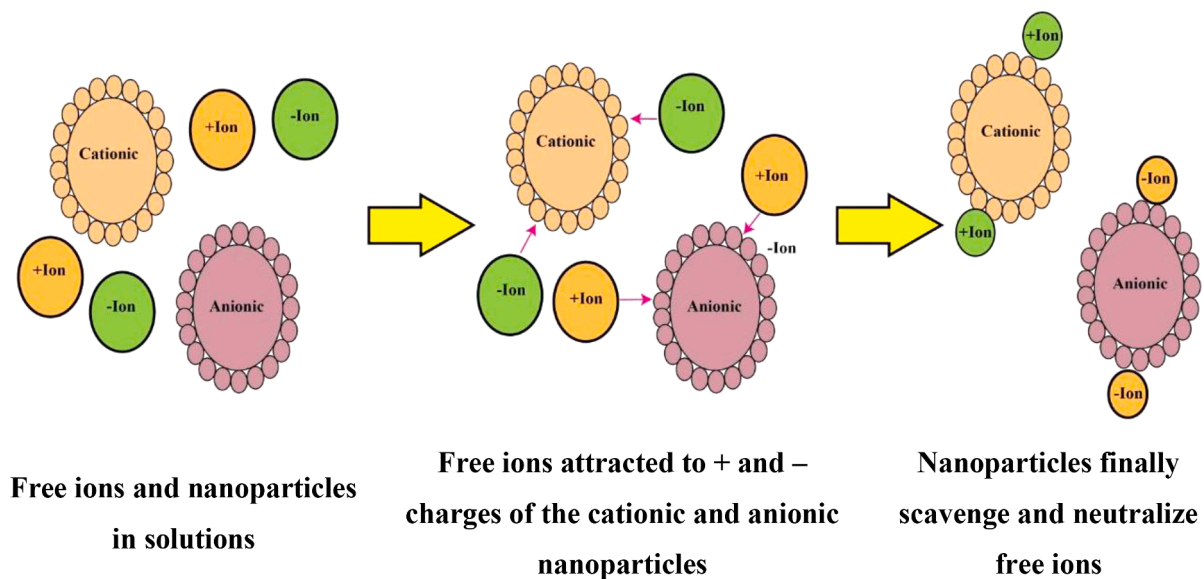


Fig. 16. Nanoparticles absorbing the ions when used as coolant in PEMFCs [79].

Choi et al. [57] further investigated the influences of coolant channel pressure on the performance of the cooling process. It was observed that the wall temperature increases in the range of 336.5 K to 344.5 K as the channel pressure increases from 1 to 1.5 bar. It is important to note that the cooling system should be controlled properly to avoid the critical heat flux. In addition, the pressure of the coolant channel should be controlled to optimize the working temperatures. At the critical heat flux, the boiling regime transits from nucleate to film boiling. The vapor film acts as a barrier between the wall and liquid, which leads to reduction of the heat flux with further increase in the temperature until the Leiden-frost point is reached. This destructive phenomenon can be avoided by supplying extra cooling liquid, finding the point in which the critical heat flux occurs and considering a proper safety factor [95].

2.1.4.1.2. Passive cooling methods. Passive cooling methods in fuel cells include the followings.

Cooling with heat spreaders

Another approach to cooling of fuel cells is the use of heat spreaders,

which act like a heat sink. Heat spreaders have high thermal conductivity and are employed near the flow channel plate (see Fig. 20). In heat spreaders, heat is firstly transferred by conduction and subsequently it is dissipated to the environment by forced or free convection. In large stacks, the use of spreaders reduces the size of the cooling system. Wen et al. [297] examined experimentally the potentials of pyrolytic graphite sheets, with high thermal conductivity, as heat spreaders in a single cell and 10-cell stack. They showed that the maximum power of the 10-cell stack can be increased up to 15% using five pyrolytic graphite sheets as the heat spreaders. To avoid high temperature gradients across the active area; the thermal conductivities of the cooling plates should be very large. Because of their large thermal conductivity and small density, graphite based materials such as pyrolytic and expanded graphite are frequently used for heat spreading in PEMFCs. In a combined passive/active technique, Wen et al. [298] used pyrolytic graphite sheets and fans for the thermal management of a PEMFC stack. The weightlessness, thinness, and large value of thermal conductivity were

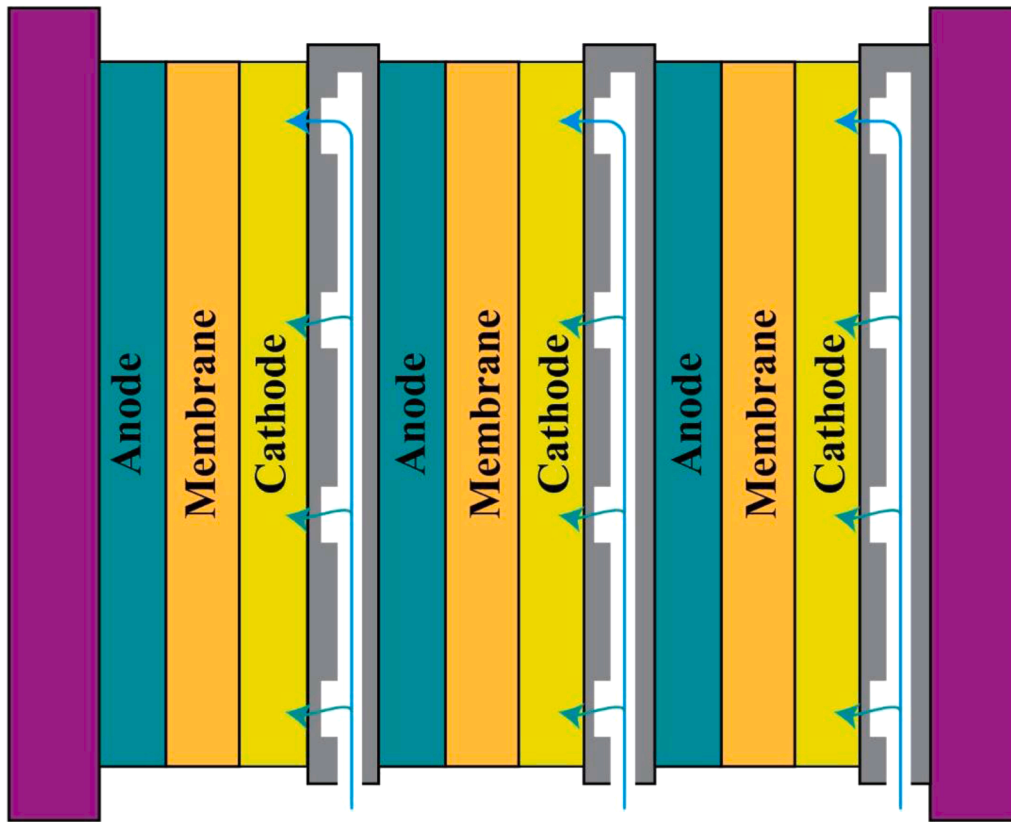


Fig. 17. Evaporatively cooled stack with cathode liquid water usage [95].

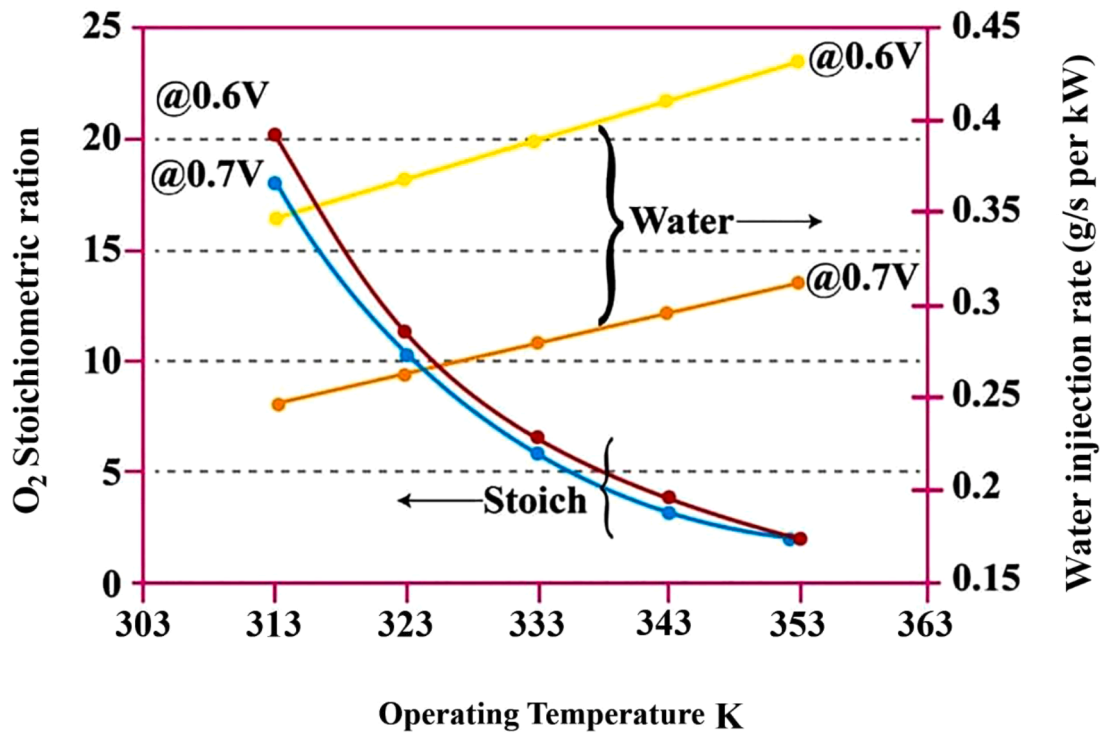


Fig. 18. The rates of water injection needed at various working conditions for the evaporative cooling of the stacks [24].

identified as the advantage of graphite sheets. Further, they reported that with the expense of higher power consumption by the fans, cooling performance of the stack improves at higher airflows.

Compared with the thermal management of low-temperature PEMFC, that with a heat spreader for high-temperature PEMFCs is simpler. Working temperatures higher than 373 K makes this thermal

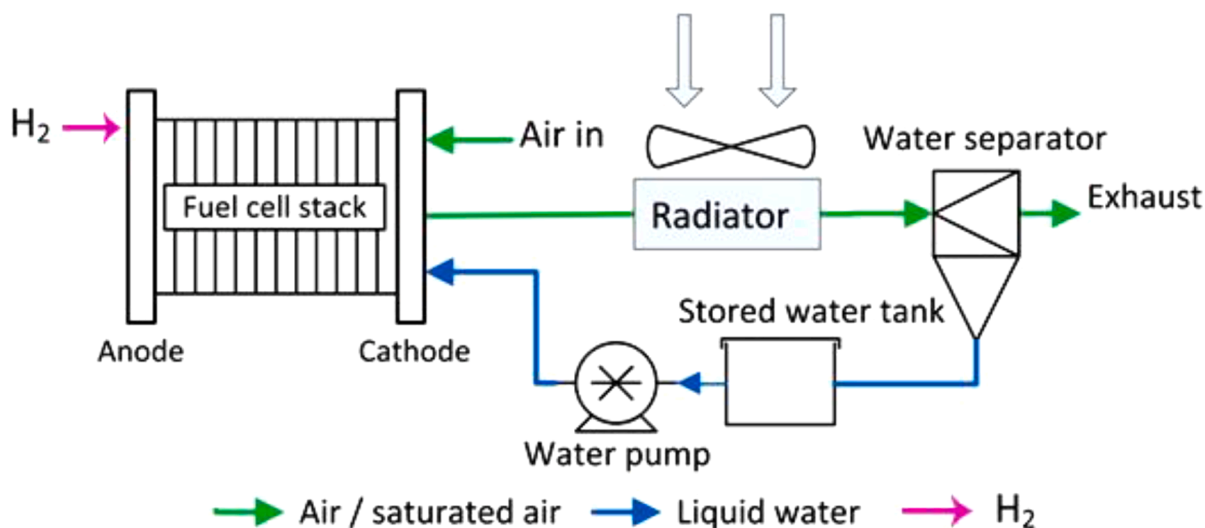


Fig. 19. An evaporatively cooled thermal management system designed for PEMFCs [97]. The cooling system was designed for a PEMFC with the power of 60 kW.

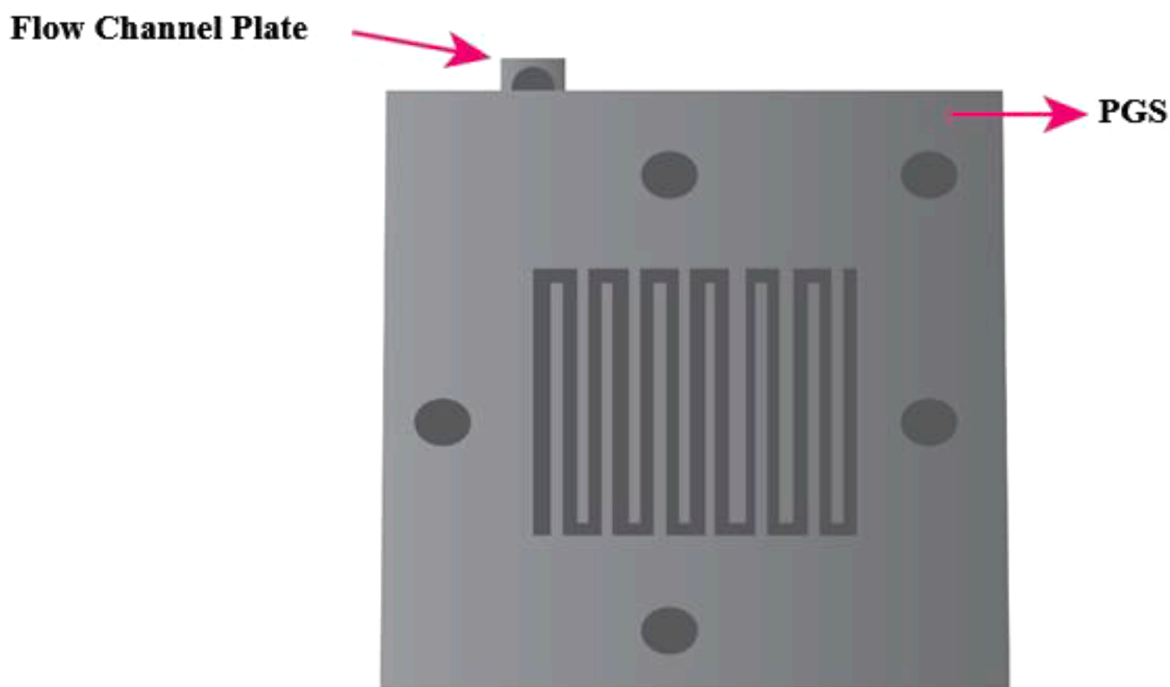


Fig. 20. Heat spreader made by pyrolytic graphite sheets aligned with the serpentine flow channel plate [296]. The cooling system was designed for a PEMFC with the power of 1 kW.

management strategy practical for PEMFCs with larger active areas [16, 251].

Recently, Tolj et al. [279] used heat spreaders to cool down a 1000 W PEMFC stack. The stack, shown in Fig. 21, included 60 cells and was cooled with air. The annotated air-coolant flow directions through the edge-cooling fins are displayed in Fig. 21 (Blue arrows). The authors concluded that the geometry of the heat spreader fin has a considerable effect on the overall temperature distributions. The maximal cell temperature drops as the guide vanes for the air flow are installed on the side plates. Therefore, the mass flow of the reactants can be quite uniformly distributed along the stack height. This leads to a relatively higher forced convection airflow rate that results in uniform temperature profile along the stack height. The highest temperature and mean temperature of the stack reduced in the ranges of 350.5 K to 336.5 K and 330.5 K to 319.5 K, respectively as the heat spreader fins were redesigned. This

clearly reflects the importance of the design of the flow distributors for heat spreading in stacks of fuel cells.

Cooling with heat pipes

Heat pipes are used widely for cooling purposes in many industries. The structure of a heat pipe can be divided into three zones of evaporator, adiabatic, and condenser on the basis of the dominant mode of heat transfer. Thanks to their great capability in heat conduction they can deliver high amount of thermal energy over a large distance with no extra power inputs [90]. Therefore, heat pipes could be used to cool down PEMFC stacks [242]. However, the design and fabrication of these devices for incorporation with PEMFCs have been a challenge. The literature confirms an acceptable performance of heat pipes in cooling of fuel cells. For example, it was reported that using a pulsating heat pipe (a kind of heat pipe with snake-shaped structure) could enhance the heat transfer rate from a PEMFC stack to the environment. In this design, the

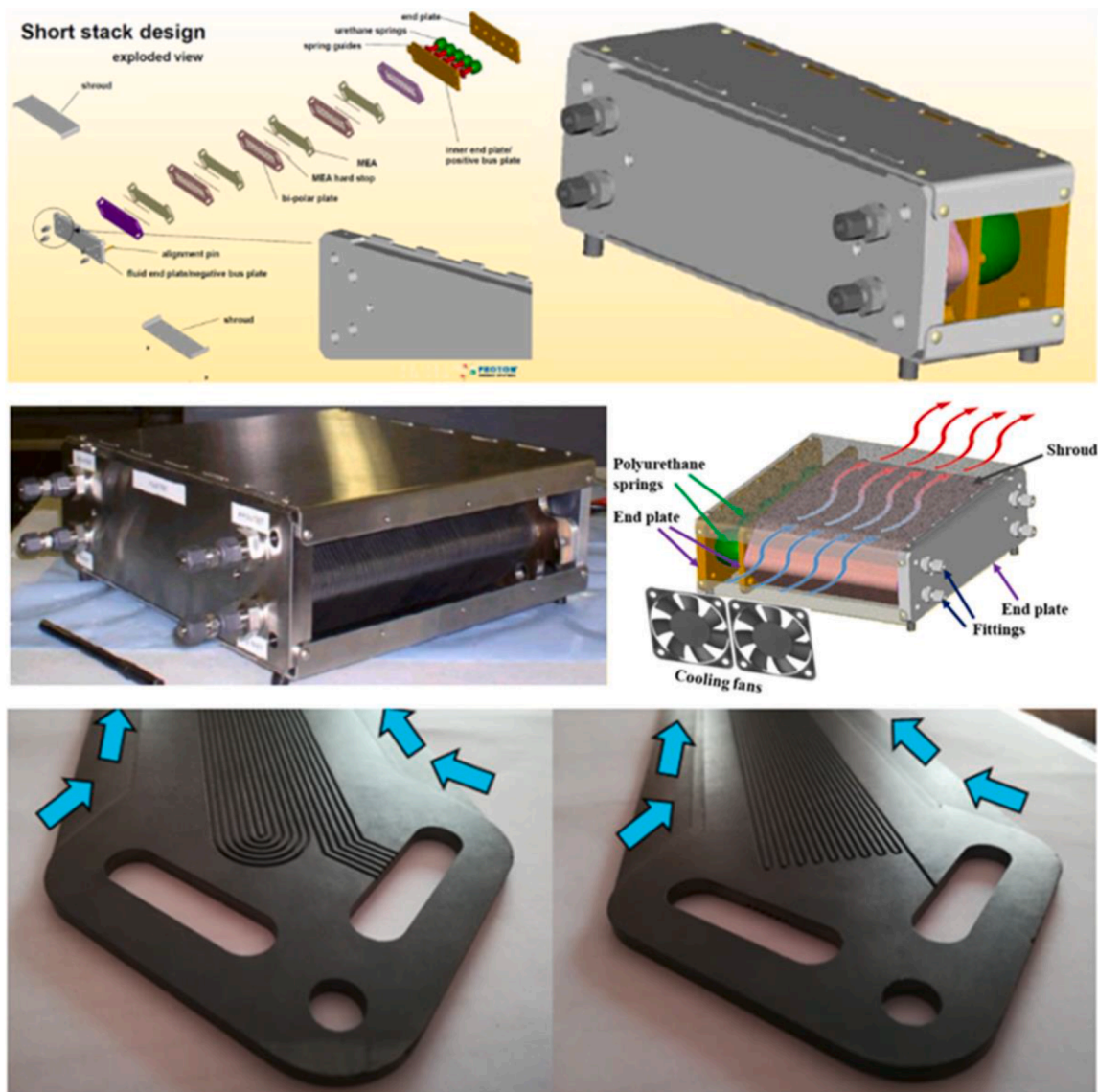


Fig. 21. The fuel cell stack investigated by Tolj et al. [279]. The cooling system was designed for a PEMFC with the power of 1 kW and an operating temperature of 333 K.

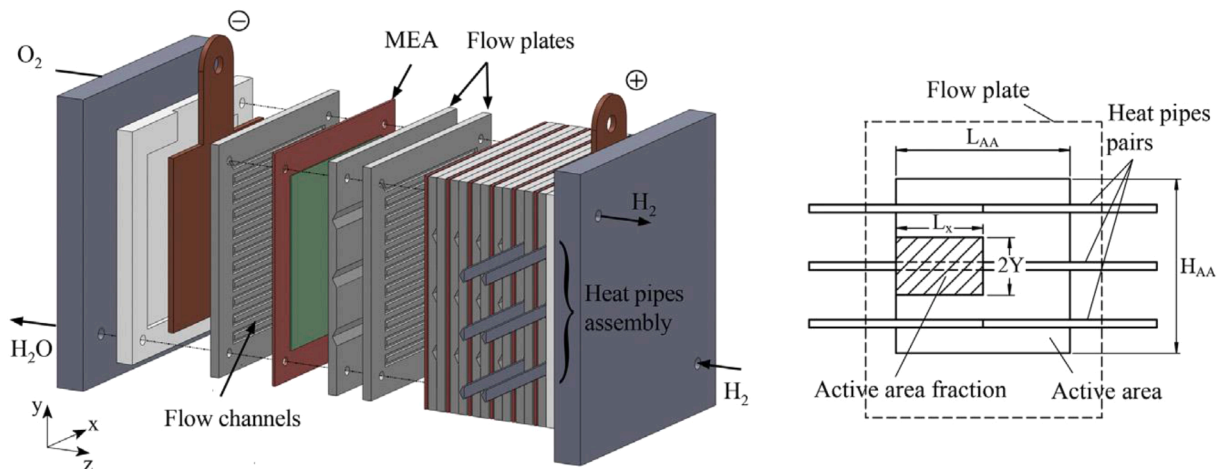


Fig. 22. Cooling system designed by Vinício Oro and Bazzo [287]. The cooling system was designed for a PEMFC with the thermal power in the range of 2 to 14 W and an operating temperature in the range of 343 K to 363 K.

evaporator part of the heat pipe is in contact with the bipolar plates and the condenser is in contact with the stack [60]. Clement and Wang [60] suggested that their pulsating heat pipe had the potential to be used in a 200 cm² fuel cell, and could provide cooling in the range of 100 to 120 W. Vinício Oro and Bazzo [287] investigated the potentials of a flat heat pipe for PEMFC cooling. The heat pipe was placed in the active area of the stack, see Fig. 22. They found that this design could successfully meet the heat dissipation and working temperature requirements of PEMFCs.

It should be noted that mini/micro heat pipes can be used as advanced thermal controllers for mini fuel cells with power generation in the range of 10 W to 100 W. Loop heat pipes, sorption heat pipes, and pulsating heat pipes can control the temperatures of portable fuel cells where the power generation exceeds 100 W [284]. Ultra-thin vapor chambers are essentially heat pipes that benefit from weightlessness, geometric flexibility, and very large thermal conductivity. Luo et al. [184] used these chambers for thermal management of PEMFCs. In this study, the bipolar plates of the fuel cell were combined with the evaporator section and the condenser section was extended out of the fuel cell. In PEMFCs, the bipolar plates supply fuel and oxidant to the membrane electrode assembly, removes water, and collects the electrons generated. This arrangement led to heat elimination by free or forced convection. Luo et al. found that employing ultra-thin vapor chambers results in uniform temperature distributions. Particularly for forced convection conditions, the lowest temperature difference on the substrate surface for the gas diffusion in the cathode could drop to 0.3 K [184].

Free cooling with cathode airflow

For smaller fuel cells, the cathode air flow can operate under free convection mode. This is the simple technique for cooling the cells and evaporating water at the cathode, conducted with the rather open structures at the cathode sides which lead to the increase of stack size. For the smaller PEMFCs, less than 100 W, free convection from air breathing is enough [255].

Cooling with other passive methods

Generally, the bipolar plates with larger thickness should be used for air or water ducts formed at the back of the bipolar plates leading to

increase in the cost of cooling system. In addition, the whole stack is pressurized to decrease the contact resistance. As a result, conduction of electricity and provision of coolant ducts by the plates is related to the applied compression force. This is restricted by other constraints, including the characteristics and properties of the materials in the fuel cells stacks.

Odabae and Hooman [213] and Odabae et al. [214] designed an effective air-cooled heat exchanger for fuel cells, which also decreases the contact and electrical resistances (See Fig. 23). Their design resulted in lowering the cost and minimizing the size of the fuel cell stack. A thin substrate of aluminum metal foam was placed between two adjacent cells. The thermal conductivity of the metal foam was up to 200 times larger than that for air and 20 times larger than that of water. The metal foam also provides excellent electrical conductivity between the cells, even in comparison with bipolar graphite plates [65], and therefore can improve the power generation. The manufacturing of the developed design is simpler as it eliminates the serpentine ducts cut on the back of the bipolar plate and replaces them with a metal foam substrate with larger values of the thermal conductivity. The use of the metal foam as heat exchanger was found to improve heat transfer rates and the uniformity of temperature distributions and, a maximum temperature difference of 6 K was reported.

Sasmito et al. [249] employed phase change materials and thermal insulator for the thermal management of PEMFC stacks under cold climate condition of sub-freezing. In cold weather conditions, the stacks of a PEMFC may experience freeze-thaw cycle operations so that they cannot work with the maximum efficiency for a long period of time. Also, the start-up may encounter some problems. The passive thermal management strategy, employed by Sasmito et al. [249], is displayed in Fig. 24. In this study, phase change materials were employed for alleviating stack from freeze-thaw cycles. In addition, the insulator was used to keep the temperature of the stack above the freezing point. The heat exchange between the stack and environment is governed by conduction and convection, at the molten state in the phase change material while the heat transfer mode in the insulator is conduction. The stack remains hot since the phase-change material acts as a heat source. Further, the insulator minimizes the heat dissipation to the ambient. Therefore, by

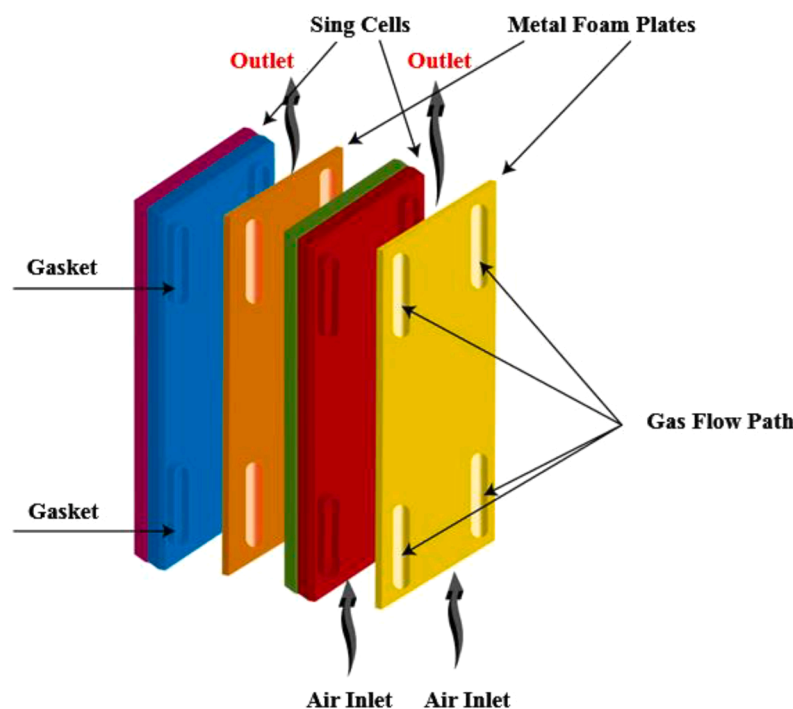


Fig. 23. The air-cooled heat exchanger designed for the fuel cells by Odabae and Hooman [213]. The cooling system was designed for a PEMFC with the thermal power in the range of 10 to 60 W and operating temperature in the range of 303 K to 363 K.

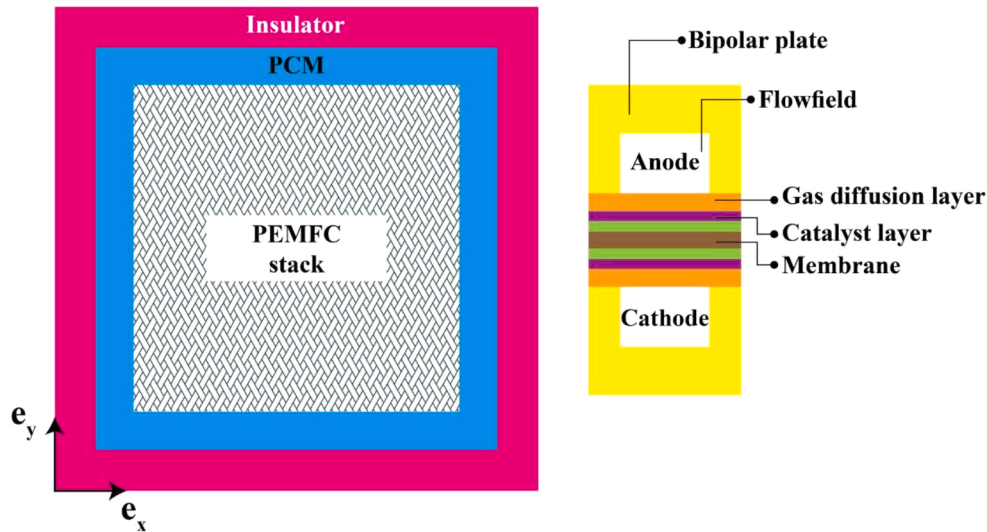


Fig. 24. Passive thermal management strategy for fuel cell in cold climate condition presented by Sasmito et al. [249]. The cooling system was designed for a PEMFC with the operating temperature of 333 K.

applying this strategy, the temperature of the stack could be kept above the freezing point for a longer time. In addition, the system becomes more compact and less power is consumed compared with other designs. The temperature of the stack would be kept above the freezing point for about two days making this design suitable for automotive applications [249].

2.1.4.1.3. *Bipolar plates for proton exchange membrane fuel cells.* Bipolar plates are important and multifunctional components of PEMFCs. Fig. 25 shows an example of a bipolar plate in PEMFC. Bipolar plates are used for uniform distribution of the gaseous fuel and air, conducting electrical current between cells, removing heat from the active area, and preventing leakage of gases and coolant [71]. The surfaces of these plates generally contain a “flow field,” that is a set of channels machined or stamped into the plate to allow gases to flow over the membrane electrode assembly. Additional channels inside each plate are employed for circulation of the coolant.

Bipolar plates have several major functions as follows [71].

- Homogeneous distribution of fuel and oxidant inside the cell.
- Facilitating thermal and water management of the unit.
- Separating individual cells inside the stack.
- Carrying electrical current away from the cell.

Bipolar plates play a key role in determining the final size, weight,

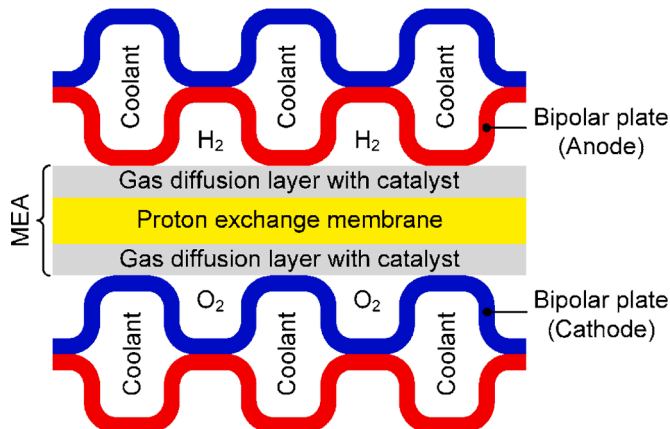


Fig. 25. Example of a bipolar plate used in PEMFC [203].

and costs of PEMFC stacks. The materials used for bipolar plates have different physical and chemical properties corresponding to the functions of the plate (see Table 4). The coefficient of thermal expansion, density, and hydrophobicity are also amongst the key physical properties of the bipolar plate material. The following properties have been recommended for the materials used in the bipolar plates [127]: Plate resistance lower than $10^{-1} \Omega \cdot \text{cm}^2$, large thermal conductivity, hydrogen/gas permeability lower than $10^{-4} \text{cm}^3 \cdot \text{s}^{-1} \cdot \text{cm}^{-2}$, corrosion rate lower than $1.6 \times 10^{-2} \text{mA} \cdot \text{cm}^{-2}$, compressive strength larger than 22 lb. in^{-2} , and density lower than $5 \text{gm} \cdot \text{cm}^{-2}$.

2.1.4.1.4. *Heat recovery options for proton exchange membrane fuel cells.* As discussed earlier, a significant amount of heat is produced during the operation of PEMFCs. Fig. 26 shows that such heat can be utilized by several combined cooling/heating and power generation technologies. Heat recovery from the PEMFCs, to supply heat and power, enhances the overall energy efficiency of PEMFCs [132, 205]. This enhanced efficiency reaches 30% to 50% for the power supply alone and up to 70% to 90% for combined heat and power (CHP) applications [206]. It has been shown that heat recovery from the stack of PEMFCs could enhance the overall efficiency of a hydrogen-based energy system to around 50% [206]. Fig. 27 shows schematically this multi-vector energy conversion and storage system wherein heat is extracted from a fuel cell, an electrolyser and a natural gas reformer.

The heat generated by PEMFCs can be used for driving sorption refrigeration cycles in combined heat and power (CCP) and, combined cooling, heating, and power (CCHP) applications. Adsorption cooling systems using vapor/solid pairs, such as water/silica gel can be integrated with a stack of PEMFCs. It is then possible to achieve an overall CCP/CCHP efficiency of about 60% to 65% [206]. Thermoelectric generator (TEG), organic Rankine cycle (ORC), and thermally regenerative electrochemical cycle (TREC) can turn the heat generated by fuel cells into power [121, 181, 336]. Combining PEMFCs with these technologies is technically conceivable. For a constant temperature of the

Table 4. The function and pertinent physical properties of bipolar plate materials [127].

Functions	Pertinent Physical properties
Distributing and managing fuel and oxidants and residual gases and liquids.	Hydrogen permeability, bubble pressure Corrosion resistance
Conducting electrical current.	Electrical conductivity
Facilitating thermal management.	Thermal conductivity
Separating the individual cells in the stack.	Compressive strength

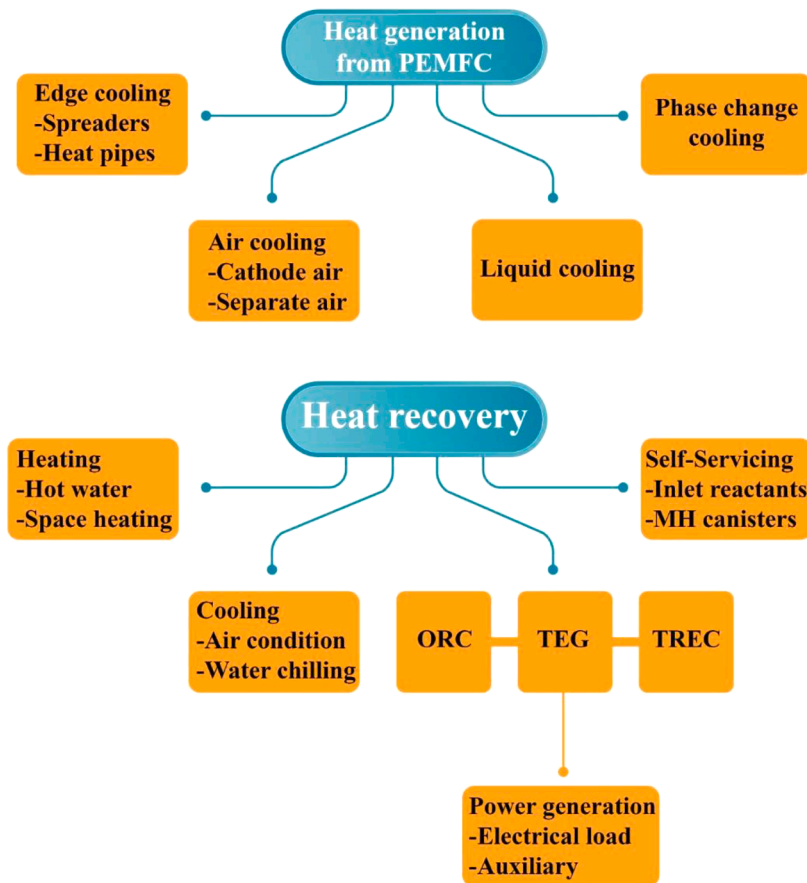


Fig. 26. Heat recovery options for PEMFCs [206].

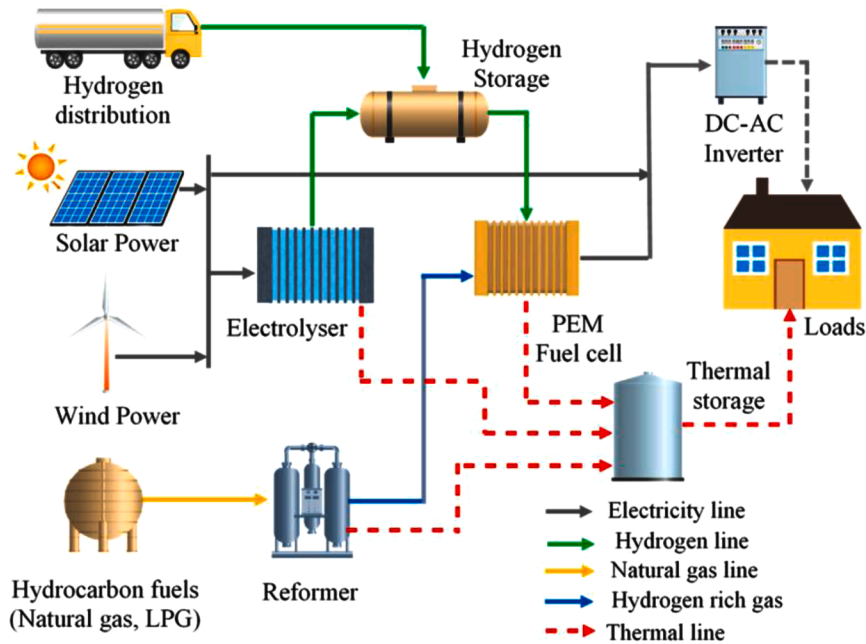


Fig. 27. A multi-vector energy system based on PEMFC [206].

heat source, integrating PEMFCs with TREC offers higher overall efficiency as compared with ORC or TEG [206]. The waste heat recovery from PEMFCs with higher operation temperatures, i.e., 393 K to 473 K, is more suitable for the usage in the power cogeneration systems in

comparison with PEMFCs with lower operating temperatures [104]. Recent investigations have shown that the waste heat captured from PEMFCs for the usage in power cogeneration improves the overall efficiency of the hybrid systems. For hybrids with TEG or ORC by about 3%

to 5% and 5% to 9% for low temperature-PEMFCs and high temperature-PEMFCs, respectively [206].

2.1.4.2. Thermal management of solid oxide fuel cells. SOFCs operate at 500 °C to 1000 °C and their thermal management faces the challenge of satisfying the high temperature reaction requirements while avoiding intense temperature gradients [89]. In addition, holding the stack temperature at a specified level is essential for achieving a suitable ion conductivity of the electrolyte [317]. Further, Laurencin et al. [165] showed that there is a strong relation between the temperature distribution and operating conditions in SOFCs. In addition, a good usage of heat is essential for achieving an effective distributed power generation, which is often the reason for employing SOFCs. Yet, poor thermal management could result in thermal stresses and efficiency decline with the subsequent shortening of the fuel cell lifetime.

Thermal management of SOFCs by heat pipes

Heat pipes have been used to control the temperature in SOFCs resulting in elimination of strong temperature gradients and the need for expensive high-efficiency catalysts [285, 326]. The planar heat pipes are integrated into the stacks of SOFCs to prevent degradation promoting hotspots and performance deterrent cold regions [76]. The concept of integrating heat pipes into SOFCs has already been successfully tested within the EU-research project BioCellus [76]. Dillig and Karl [75] reported that integrating an isothermal heat pipe into the solid oxide electrolyser/fuel cell stack considerably reduces the temperature gradients inside the cells. The extent of this reduction is related to the number of cell layers between the two heat pipe layers. Dillig [77] integrated a liquid metal heat pipe device into the planar stack structure of a SOFC (as shown in Fig. 28). As a consequence of the condensation/evaporation cycle of the liquid metal in the heat pipe, the interconnector became isothermal. Significant heat transfer in the heat pipe allows heat distribution inside the stack and an extraction of high-temperature heat from the stack. This technique can flatten the internal temperature profile of the stack and decrease the stack internal gradient in the range of 43 K to 15 K.

Zeng et al. [326] incorporated a heat pipe with liquid sodium metal into the design of a SOFC for smoothing the temperature distributions and enhancing the electrochemical efficiency. A thermally unified heat pipe/SOFC with five substrates including current-collecting, heat functional, electrolyte, cathode and anode substrates was designed (see Fig. 29). It was found that by using liquid sodium metal as the heat transfer medium, the temperature distribution in the SOFC could be

equalized. As already discussed in Section 2.2.3, this is momentous for enhancing electrochemical activities and decreasing degradation.

Thermal management of SOFCs by airflow

The flow ducts on the cathode side of the SOFCs are responsible for supplying oxygen to the cells and, can be further used to remove extra heat generated by the electrochemical reactions. This idea has been investigated in a few studies.

Tan et al. [274] used airflow alternation to control the temperature in the SOFC short stack. They found that the airflow alternation is most effective in attaining a uniform and higher cell temperature and thus, lowering dispersion of the current density. An alternate airflow parallel to the fuel flow could provide the maximum voltage performance of 0.797 V, while alternate airflow perpendicular to the fuel flows decreased the risk of local fuel depletion in comparison with crossflow stacks. As a result, proper selection of the airflow configuration inside the stacks could improve the efficiency.

Thermal management of SOFCs by using novel materials

New materials have been developed and used in different components of SOFCs to uniform the temperature distributions inside these devices. Tucker and Cheng [282] suggested a strategy to eliminate the hot spots and reduce the temperature gradients in SOFCs. They used materials with a positive temperature coefficient, which exhibit substantial changes in their electrical resistance near the desired highest cell temperatures. It should be noted that the positive temperature coefficient materials show a resistivity, which could rapidly increase when the temperature rises above the Curie temperature. This is the temperature at which a transition between the paramagnetic and ferromagnetic phases occurs [220].

Zhan et al. [327] used a metal foam as the cathode flow distributor to manage the temperature in an SOFC. They performed a comparison between the results of SOFCs with and without metal foams as displayed in Fig. 30. Their results showed that because of the significant heat conduction and uniform electron transport, uniform temperature distributions with lower values could be achieved. In addition, the metal foam with larger permeability renders better fuel cell efficiency but features higher-pressure drop.

Finally, it should be mentioned that recently, Promsen et al. [224] evaluated the cooling SOFC stacks with phase change heat transfer of saturated water. They observed that, compared to air cooling, water cooling considerably improves the temperature distribution in the stack leading to superior electrochemical performance

2.1.4.2.1. Heat recovery options for solid oxide fuel cells. As SOFCs

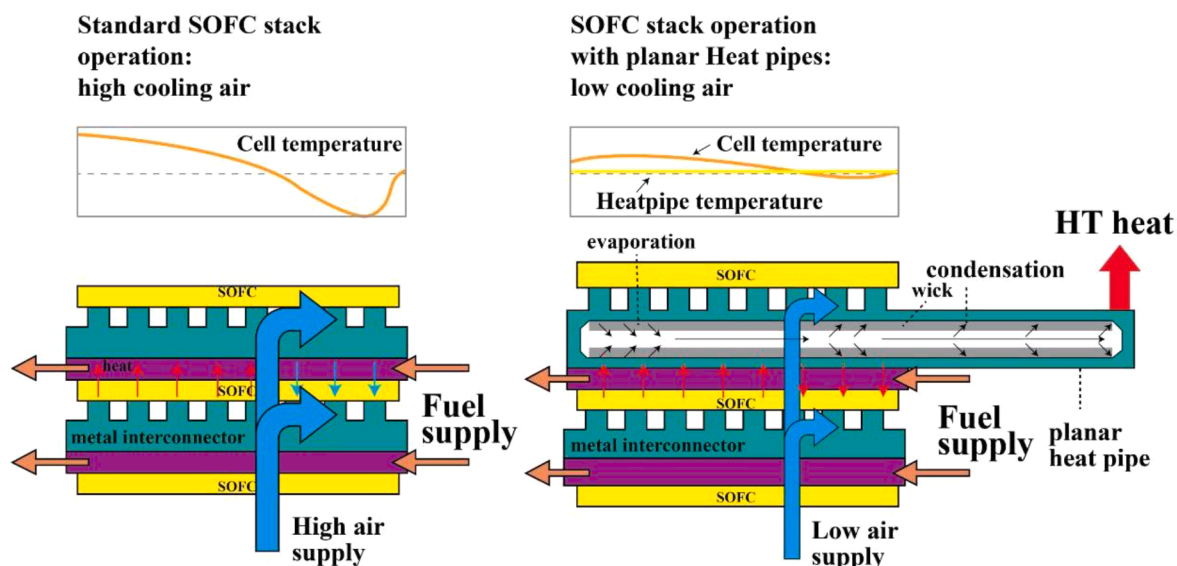


Fig. 28. Cooling system designed by Dillig [77]. The cooling system was designed for an SOFC with an operating temperature in the range of 923 K to 1143 K.

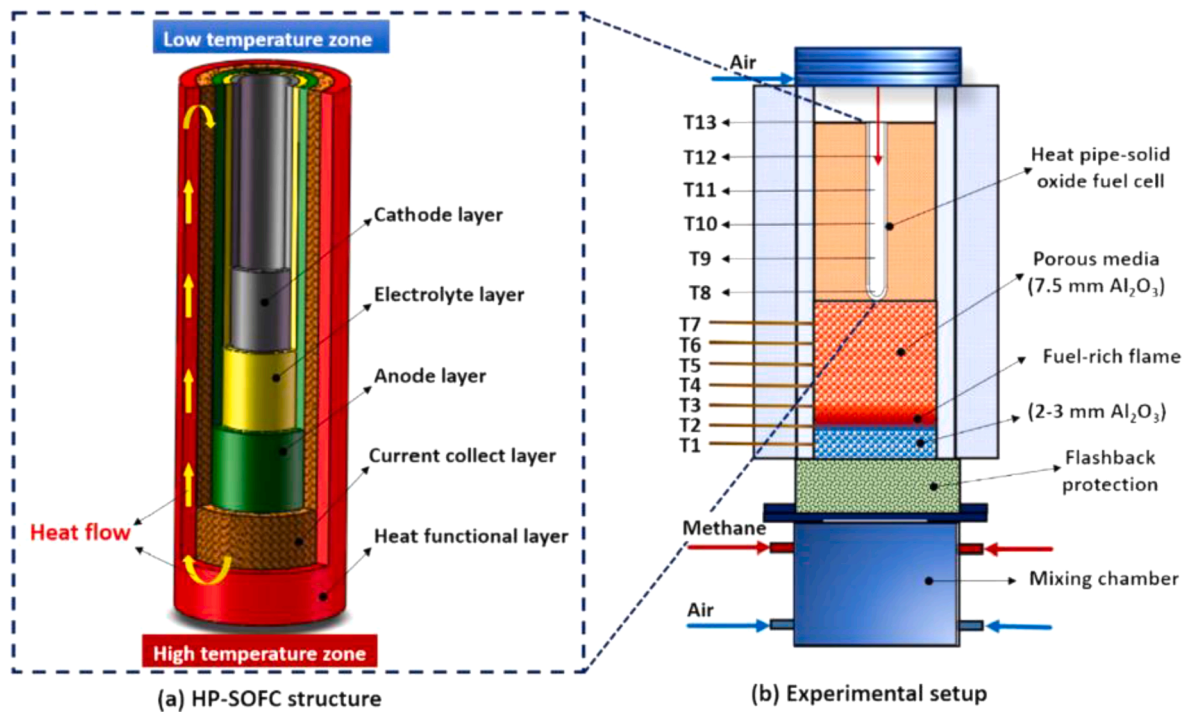


Fig. 29. A thermally unified heat pipe/SOFC designed by Zeng et al. [326]. The cooling system was designed for a SOFC with the operating temperature in the range of 1073 to 1203 K.

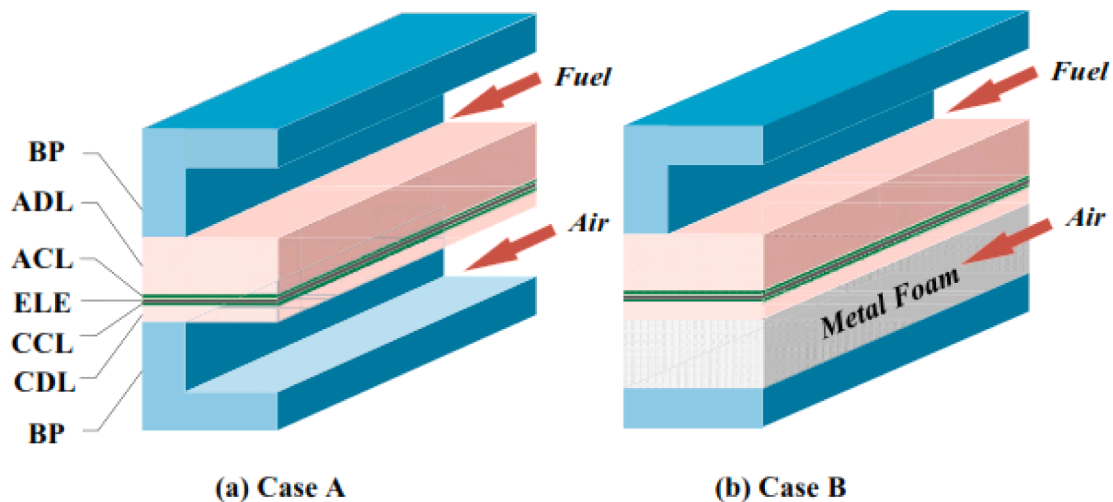


Fig. 30. SOFCs with and without metal foams considered by Zhan et al. [327]. The cooling system was designed for an SOFC with an operating temperature of 1073 K.

involve high temperatures, their waste heat could be used for fuel reforming [74]. This process includes conversion of hydrocarbons into H_2 and CO. The exhaust gas in SOFCs is very hot (around 1073 K to 1173 K) and hence can manage fuel pretreatment processes. SOFCs could be also integrated into gas turbines or micro gas turbines [174, 53]. Fig. 31 shows a schematic view of an SOFC–micro-gas turbine hybrid system. The air pressure is initially increased by the compressor, C, and then the temperature is further increased in a recuperator, RC, before being supplied to the SOFC stack. Upon expansion in the turbine, T, the exhaust gas from the SOFC is cooled in the recuperator and fuel reforming unit. Two flue gas streams, extracted from the recuperator and reforming units, are then employed for vaporization of the fuel/water mixture in the fuel vaporizer, FV. As a result, the low-temperature waste heat can be recovered. In the fuel reformer, RF, the endothermic

steam reforming occurs, and the superheater SH in which the vaporized fuel/water mixture is heated to the temperature required for reforming [61]. Generally, an SOFC combined with a gas turbine represents a combined power cycle. Unreacted fuel from a topping SOFC combusts and the heat is used by a downstream heat engine [48]. Such systems have large conversion efficiency. For example, an electrical efficiency is better than 60% and the system efficiency, including waste heat recovery for co-generation, is higher than 80% could be achieved by using an internal-reforming hybrid SOFC-gas turbine system [174]. SOFCs on their own can attain 50% net electrical efficiency and are already used in combination with multi-MW gas turbines, to attain larger efficiency for electricity generation [53, 64, 174].

2.1.4.2.2. Options to decrease the operating temperature of solid oxide fuel cells. SOFCs operate within the temperature range of 873 K to 1273

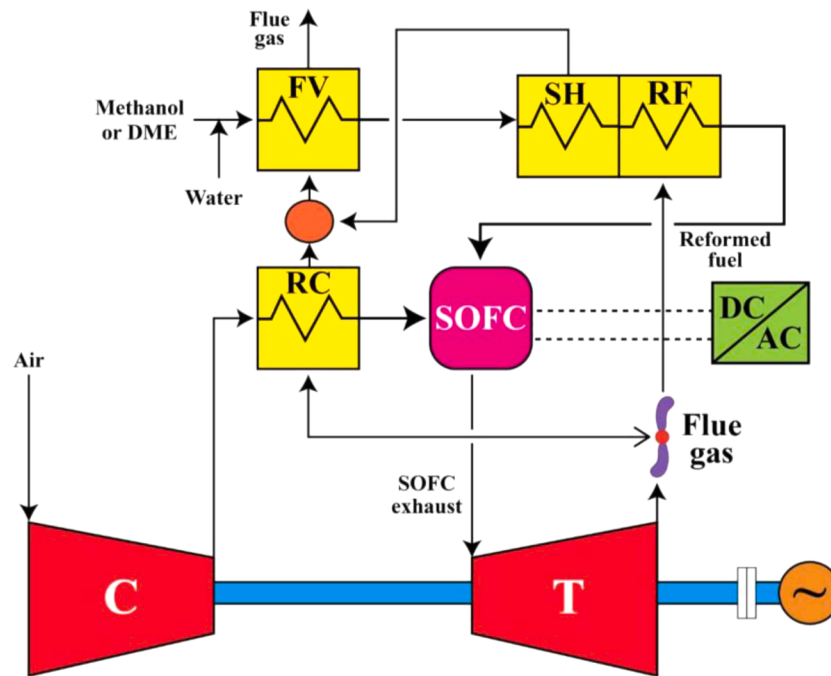


Fig. 31. A schematic view of the externally reformed SOFC–micro-gas turbine hybrid system [61].

K. This high temperature complicates the design of external reformers, piping, heat exchangers and pumps. In addition, long start up time, costly metallic interconnects and sealants and less durability of cell components [94, 216] constitute other problems. These issues hinder commercialization of SOFCs. Consequently, several efforts have been made to reduce the working temperature of SOFCs down to 673 K to 1073 K [84, 105]. There are two options to decrease the operating temperature of SOFCs, while still achieving comparable efficiency to those operating at higher temperatures. First, the thickness of the electrolyte is reduced. This leads to smaller area specific resistances of the fuel cell. Second, new materials are developed to generate a similar behavior. In this option, the ionic conductivities of the electrolytes are improved at lower temperatures. Several approaches have been taken to improve the ionic conductivity of ceria-based electrolytes for intermediate temperature-SOFCs. These approaches are manipulating ionic defects by doping or co-doping with aliovalent cations, nanocomposites, and tailoring the strain of the hetero-structure interface in the electrolyte thin film [7] while improving the performance of the electrodes [40].

It is important to note that decreasing the operating temperature of SOFCs suppresses kinetics of the electrodes and degrades the system performance. Yet, the performance of SOFCs at lower operating temperatures could be enhanced by improving the electrode materials. For example, it has been demonstrated that the nanostructure engineering of electrodes could enhance the catalytic performance [78]. This is through minimizing the electrode polarization resistance for oxygen reduction and fuel oxidation reactions at the nanoscales in comparison with the conventional electrode designs [78]. It should be noted that by decreasing the operating temperature of SOFCs, a wider range of materials become employable. This results in cheaper fabrication, particularly regarding the interconnect and balance-of-plant components. For example, low-temperature SOFCs, with operating temperature lower than 923 K, can further decrease the system costs due to the wider material options for interconnect and compressive ceramic seals/nonglass. In addition, for operating temperatures lower than 873 K, both radiative heat transfer and sintering rate are exponentially reduced. These facts decrease the insulation cost and the primary efficiency degradation mechanisms. At even lower operating temperatures,

lower than 623 K, inexpensive stamped stainless-steel interconnect, elastomeric/ polymeric seals such as Kapton, and off-the-shelf BOP can be used [291].

Another reason to decrease the operational temperatures of SOFCs is to approach the maximum theoretical efficiency. In contrast to the temperature dependence of internal combustion engines, the theoretical fuel cell performance increases as the temperature drops [291]. As an example, the maximum theoretical efficiency of an SOFC employing carbon monoxide as fuel, is increased from 63% at temperature of 1173 K to 81% for temperature of 623 K [291]. The readers are referred to the work of Kaur [161] for further information on the new materials employed within SOFCs.

Operating at lower temperatures (<623 K) also allows faster start-up and shut-down, decreased corrosion rates of metallic components, enhanced durability (sintering and component inter-diffusion are accelerated at larger values of temperature), stronger construction through the usage of compressive seals and metallic interconnects [291]. Introducing SOFCs with lower operating temperatures, in the range of 773 K to 1023 K, can open new arenas for applications in mobile, remote telecommunications, and IT applications [161]. In addition, intermediate temperature-SOFCs can be used for other important applications, including regenerative fuel cells, truck APUs, gens replacement, and power for isolated communities in developing countries. In general, the major applications of intermediate temperature-SOFCs are in the power range of sub-10 kW [161]. It has been demonstrated that the intermediate temperature-SOFCs operation with considerably low cell resistances and high-power densities under the working temperatures of 673 K to 873 K is feasible [130, 292]. There are a few commercial developers of intermediate temperature-SOFCs such as Mitsubishi Materials Corporation and Kansai Electric Power Company [259] and Ceres Power Ltd. [88]. For further information about the commercialization of intermediate temperature-SOFCs, readers are referred to [88].

2.1.4.3. Machine learning techniques to control temperature of fuel cells. Machine learning techniques such as Artificial Neural Network (ANN) could be employed as an alternative to high-fidelity modeling of complicated non-linear systems such as fuel cells. In general, machine

learning requires input training data obtained experimentally and computationally. According to the inputs, the machine learning techniques can be used to generate meaningful solutions for complex problems, see for example Mohebbi Najm Abad et al. [196] and Alizadeh et al. [10]. These techniques are also capable of producing mathematical correlations for highly complex configurations with large number of input parameters. Such correlations can be employed by fuel cell designers for optimization purposes under particular operating conditions [106].

Since the performance of fuel cells is strongly temperature dependent, it is important to dynamically control their temperature. As discussed in section 2.2.1., the cell temperature features nonlinear relationships with gas fluxes, gas temperatures, and the surrounding temperature. This makes the temperature control in fuel cells a highly cumbersome problem that is not amenable to traditional control approaches [28, 128]. ANN has been found suitable for controlling the nonlinear and intermittent problems. Dong et al. [81] designed a temperature controller for PEMFC by the oxygen, hydrogen, and water-cooling flow rates. These flow rates have distinct effects and accordingly, a divided-area controller should be used. The fuzzy logic type was used as the activation function of the neural network. The Sugeno fuzzy logic system was also applied to identify the controller. Dong et al. [81] observed very smooth flowrate control and low fluctuations during the transitional period.

Tao et al. [275] developed learning fuzzy neural networks to keep the temperature of a PEMFC by the gas flow rate. The neuron-fuzzy controller adjusts the anode and cathode flows to control the stack temperature. Controlling the temperature by the gas flow might impart some effects on the flow rates of the reactant gases. However, these effects were found negligible in this study in which the system featured low flow rates. The controller was regulated via the backpropagation algorithm and based on the residual temperature error. The suggested design was tested in the start-up simulation and the tests showed that the system could readily reach the desired temperature of 353 K with minimal fluctuations.

Li et al. [173] employed ANN to control the temperature of a low-power PEMFCs. Their results showed that this technique was superior to the traditional PID control techniques. A PID, (proportional integral derivative) controller employs the control loop feedback and is usually recognized as the most stable and accurate controller. This controller is widely used in industrial applications to control temperature, pressure, flow, speed and other process variables. Li et al. [173] used a gas heating resistance to control the temperature. The PID parameters were varied over time showing minor overshoot and good stability, yet the temperature convergence time was slow. [91] used the feedforward ANN with three layers to investigate the temperature effects of the cell and reactant gases on the voltage. These authors found that their model could predict the experimental data very well and that the best efficiency could be obtained as temperatures of the cell and reactant gases approach each other. Note that when the cell temperature is higher than that of gases, the membrane dries out and this affects considerably the proton conductivity. Further, when the cell is colder than the reactant gases, the membrane might be flooded. An extra amount of water fills up the pores and prevents access to active sites and blocks the transport of products and gaseous reactants.

A survey of literature reveals that only few adaptive neural approaches so far have been developed for the dynamic temperature control in fuel cells. The existing studies in this field indicate that the neural PID controller is an excellent control tracking for high current with relatively low over-shoots. However, for low currents, the neural-feedback can provide better performance [177].

2.1.4.4. Thermal management of other types of fuel cells. As stated earlier, the bulk of literature on fuel cell cooling is concerned with PEMFC and SOFC. Studies on the cooling of other types of fuel cell are

far less frequent. In this section, the existing studies on the thermal management of other types of fuel cells are reviewed. It is important to note that the scarcity of these studies impedes finding clear trends and making systematic conclusions. Nonetheless, an attempt is made here to present the findings of each study.

Water vaporization in the cathode for cooling:

Dohle et al. [80] investigated water vaporization in the cathode for the thermal management of a direct methanol fuel cell. They considered the operating temperature range of 333 K to 403 K for this fuel cell. Expectedly, vaporization of liquid water was more intense at higher temperatures of the fuel cell stack boosting the cooling process. In addition, the generated heat by the fuel cell could be recovered by including a heat exchanger in the anode loop. It was found that increases in the operating temperatures cause a considerable drop in the thermal efficiency due to the heat loss as a result of vaporization of water in the cathode. It should be noted that the thermal efficiency was defined as the thermally useful energy relative to the heating value of methanol. In direct methanol fuel cells, the liquid methanol can generally act as a coolant for the stack and as a result, this type of fuel cell can be effectively cooled by the liquid fuel itself [191]. This means that direct methanol fuel cells do not need any dedicated system for thermal management of stack and cooling is done without any parasitic power loss [191].

Thermal control system:

Yuan et al. [323] investigated an anode self-adaptive thermal control for the usage in the passive direct methanol fuel cells. It is noted that in such passive fuel cells, external pumps or other auxiliary equipment are not used for the supply of oxidizer and fuel. In their design, the heating unit was controlled by a single chip microcomputer and a relay that could maintain the operation of direct methanol fuel cell at the optimal temperature. It was shown that the optimal operating temperature of passive direct methanol fuel cells is 2 to 3 times larger than the room temperature in °C [323].

Usage of simulation to provide temperature maps of fuel cells for cooling system

Methanol crossover in direct methanol fuel cells is closely related to the evolution of the transient temperature as the methanol crossover rate increases with temperature and methanol concentration. The anode and cathode kinetic parameters improve with a virtual increase in temperature in direct methanol fuel cells but thermal runaway, which occurs when the amount of heat produced within a cell exceeds its heat-dissipation capacity, is greatly exacerbated by insufficient heat dissipation. As a result, a detailed theoretical investigation on the unsteady thermal behavior of direct methanol fuel cells is necessary to obtain a better understanding of these complex interactional phenomena. Such investigation helps to optimize the material and component design of direct methanol fuel cells and eventually accelerate the commercialization of direct methanol fuel cells technologies [54].

Chippa et al. [54] developed a 1D unsteady model for the direct methanol fuel cells to investigate the unsteady thermal characteristic of this type of fuel cell under different operating conditions. The results indicated that the cell performance and efficiency were highly related to the water, methanol, and heat transfer in the fuel cell. It was suggested that increasing transient cell temperatures in a fuel cell would be beneficial as it would increase mass transfer and chemical kinetics. Temperature increase could also lead to an increase in methanol crossover from the anode to the cathode, which could increase the mixed cathode overpotential, ultimately reducing the fuel cell's efficiency. High concentration of methanol-feed and/or low external heat transfer coefficient in the direct methanol fuel cell, could lead to thermal runaway phenomenon. This is a situation in which increasing the cell temperature increases the rate of methanol crossover which then leads to further temperature elevation and damages the fuel cell. As a result, the model shows the necessity of an efficient cooling module for stabilization of cell operation and improving cell performance. The cooling module is more necessary at higher concentration of methanol in

portable applications of direct methanol fuel cells.

Bosio et al. [39] focused on the thermal management of the molten carbonate fuel cell. This type of fuel cell operates at the temperature range of 925 to 955 K. The input anodic and cathodic gas with the temperature of about 855 K is required for good ionic conduction in the cells. In addition, a maximum local temperature larger than 960 K must be avoided as the higher temperature may lead to electrolyte evaporation and corrosion [233]. The first issue is manageable, while resolving the second one requires providing many local measurements or, more properly, reliable detailed simulations [39]. Bosio et al. [39] used the SIMFC (Simulation of Fuel Cells) to calculate the temperature distribution on the cell plane of a molten carbonate fuel cell. They found that the temperature map of the plane could be very irregular and that some sections of the cell might operate under critical conditions. This could happen even if the mean temperature was not too high. Various methods can be applied to achieve a more uniform temperature distribution on the cell plane. It was shown that the fluid-dynamics of cathodic and anodic gases on the cell plane could dominate the cooling process [273].

Usage of double pipe heat exchanger design

Ariyanfar et al. [18] used double pipe heat exchangers to cool down the alkaline fuel cells. In general, the electrolyte has a cooling role in this type fuel cell. In their employed heat exchanger, the electrolyte and water were the hot and cold fluids and flowed through the inner and outer pipes, respectively. Their results showed that decreasing the electrolyte temperature from 343 to 313 K leads to about 2% improvement in the overall efficiency of fuel cell.

Usage of separator

Kim et al. [153] performed a numerical study to investigate the potentials of a separator for controlling the stack temperature in the molten carbonate fuel cell. A separator with three flow paths was used to control the stack temperature while keeping a high cell potential. This included two flow paths for the electrodes and one path at the center of the separator for the flow of nitrogen for cooling. It was found that the separator could control the stack temperature of a co-flow stack with an external reformer under atmospheric pressure.

Heat recovery option

Ishizawa et al. [133] designed an efficient heat recovery module for phosphoric acid fuel cells. In their design, a shell-and-tube heat exchanger and a direct-contact cooler were used to recover high-temperature heat and water efficiently. The reformer and cathode exhaust gases were firstly supplied to the heat exchanger and then to the cooler. The high temperature heat in the range of 333 to 358 K was recovered, and the heat recovered from the coolant was utilized in a dual-heat-input absorption refrigerator. The water required to operate the fuel cell was also recovered from the exhaust gases. Wu et al. [305] used the thermoelectric generator and the thermoelectric cooler to recover the waste heat of a phosphoric acid fuel cell. Combining thermoelectric generator and the thermoelectric cooler allows recovering the waste heat to be then used for cooling generation. Wu et al. concluded that the efficiency and power density of the hybrid system increase by about 2.8% and 2.3% compared with a stand-alone phosphoric acid fuel cell. Zhang et al. [330] used an absorption refrigerator to recover the waste heat generated by a molten carbonate fuel cell. It was shown that, compared to single molten carbonate fuel cell, hybridization improved the maximum power density and efficiency by 3.2% and 3.8%, respectively. Abdollahipour and Syyaadi [3] used regenerative electrochemical cycles for heat recovery from molten carbonate fuel cell and extra power generation. They showed that the higher operating temperatures of the fuel cell could improve the power output and efficiency of the hybrid system.

3. Electrolysers

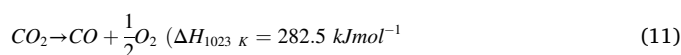
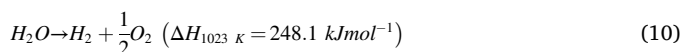
Electrolysers employ electrical energy to electrochemically decompose a substance, e.g. water into oxygen and hydrogen. By using water electrolysers, ultra-pure hydrogen is produced in a carbon free process

when the electricity is provided by renewable energy sources. The produced 'green hydrogen' can be subsequently converted back to electricity in fuel cells, or be mixed with natural gas to produce a low-carbon fuel blend for heat and power generation [86]. Production of green hydrogen is a rapidly growing application of electrolysers [204], as there are active plans for the partial and eventually total replacement of natural gas with hydrogen [86]. Often electrolysers consume the surplus of the renewable power to produce hydrogen as a means of resolving the inherent intermittency issue of the renewables. In this context, electrolysers are effectively energy storage devices that store electricity in the form of an energetic molecule (hydrogen) [150]. It follows that the performance of electrolysers directly affects the efficiency of the energy storage and is therefore of high significance.

The operating parameters of electrolysers including temperature and pressure vary from one type to another. Polymer electrolyte membrane and alkaline electrolysers operate at moderate temperatures lower than 353 K and 493 K, respectively. However, the solid oxide electrolysers operate at higher temperatures, larger than 873 K. The key operating parameters and efficiencies for all types of electrolysers are summarized in Table 5.

3.1. Basic thermodynamics of water and carbon dioxide electrolysis

Both carbon dioxide and water electrolysis are highly endothermic processes and require 3.50 and 3.07 kWh of heat per Nm³ of carbon dioxide and hydrogen, respectively, at 1023 K.



The enthalpy of these reactions is quite weakly temperature dependent. According to Gibbs relation

$$\Delta H = \Delta G + T \times \Delta S, \quad (12)$$

where ΔG is the Gibbs free energy change that should be supplied in the form of electrical energy. The entropic part, $T \times \Delta S$, should be provided as thermal energy (Bøgild [34]). ΔS has a positive value for both reactions emphasizing the fact that the reactions do not occur spontaneously. Fig. 28 displays the energy demands for water and carbon dioxide electrolysis. Evidently, the electrical energy demand or ΔG decreases as the temperature increases. For example, at a temperature of 353 K, ΔG is 93% of ΔH . However, at a temperature of 1023 K, it drops to 77% of ΔH (Bøgild [34]). The required heat in electrolysers can be supplied by external sources, including nuclear reactors, solar thermal systems, and exothermic chemical reactions in stacks of SOECs. In addition, in a simple process, heat is supplied by Joule heating due to the loss mechanisms in the stacks of electrolyser. These loss mechanisms are normally lumped together in the so-called 'area specific resistance', ASR, which consists of ohmic resistances and activation over-potentials at both anode and cathode. The activation over-potentials include two parts: over-potential of kinetic activation energy and over-potential by mass transport limitation (Bøgild [34]). As shown in Fig. 32, at high temperatures, a considerable part of the heat needed for the electrolysis process is supplied by the system itself [137]. This provides an opportunity to utilize the heat inevitably generated by the passage of electrical current through the cells, and to reduce the overall electricity consumption and cost of hydrogen generation. In fact, part of the energy required for the dissociation of water is now supplied in the form of heat. As a result, from the thermodynamics viewpoint, electrolysis can be enhanced by operating at higher temperatures [137].

There are high temperature-PEMEs, operating at about 433 K. In comparison with low temperature-PEMEs, the electrical energy demand of the high temperature-PEMEs is smaller as a portion of the energy input is in the form of heat. This makes high temperature-PEMEs

Table 5

The main type of electrolyzers with their characteristics and common operating conditions [103, 168, 199].

Electrolyzers	Working temperature	Working pressure	Cathode gas	Electrolyte/ membrane	Anode gas	Hydrogen generation Efficiency
PEM	313 K to 323 K	Lower than 30 bar	Hydrogen	Nafion® H^+ /Polymer Electrolyte Membrane	Oxygen, water	50 to 70%
Alkaline	338 K to 493 K	Lower than 30 bar	Hydrogen, steam	OH^- /KOH Electrolyte	Oxygen, water	65 to 75%
Solid Oxide	873 K to 1273 K	Lower than 10 bar	Hydrogen, steam	O^{2-} /ZrO ₂ , La _{0.5} Sr _{0.2} Ga _{0.5} Mg _{0.2} O ₃	Oxygen	70 to 90%

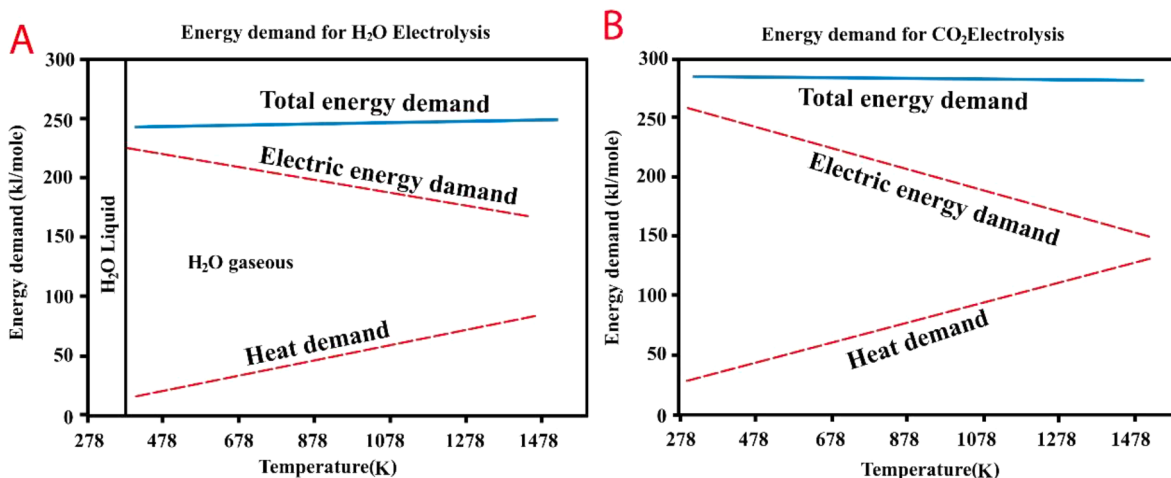


Fig. 32. Energy demands for water and carbon dioxide electrolysis at high temperature [137].

suitable for utilization of industrial waste heat. SOEs often operate at around 1073 K and therefore require very high-grade waste heat that limits their application for waste heat utilization [141]. The capability of high temperature-PEMEs to use a wider range of waste heat, has turned them into a promising technology for hydrogen generation. This is particularly the case, when they are driven by nuclear, wind or solar power [141].

3.2. Electrical, transport, and reaction resistances in electrolyzers

The efficiency of electrolyzers depends strongly on their resistances. Generally, the resistances in electrolyzers could be categorized into three groups related to electrical, transport, and reactions. Electrical and transport resistances lead to heat production based on Joule's law and transport phenomena. Energy losses due to these resistances are known as the Ohmic losses [31, 215].

3.2.1. Electrical resistance

In electrolyzers, the electrical resistance is directly responsible for heat generation that results in the dissipation of electrical energy to heat. Electrical resistance in a water electrolysis module features the following three basic parts [325]:

- The resistance within the system circuit.
- The mass transfer phenomenon such as ions exchange in the electrolyte.
- The gas bubbles, which cover the surface of the electrode and diaphragms.

With the progress of the electrolysis, O₂ and H₂ bubbles appear on the surfaces of the anode and cathode, respectively. These bubbles detach from the surfaces when they are big enough. Coverage of the electrode surface by the gas bubble can directly increase the electrical resistances of the whole module. This is by reducing the connection of

the electrolyte and the electrodes, preventing the electron transport, and boosting the ohmic losses of the whole module. It should be noted that the resistances of electrodes and connection circuit are specified by the types and sizes of the materials, manufacturing techniques, and the conductivity of the individual components [325].

3.2.2. Transport resistance

Convective transport has a critical role in the transfer of ions, heat wastage, temperature distribution, and characteristics of gas bubbles within the electrolyte. Viscosity of the fluid and flow fields around the electrolyte dominates the ion transfer process, temperature distributions and the bubble size. Further, detachment of bubbles and increasing velocity affect the current and potential distributions in the cells. With the progress of the electrolysis, electrolyte concentration increases and fluid viscosity rises [325].

3.2.3. Electrochemical reaction resistance

In anodes and cathodes, the reaction resistance results from overpotentials required to overcome the activation energies of electrons forming on the surface of oxygen and hydrogen. This leads to an increase in the overall potential of the cell. These are the intrinsic energy barricades of the reactions, which determine the kinetics of the electrochemical reactions [25]. Reaction resistance or overpotential is the intrinsic resistance of the electrochemical reaction related to the surface activity of the electrodes [182]. Clearly, the strategies in any effort to enhance the energy efficiency of electrolyzers should involve minimization of these resistances.

3.3. Temperature effects on the efficiency of electrolyzers

Temperature strongly influences the efficiency of the electrolysis cells. Electrolysis is more efficient at higher temperatures [209]. Thermodynamics of a water molecule indicate that as temperature increases, the splitting reaction potentials decline. Further, ionic conductivities

and surface reactions of electrolytes increase at higher temperatures [283]. Water electrolysis at higher temperatures requires less energy to achieve any given current density as compared with the low-temperature electrolytic processes [33, 269].

Alkaline water electrolysis [325], solid oxide electrolysis [208], microbial electrolysis cells [144], and polymer electrolyte membrane water electrolysis [98] are the existing electrolysis technologies for hydrogen generation. Fig. 33 displays the effects of temperature on the cell potentials to generate hydrogen by water electrolysis [33, 288]. The map of cell potential temperature consists of three areas, separated by equilibrium voltage and thermo-neutral voltage lines. The equilibrium voltage represents the theoretically lowest potential that is needed for dissociation of water by electrolysis. The equilibrium voltage drops as the temperature increases. The thermo-neutral voltage is the real lowest voltage, which should be applied to the electrolysis cells. Above this line the electrolysis is exothermic and below that, it is endothermic. The thermo-neutral voltage consists of the over potential of the electrodes that are weakly related to temperature. As a result, the thermo-neutral voltage only increases slightly with temperature. In Fig. 33, if water electrolysis occurs in the shaded area, the reaction is endothermic [325].

In a numerical study, Kai et al. [145] investigated the influence of temperature on the performance of polymer electrolyte membrane water electrolyzers (PEMWE). It was found that operation at high temperatures, particularly at those higher than the saturation temperature, reduces the saturated liquid leading to shortage of water and an increase in the over-voltages. Boosting the temperature with pressurization monotonically decreases the anode activation overvoltage. For example, increasing the temperature in the range of 373 K to 393 K and boosting the pressure in the range of 0.13 MPa to 0.22 MPa leads to decrease in the electrolysis voltage from 1.57 V to 1.51 V. It should be noted that operation at high temperatures can improve the economy of PEMWEs. Increasing the operational temperatures activates electrochemical reactions in PEMWEs and reduces the electrolysis voltage, facilitating high current density with a smaller electrode area [311].

3.4. Thermal management of electrolyzers

Coupling of electrolyser with electricity sources implies large load gradients and changes in the rates of internal heat generation/consumption, leading to changes in the temperature profiles of the stack [75]. This causes thermal stress in the ceramic cell and induces micro-cracking with a subsequent decrease in the cell lifetime [75].

Hence, the theoretically rapid adaption to electrical load in electrolyzers is strongly limited by inertial thermal adaptation of the cells and stacks [45]. It is, therefore, essential to develop temperature management strategies to combine electrolyzers and electric power sources.

3.4.1. Low temperature electrolyzers and their thermal management

Low temperature electrolyzers, such as PEMs and alkaline electrolyzers, require constant cooling to keep the stack within a desirable temperature range under all feasible conditions. Temperature in small-scale electrolyzers is usually controlled externally, while the temperature of large-scale electrolyzers designed for industrial applications should be internally managed. This is because of the extensive cell surface area (about 1000 cm²) in industrial electrolyzers compared to that of small-scale electrolyzers (lower than 100 cm²) [278].

In this review, among low temperature electrolyzers, it is mainly focused on PEM electrolyzers. It is expected that PEM electrolyzers will continue to operate at a higher current density in the near future than alkaline technology. The latter, however, has remained stagnant. Having a high current density also indicates heat accumulation, which implies that there is more load on the cooling system. Therefore, current density is a critical parameter in the analysis of low temperature electrolyzers where cooling and heat recovery happen. It is shown that a cooling solution for PEM electrolyzers may be easier to adapt to an alkaline electrolyser than the other way around [278].

Usually, two techniques are employed for internal thermal management of electrolyzers. The temperature of electrolyzers can be either controlled by the surplus of process water or by the cooling fluid running in a separate circuit. A combination of the two methods is also feasible and is useful for sharing the load when cooling is the sole purpose. Nonetheless, for reusing the heat in other processes, it is essential to control the heat in closed circuits. Thus, in this case, it is better to use only one technique [278].

3.4.1.1. Surplus flow of the process water. The main benefit of controlling the temperature with the surplus of process water is the considerable rate of heat transfer between cell and water. In this case, the current collectors and electrodes are perforated to retain the membrane moist and to enhance reaction kinetics by providing a large contact area. Accordingly, this method offers the advantage of highly efficient transport of heat. The major drawback is the risk of pollution. A system cooled by process water would need large circulations of demineralized water. Consider a system fully relying on process water cooling. The

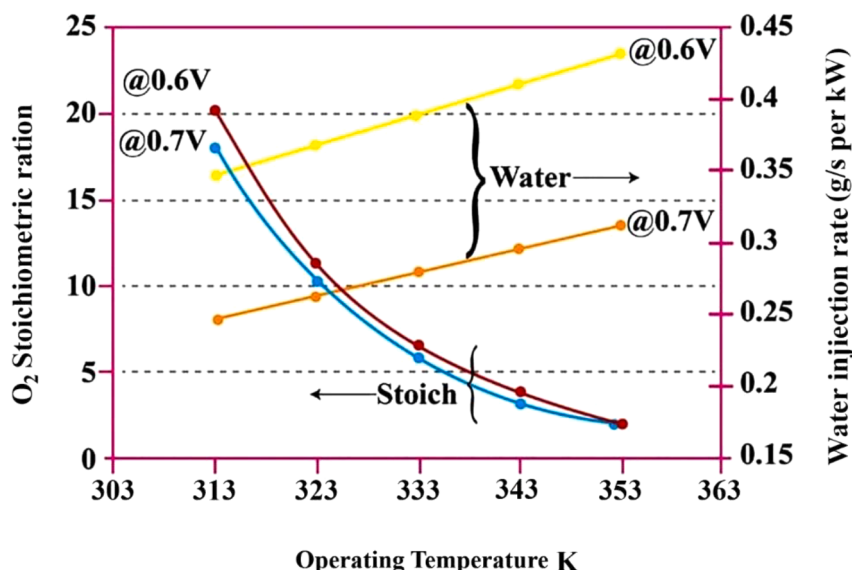


Fig. 33. The effects of temperature on the cell potentials for generation of hydrogen by water electrolysis [325].

following equation shows the molar-based flow of cooling water needed for each mole of water consumed [286]:

$$\sigma_{H_2O} = \frac{2F}{M_{H_2O} C_{P,H_2O} \Delta T} (U_{cell} - U_m) \quad (13)$$

where M_{H_2O} and C_{P,H_2O} are the molar mass and specific heat of water, respectively. ΔT denotes the desired temperature difference between the inlet and outlet. Further, U_{cell} and U_m demonstrate the cell voltage and the thermoneutral voltage under the operating conditions, respectively. The flow rate has an inverse relation with the temperature difference, ΔT , between the outlet and inlet of the cells of electrolyser. There exist a few reasons for minimization of ΔT . Villagra and Mille [286] reported that the degradation and aging rate increase with increasing temperature gradients across the cells. In addition, several cell characteristics such as activation overpotential or ohmic resistance are temperature dependent. Hence, strong temperature gradients within the cells ($\Delta T > 10$ K) lead to heterogeneous loading of the cell, which adversely affects the efficiency. As an example, $\Delta T = 10$ K for the electrolyser operating at the cell voltage of $U_{cell} = 1.9$ V leads to a feed factor of $\sigma_{H_2O} \sim 105$. This means that for each mole of water used by the cells, 105 mol of cooling water is required. In addition to the possible issues concerning pressure drop, a large feed factor intensifies the hazard of pollution. From the process water leaving the electrolyser, heat can be captured prior to recycling it back into the cell. On average, a water molecule is circulated 105 times before splitting into oxygen and hydrogen. It is, finally, noted that this cooling method might introduce major practical difficulties, as demineralized water is a powerful solvent for many materials used in the system.

3.4.1.2. Separate cooling circuit. There are no pollution concerns with the separate cooling systems. This cooling method stretches the range of design parameters because it does not interfere directly with the cells. However, some extra ducts are required for cooling of the fluid somewhere in the stack. This type of ducts can be placed in the bipolar plates separating the cells. However, since electrolysers are already quite compact, there is a limited space for cooling ducts. This renders the separate cooling circuits more applicable to fuel cells [278]. Two structured thin plates are combined into a bipolar plate to manufacture ducts for distribution of the flow over the outer surface and internal cooling ducts (See Fig. 34).

3.4.1.3. Bipolar plates and channels. There exist several methods for designing an integrated cooling system for electrolysers. Firstly, the plates are connected to the cells inside the stack in series to ensure that the cooling ducts inside the plate do not occupy a large volume. This causes an increase in the ohmic resistance of the bipolar plates and hence, the stack efficiency drops. In addition, the flow distribution of the process water and produced gases are managed by the bipolar plates. The precise shape of the ducts for distribution of the flow is distinctive for each electrolyser and is directly related to the design factors such as size of the system, operating temperature, number of cells, cathode and anode pressures and the load range. The design details for the cooling networks are protected by the designers and a standard large-scale design can be hardly found in open literature. Tiktak [278] designed a cooling system for the medium to large-scale polymer electrolyte membrane based electrolysers. Fig. 35 shows the schematic view of the proposed cooling system. The thickness of each substrate and the size of the ducts were selected according to the data available in the literature [167, 185].

3.4.2. High temperature electrolysers and their thermal management

High temperature electrolysers operate at the temperature in the range of 500 and 900 °C [85]. In general, the performance of electrolysers can be enhanced by operating at high temperature. This reduces the electricity consumption but demands a heat input and calls for

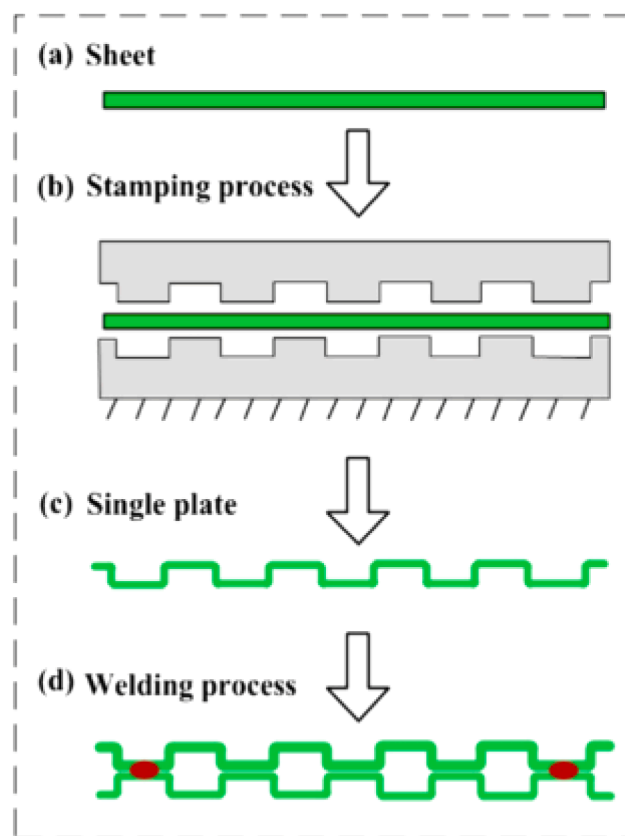


Fig. 34. Simple manufacturing for bipolar plates equipped with ducts for cooling and distribution of flow in the cathode and the anode chamber [227].

recovering of the waste heat from the products of electrolysis. As discussed earlier, some of the energy needed for water splitting can be supplied by heat instead of electricity, thus decreasing the overall electrical energy consumption. Heat can be supplied by coupling the electrolyser with high temperature reactors or renewable sources of heat such as geothermal energy. Provision of heat to electrolysis by a geothermal source is often much more economic than that by high temperature reactors [186]. Nonetheless, operation at high temperatures adversely affects the materials durability owing to micro-structural defects, thermal stresses and chromium migration.

Based on the energy balance at the electrolyser level, there exist three operational modes for high temperature electrolysers. These include endothermal, isothermal, and exothermal modes. Under the endothermal mode, the steam temperature drops from the input of the electrolyser to the output. This mode offers the best energy efficiency yet features the highest generation cost as endothermal electrolysers are much more expensive than exothermal ones. Under the isothermal mode, the steam temperatures the input and output are the same. The energy efficiency is superior to that of the exothermal mode. However, the electrolyser cost is so high that outweighs the improved efficiency [186]. Finally, under the exothermal mode, the steam temperature increases from the input to the output of the electrolyser. This mode has the poorest energy efficiency amongst all categories, but offers the cheapest generation as its investment costs are the lowest of the three categories [260]. Central to improving the efficiency of high temperature electrolysers is the recuperation of heat at the system outlet by heat exchangers. Stainless steel heat exchangers can be used at medium temperatures (<650 °C), while nickel based heat exchangers are suitable for high temperatures (between 650 °C to 850 °C). Finally, ceramic based heat exchangers can be used for very high temperatures (>850 °C) [260].

The electrolysis reaction itself is an endothermic reaction [222].

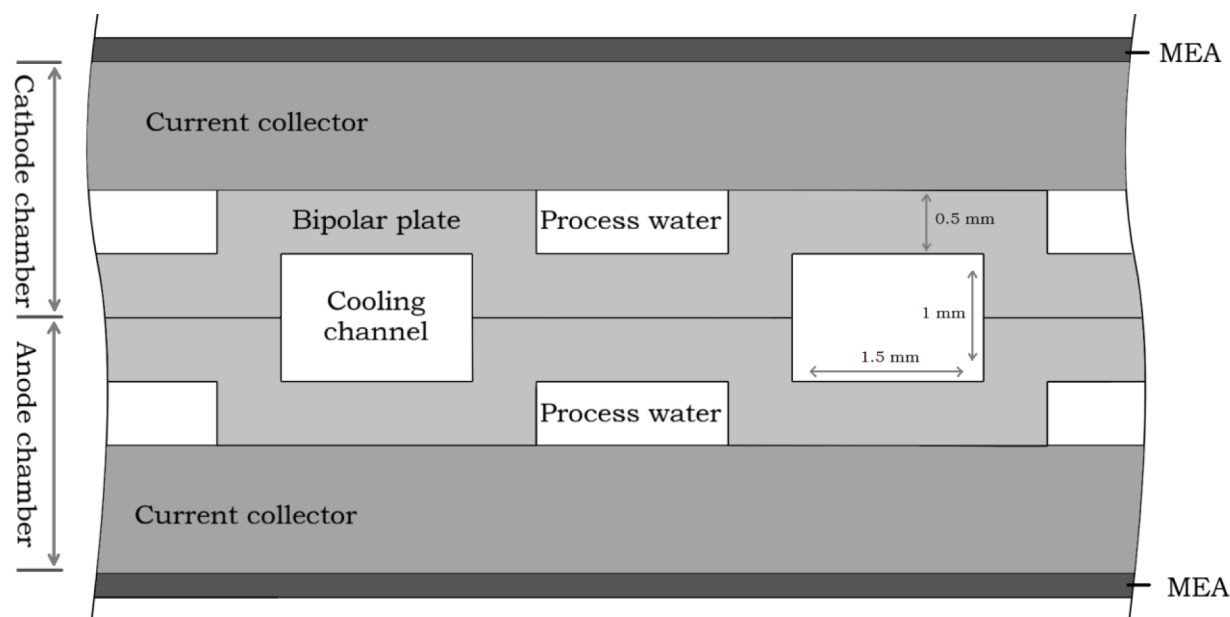


Fig. 35. Cross-sectional view of the cooling ducts between two-membrane electrode assembly [278].

Therefore, if the supply of electricity is insufficient to meet the energy requirements, the electrolytic process will draw heat from the gases passing through the cells leading to a temperature drop in the chamber. This manifests the endothermic mode of operation [222]. Solutions have been developed for operation of high-temperature electrolyzers under endothermic mode. For instance, Laurencin et al. [166] introduced a technique in which energy is stored during the exothermic mode and consumed during the endothermic mode of operation in the electrolyser. The duration of exothermic and endothermic modes is determined by the operator.

There is currently a rapidly growing interest in using the surplus of renewable power (chiefly from wind and photovoltaic) for electrolysis of water and production of hydrogen [52, 169, 239]. However, renewable electricity sources are usually intermittent, which do not allow for steady operation of electrolyzers. In addition, electrolyzers comprise some elements that are highly sensitive to thermal gradients. As a result, any strong temperature variation in the electrolyser can lead to deterioration and failure of these elements. When electrolysis energy is supplied by intermittent renewable power, encountering an energy deficit is quite likely. The electrolytic process then draws the missing energy from the environment where it takes developing a thermal gradient in the enclosure. [222]. Such thermal gradients can reach about 50 K/cm [222]

Perret [221] developed a technique to manage the thermal gradient in the cell stacks constituting the electrolyzers at higher temperatures. In their design, the water vapor is circulated in the cell stacks by independent channels for homogenization of the temperature before directing it towards the cathodes. Under the exothermic mode, the surplus of heat can be transferred from the cell by circulation of a relatively cooler water vapor. Vapor circulation, yet with relatively higher temperature than the cell, can be utilized to supply the heat deficit under the endothermic mode. Clearly, availability of a high temperature steam is a prerequisite of this technique. Yet, it features a drawback of requiring a flow circuit throughout the electrolyser making it architecturally complex. [21] put forward a thermal control strategy for electrolyser adoptable to both endothermic and exothermic modes. This included measuring the cell temperature and altering the applied voltage to the cell correspondingly such that the temperature remains within a certain range. When the cell temperature was below a predetermined upper temperature threshold, the controller decreased the operational voltage to a value lower than the thermoneutral voltage of

the electrolyser. However, when the cell temperature falls below a predetermined lower temperature, the operational voltage was increased to a value larger than the thermoneutral voltage.

A control strategy was proposed by Colombo [62] to manage the cell temperature during the dynamic operation of a high temperature SOEC. In their study, temperature was controlled by manipulating the air flow rate at the anode side. Here, the air flow was, first, used to remove the oxygen generated by the electrolysis process. This method is suitable for production of hydrogen, not oxygen, as separating oxygen and nitrogen in air is an energy intensive process. Second, it provided active cooling or heating for the stack. Two different strategies, including constant PEN (Positive electrode- electrolyte- negative electrode) average temperature strategy and constant air inlet temperature strategy, were implemented as Proportional Integral (PI) feedback controls for the system response to fluctuations in input power (see Fig. 35). The first strategy aims to hold the mean operating temperature of the cell at 750 °C. The maximum and minimum cell temperatures are 766 °C and 733 °C, respectively. In this strategy, the controller reacts to temperature change by manipulating the inlet air flow. Power consumption of the blower and air inlet temperature are regulated to manipulate the inlet air flow. The first control strategy is displayed in Fig. 36a. The second control strategy maintains the air inlet temperature and volumetric flow constant under different ranges of the operating conditions. Here, the cell mean temperature is varied between a maximum and a minimum values. When the difference between air inlet and outlet temperatures reaches one of the set points, the air flow increases to cool or heat the cell and maintain the cell operating temperature within the required safety range. This control strategy is disclosed in Fig. 36b.

For the SOECs operating in the endothermic mode, there are two procedures to control their thermal gradients. These include (i) heating by recovery of the stored thermal energy under the exothermic mode, (ii) using the thermal energy of high-temperature fluids inside the stack. Petipas et al. [223] used airflow regulation for the thermal management of SOECs (see Fig. 37). Their system had two units, including SOEC and Balance of Plant (BoP). At the SOEC inlet, steam at 1073 K was supplied and a conversion of vapor to hydrogen with the fixed rate of 75% was achieved, indicating that the flow of vapor was proportional to the supplied power. The produced gases at the cathode were a mixture of vapor (25%) and hydrogen (75%), while those at the anode included a mixture of air sweep and oxygen. To restrict the temperature gradients within the cell to 10 K/cm, the exit temperature varied in the range of

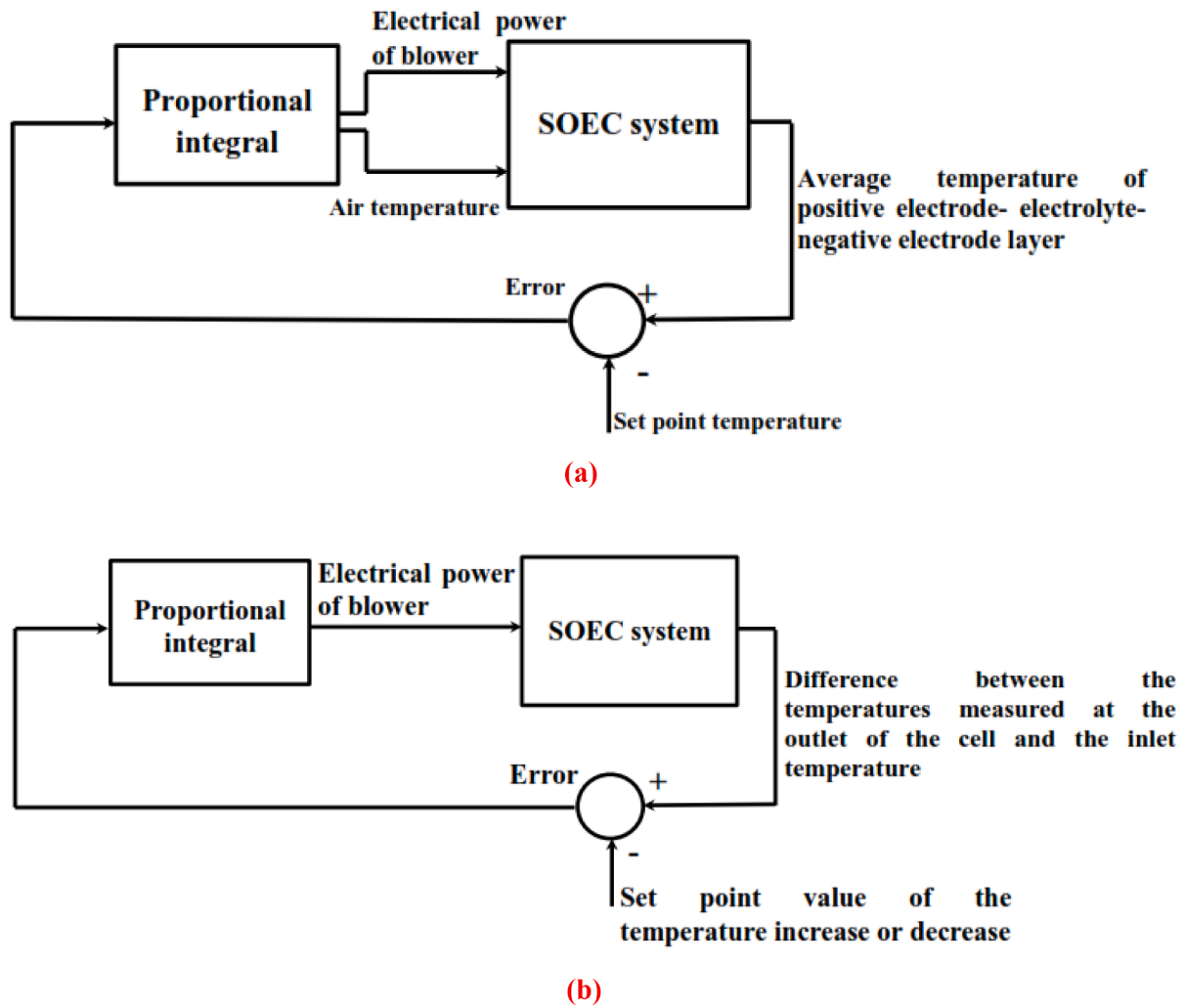


Fig. 36. The control strategies applied to the cell temperature during the dynamic operation of high temperature SOEC [62].

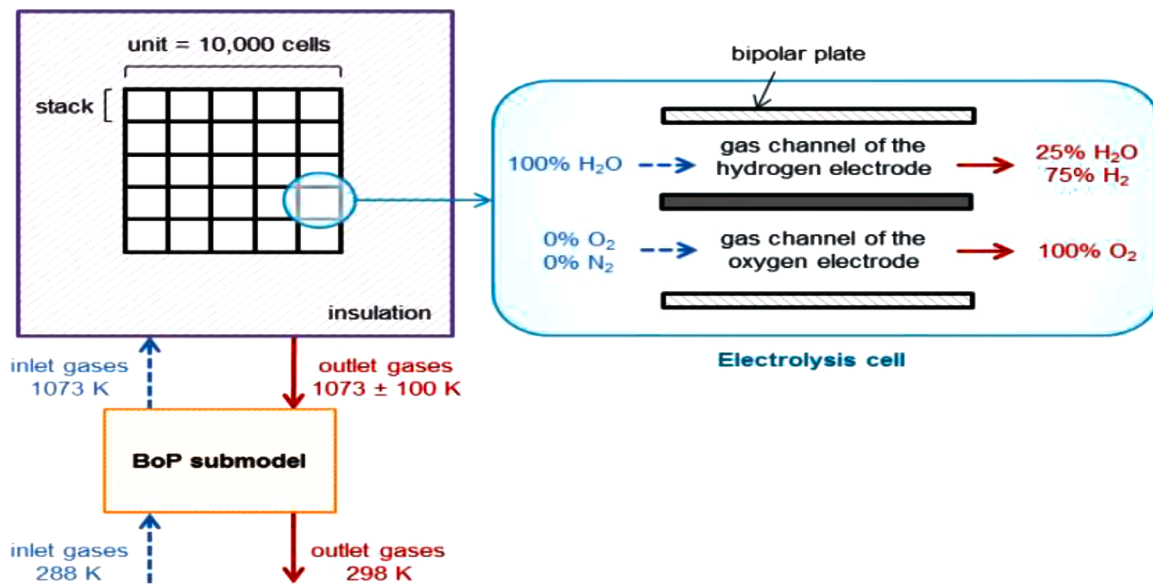


Fig. 37. Schematic view of the SOEC considered by Petipas et al. [223].

973 K to 1173 K setting the lowest power of SOEC unit to 0.633 MW (endothermic mode) and the largest power of 1.101 MW (exothermic mode). BoP had different components, including compressor, heat exchanger, pump and heater. The gases at the outlet were cooled by the inlet water using a heat exchanger. Temperature of the gases exiting the SOEC unit dropped from 1073 to 373 K and 30% of the unreacted vapor was condensed. Further decrease in this temperature from 373 K to 298 K was achieved by pumping the cooling water. The produced hydrogen was subsequently compressed and cooled down to 3000 kPa and 298 K, respectively. Also, part of the recovered heat was used for heating up the inlet gases. Liquid water entered BoP with the temperature of 288 K and the heat recovered from the outlet gases and hydrogen compression was used to vaporize 80–95% of that. An electrical heater ensured more vaporization and a temperature rise from 373 K to 1073 K. It was shown that, in endothermic mode, employing air flow could reduce the thermal gradients throughout the cell from -3.25 K/cm to -1 K/cm. A stronger drop from 4.55 K/cm to 1.55 K/cm was reported in exothermic mode. The flow rate of air should be regulated in accordance with the thermal requirements of the electrolyser and for efficiency enhancement.

3.4.3. Reversible solid oxide cells

The reversible solid oxide cells, RSOCs, are single devices, which can act as SOFC and SOEC [109]. Under SOFC mode, it produces electricity and heat by establishing an electrochemical reaction between air and a fuel such as H_2 , natural gas, hydrocarbons or syngas at high temperatures in the range of 1023 K to 1173 K [190]. Under SOEC mode coupled with a power source, they generate chemical energy by electrolysis of H_2O , CO_2 or $H_2O + CO_2$ [6, 109]. The working temperature of RSOCs varies in the range of 923 and 1270 K. This temperature range permits the use of only solid substrates, reaching a good conductivity through solid state diffusion mechanisms [6]. Ceramic materials generally show good stability and conductivity at high temperatures and therefore, it is possible to achieve a target electrolyte resistance of $0.01 \Omega^{-1}cm^{-1}$ by using these materials. Fig. 38 displays the voltage-current characteristic for RSOCs. In this figure, the current is negative under SOEC mode, while it is positive under SOFC mode. The cell voltage under each mode of operation can be calculated as a deviation from the open circuit voltage by a current-dependent overpotential, η [59]:

$$V_{SOFC} = E_N - \eta \quad (14)$$

$$V_{SOEC} = E_N + \eta \quad (15)$$

In practice, RSOCs are not strictly isothermal because of the temperature gradients associated with spatially varying driving potentials related to heat transfer, charge transfer, species transport, and in-situ reforming reactions. In this context, thermoneutral voltage is defined as the cell voltage that leads to equal gas temperature at the inlet and outlet of the cells [149].

3.4.3.1. Thermal management of reversible solid oxide cells. Thermal management is an essential requirement for RSOCs. In the SOFC mode, the reactor is strongly exothermic, while operation under SOEC mode makes it highly endothermic [246]. Several techniques are used for thermal management of RSOCs. Bierschen et al. [30] proposed the solid oxide cell, SOC, storage chemistry where the fuel cycles between water-carbon dioxide-rich and methane-hydrogen-rich gases. Fig. 39 shows the schematic diagram of the RSOC considered by Bierschen et al. [30]. The electrical energy can be stored as the water-carbon dioxide-rich mixture is electrolyzed (dashed arrows), while the electricity is generated (solid arrows) in SOFC mode using the resulting methane-hydrogen-rich fuel. Pure oxygen is produced during electrolysis and is stored for use during fuel-cell operation. The unique feature of this method is formation of methane during the electrolysis, a less endothermic process than the usual hydrogen or carbon monoxide forming reactions, enabling enhancement of efficiency. Note that in SOEC mode, the energy is stored in a fuel, and then under the SOFC mode, energy of this fuel is partially converted back to electricity. The efficiency is defined here as the ratio of energy supplied during discharging to energy consumed during charging. Bierschen et al. found that a thermal balance could be achieved by coupling the exothermic methanation reaction, with the endothermic electrolysis reaction in the SOC reactor. Through utilizing this technique, the thermo-neutral or even exothermic operation of SOC reactor under the SOEC mode could be attained. A similar strategy for thermal management has been used in more recent studies [138, 149, 300]. Nonetheless, this technique faces some challenges. Thermodynamically, most applicable exothermic reactions, including methanation, need a combination of low reaction temperature in the range of 400 to 650 °C and/or high pressure of about 30 bar. As a result, one needs to develop a SOC reactor with small electrochemical loss at that reaction temperature while operating at high pressure. Low and intermediate temperatures SOC reactors are currently under construction and in the developing phase [246].

Santhanam et al. [246] developed a novel technique for thermal management of RSOCs. Fig. 40 shows the schematics of the process proposed by Santhanam et al. [246] under SOFC and SOEC modes. Integration of heat storage with RSOC helps store the heat generated during the exothermic operation of RSOC. The stored heat can be, subsequently, employed during the endothermic operation of RSOC (SOEC mode) or to supply thermal energy for other interlinked processes. The integration of high-temperature heat sources is suitable for endothermic electrolysis operation, enabling higher roundtrip efficiencies [41, 212]. In the future, one can envisage a heat storage integrated RSOC energy system in industrial and chemical processes where high temperature heat is utilized or generated [1, 38, 119].

RSOCs can be a cost effective technology for electrical energy storage with a good roundtrip efficiency, more than 70%, and higher energy density as compared with batteries [331]. They feature two distinct modes of fuel generation (electrolysis mode) and power generation,

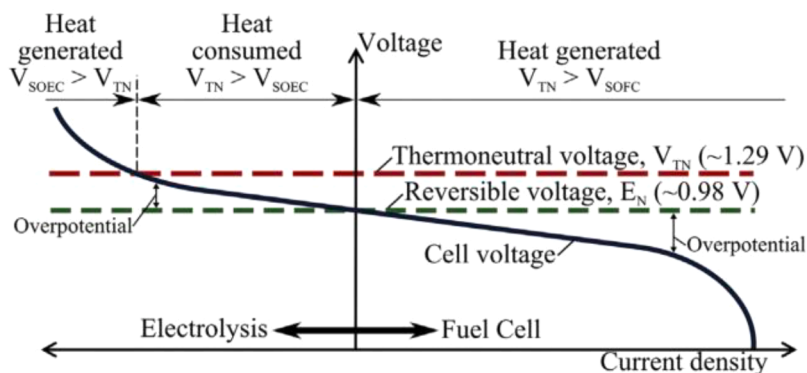


Fig. 38. Representative voltage-current characteristic of RSOC [59].

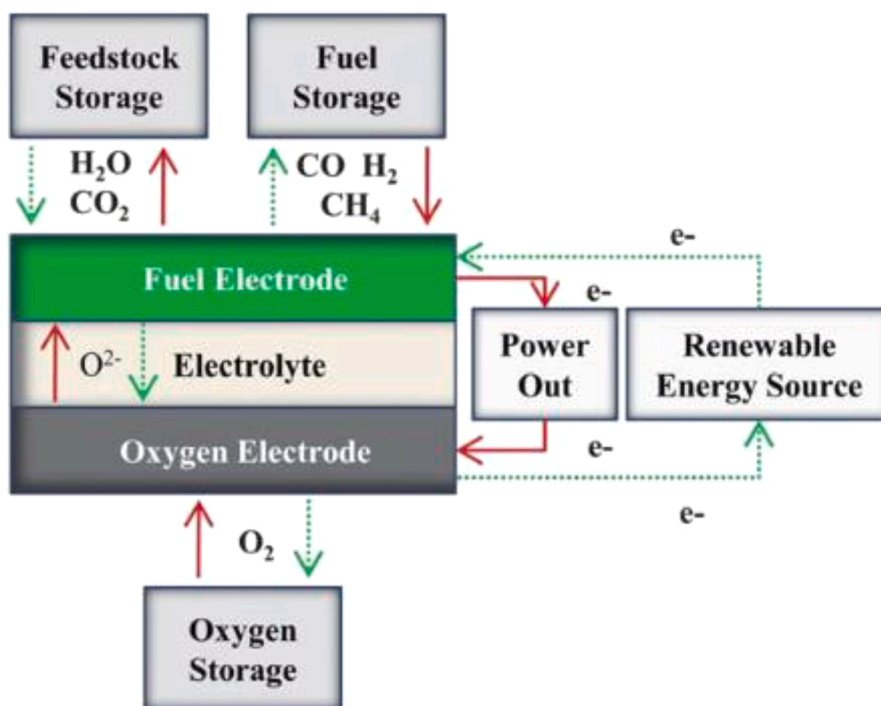


Fig. 39. Schematic diagram of the RSOC considered by Bierschenk et al. [30].

(fuel cell mode,) can be observed. A stand-alone energy storage system is realized from this technology as these two operating modes are coupled with intermediate storage of reactants and products. An essential characteristic of RSOCs that enables high roundtrip efficiency is the production of methane in electrolysis mode for offsetting the typically endothermic conversion process. Methanation is promoted by high pressure and low temperature conditions. This means that intermediate-temperature RSOCs with the operating temperatures lower than $700\text{ }^{\circ}\text{C}$ are important for a good performance [299]. The roundtrip efficiency of RSOCs, used as electric energy storage, can be improved by a suitable thermal management strategy. Different thermal behaviors during SOFC and SOEC modes can induce thermal stress, which damages the cells. [72] proposed a novel thermal management strategy for the RSOC used as an electricity storage system. They stored the heat generated under SOFC mode as latent and sensible heat in a PCM and high density and high specific heat material, respectively. The stored thermal energy could be employed during the electrolysis operation. Heat was stored directly inside the stack employing sensible heat storage for a small size electrical energy storage plant or a PCM thermal storage for the large size one. They used aluminum oxide as the ceramic material and the eutectic metal alloy with good thermal conductivity and small volume changes as the PCM. A schematic view of their stack configuration is shown in Fig. 41. The thermal storage material was placed near the stack, and to decrease the contact thermal resistance, micro-channels were employed, rendering higher heat transfer rates and lower thermal gradients. It should be pointed out that due to the high operating temperatures of RSOCs, the stack requires heating when performing electrolysis. This heat can be stored when the cell generates electricity leading to increases in the roundtrip efficiency. It should be noted that the resultant thermal stress under SOFC and SOEC modes could damage the cells [72].

Mottaghizadeh et al. [197] integrated the cascaded latent heat storage module with suitable PCMs with the commercially available RSOC. A downstream process like methanation was also used in the system for further enhancement of thermal management. This resulted in a fully thermally self-sustained process in the RSOC reactor. For this purpose, the heat produced during the SOFC mode was stored and

utilized during the SOEC mode. It was found that employing PCMs could facilitate the thermal management of the system and eliminate the need for external heat sources. It should be noted that melting point of the employed PCM should be very close to the storage temperature of system. Mottaghizadeh et al. [197] used LiF with the melting temperature of $848\text{ }^{\circ}\text{C}$ and fluoride salt with the melting temperature of $749\text{ }^{\circ}\text{C}$ as the PCM.

In their recent work on RSOCs, Weng et al. [301] proposed a strategy for reducing the cell operating temperature by porosity control. The performance of RSOCs is affected by the quality of anode. In general, the anode components in RSOCs should have a porosity to function properly [125]. The anode acts as a transport medium for the hydrogen oxidation process and serves as the catalyst in the electrochemical process occurring inside the RSOCs [302]. Hence, it should have a permeable structure. Decreasing the cell operating temperature enables use of less costly materials for the cell fabrication. It was found that the operating temperature decreases from $800\text{ }^{\circ}\text{C}$ to $750\text{ }^{\circ}\text{C}$ as the cell porosity decreases from 40% to 30%. It should be noted that lower cell porosity results in gas starvation, while it offers high electronic/ionic conductivity. Weng et al. [301] also found that SOFC mode shows high sensitivity to porosity changes; however, SOEC mode is more sensitive to temperature changes. Hence, porosity control is preferred for temperature reduction under the SOFC mode.

Most recently, Mottaghizadeh et al. [198] employed a network of heat exchangers to control SOFC mode of RSOC. In their design, the SOFC meets the building electricity requirement and heat generated during its electrochemical reactions can be transferred to the SOEC for endothermic operation and standby demands. It was shown that the mean temperature and local temperature gradients of the SOFC and SOEC modes stay within the desired ranges.

It should be pointed out that operating at or near the thermoneutral voltage can simplify the thermal management of the stack of RSOCs as no excess gas flow is needed and thermal stress in components is minimum. Indeed, in the electrolyser mode, there is no demand of air flow for supporting the reactions. The pure oxygen resulting from electrolysis is often stored as a valuable commodity in large-scale electrolysis plants. However, there are reasons for employing a sweep gas on the oxygen

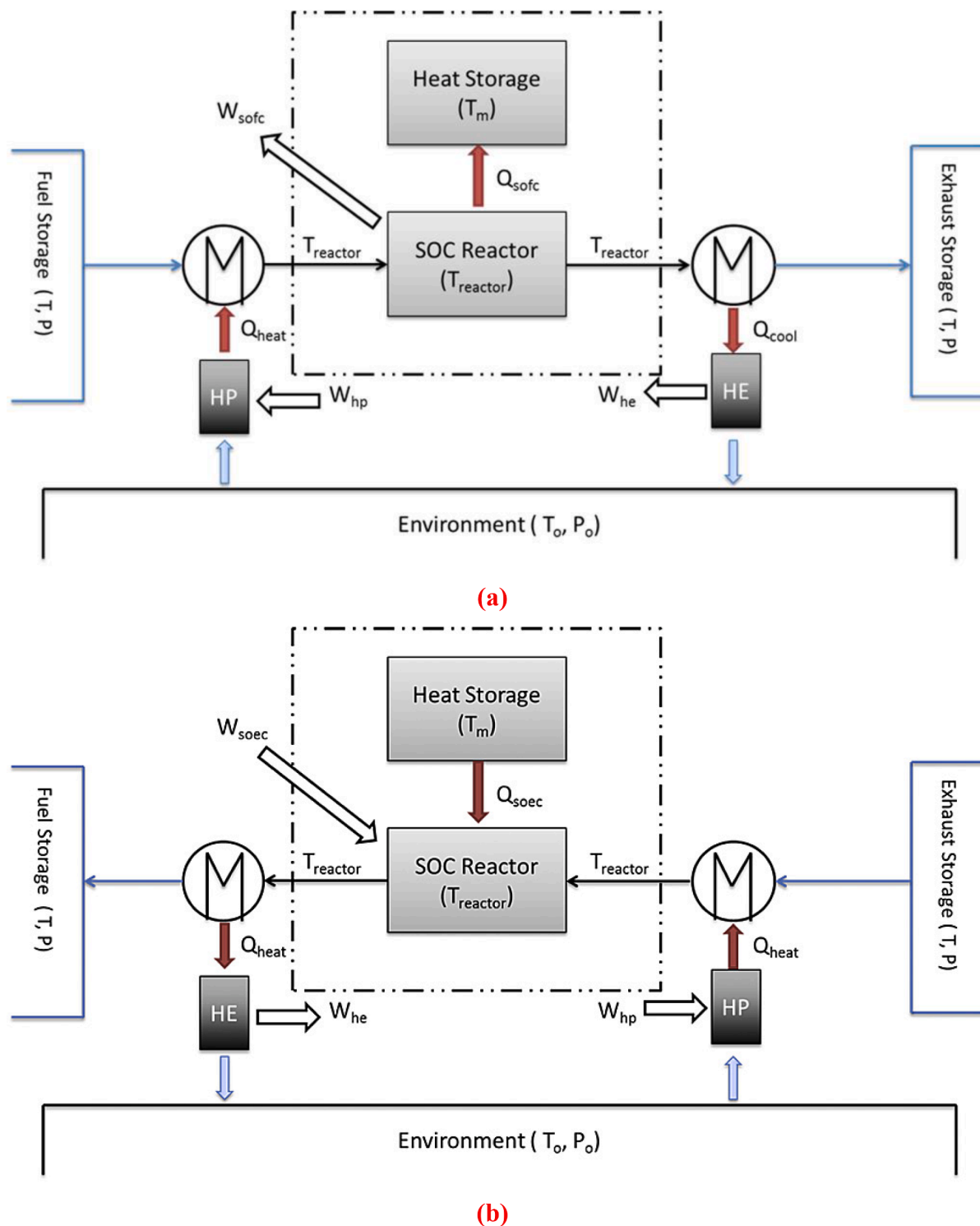


Fig. 40. Schematic diagram of the process proposed by Santhanam et al. [246] in a) SOFC mode; b) SOEC mode.

side. First, employing a sweep gas the performance does not reduce significantly due to minor leakage of hydrogen from the hydrogen/steam side to the oxygen side of the cell. Second, handling of pure oxygen at high temperatures imposes serious materials issues. Lastly, employing sweep gas on the oxygen side of the electrolyser cell decreases the partial pressure of oxygen and mean mole fraction. Thus, it reduces the open cell potential and makes the electrolysis process more efficient. There are a number of extra thermodynamic implications related to the thermoneutral voltage. In general, operation of

electrolysers at or above the thermoneutral voltage eliminates the need for high temperature electrolysis, wherein the input heat provides a fraction of the total energy demand [211]. To operate isothermally above thermoneutral voltage, heat rejection is required [211].

4. Supercapacitors

In contrast to ordinary capacitors, supercapacitors utilize electrode materials with high surface area and thin dielectric materials to achieve

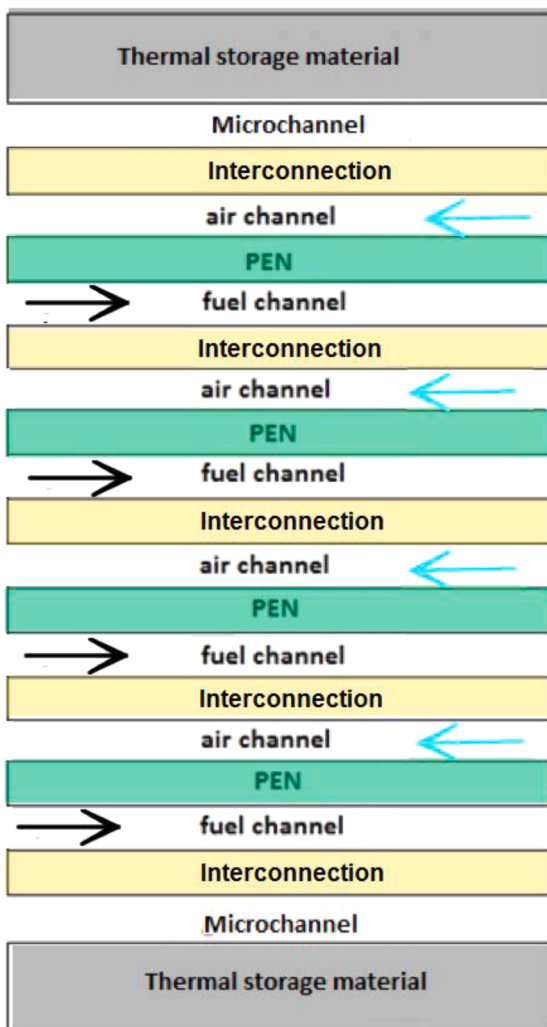


Fig. 41. Stack configuration considered by [72].

greater capacitance [315]. Supercapacitors can be employed independently or in a combined system together with modern batteries to enhance the overall performance [68]. It should be highlighted that combining a supercapacitor and a battery allows for fast release of a large amount of electrical energy, enlarging the specific power significantly ($\sim 10^4 \text{ W.kg}^{-1}$) [261]. Usually, supercapacitors provide about five times the specific power rendered by an ordinary lead-acid battery [68]. Thus, under large power conditions, such as high discharge rate, the supercapacitors provide larger values of specific energy as compared with lead-acid batteries. Further, a supercapacitor could be incorporated into a battery-based energy storage module for decoupling the power and energy specifications. This leads to size reduction and prolonging the lifetime of the entire energy storage module [110]. Supercapacitors are further used in the photovoltaic systems [27] as well as a number of portable electronic equipment. In addition, supercapacitors are usable as the primary source of energy with the advantage of quick recharging. Importantly, supercapacitors are usable over a wide range of temperature, 233 K to 358 K, while an ordinary battery is limited to a much narrower range of temperature. For example, lithium-ion batteries operate between 263 K to 313 K [341]**. In contrast with batteries, the electrode materials employed in a supercapacitor do not undergo phase change or/and chemical reactions during charging/discharging cycles. Consequently, supercapacitors exhibit a very high cyclability and life span because of their inherent reversible mode of operation [156].

In general, fuel cells and batteries exhibit very large values of specific energy but with small specific powers. However, an ordinary capacitor

although exhibiting high specific power because of the significant electron mobility within the conductive plates, cannot deliver a large specific energy for long-range applications [262]. Therefore, supercapacitors can fill the gap between the fuel cells, batteries and capacitors in the Ragone plot. A supercapacitor exhibits much bigger specific power in comparison with the fuel cells and batteries and larger specific energy in comparison with the ordinary capacitors.

4.1. Structure of supercapacitors

The general architecture of a supercapacitor is shown in Fig. 42. There are two electrodes in a supercapacitor, with a separator sandwiched between them. Symmetric cells have similar electrodes, while asymmetric cells can have different electrodes. The separator is wetted by electrolyte and is used to prevent the electrical connection between the electrodes. The materials usually used for separators are ion-permeable to allow ionic charge transfer. At the same time, the materials should have high electrical resistance, high ionic conductance, and low thickness to provide the maximum performance. In most cases, paper or polymer separators are employed together with organic electrolytes, while ceramic or glass fiber separators are generally integrated with aqueous electrolytes [257]. There is a voltage restriction at one electrode due to the electrolyte breakdown potential. The equivalent series resistance of the cells is highly related to the electrolyte conductivity. Aqueous electrolyte has the breakdown voltage of about 1 V that is considerably lower than that accessible with an organic electrolyte (about 3 V). However, the conductivity of an aqueous electrolyte is higher than that of an organic electrolyte that can be suitable for high power devices. Aqueous electrolyte also has favorable features such as low costs and easy handling [110].

4.2. Effects of temperature on supercapacitors

The operating temperature of the supercapacitors leaves considerable effects on their components and performance characteristics. These effects are briefly reviewed in this section.

4.2.1. Effects of temperature on electrolytes

The temperature range of the electrolytes is normally between 233 and 343 K. Temperature affects electrolyte thermophysical properties as follows.

- **Ionic conductivity:** With a rise in temperature, ions move more freely, increasing the ionic conductivity of electrolytes.
- **Viscosity:** The viscosity of electrolytes drops as the temperature increases and has an inverse relation with the ionic conductivity as can be observed from Walden's rule [322].
- **Diffusion coefficient:** Increasing ion mobility results in a higher diffusion coefficient for electrolytes at higher temperatures.

Temperature also affects the stability of electrolytes. Beyond the temperature range of 233 K to 343 K, the ionic conductivity of electrolyte considerably drops or decomposition in electrolytes occurs (releasing toxic gases), causing a decay in the electrochemical performance.

4.2.2. Effects of temperature on separators

Separators can be used for preventing direct contact between negative and positive electrodes, while allowing fast transportation of ionic charge carriers. For applications at higher temperatures, the mechanical strengths of separators are generally important and should endure the demanding operational environments. As decomposition temperatures are approached, separator begins to shrink, causing short circuiting between the electrodes and an eventual thermal runaway. Apart from high thermal stability, separators should have strong shutdown features. This is because above a certain temperature, the separator melts and



Fig. 42. Architecture of a supercapacitor González et al. [110].

transforms to a thin film, stopping the pathways of ionic conduction by elimination of pores and an eventual prevention of thermal runaway [225]. In addition to thermal stability, performance indicators including capacitance, ESR and, therefore, power densities are influenced by porosity of the separator materials and their thickness at excessive temperatures. When the temperatures is very low, i.e. <243 K, the ions mobility decreases. Under this condition, porosity of the separator membrane plays a critical role in the overall performance, particularly for a system with a more viscous electrolyte [309].

4.2.3. Effects of temperature on electrodes

Electrode used in supercapacitors generally consists of active electrode material, binder, and conducting agent. Thermal stability and thermal conductivity considerably affect the thermal performance of the supercapacitors, particularly at high temperatures. In this section, the thermal conductivity and stability of the materials used in supercapacitors electrodes are discussed.

4.2.3.1. Active materials. It has been shown that the main contributor to the thermal resistance of supercapacitors is their electrodes [122]. In practice, many factors, including structures, morphologies, and testing conditions, affect thermal conductivity of the electrode used in supercapacitors even for the same materials. As a result, it is important to understand the thermal characteristics of electrode materials when designing a supercapacitor [112]. Further, it should be mentioned that the thermal conductivities of the electrode with or without liquid electrolyte are very different. In general, the electrodes can be wetted to efficiently dissipate heat in supercapacitors. Using electrodes with high porosity is usually not helpful for conduction of heat, while it contributes to the storage of charge over the surface of electrodes. Higher pressures applied during manufacturing, enhance the thermal conductivity of the electrodes made of activated carbon [44]. At higher pressure, a reduction in thermal resistance is gained as more carbon fibers are in contact with the current collector. It follows that these aspects should be considered when electrode materials are adopted with large pore volumes or low packing densities (e.g., nanofibers). For the purpose

of electrode manufacturing and amongst transition metal oxides, MnO_2 offers a good thermal stability [229], while RuO_2 coated electrodes have also shown favorable thermal stability [154]. During heating of RuO_2 electrodes, capacitance increases due to enhanced proton/electron transport. This could be because of an increase in the number of reaction sites, or a decrease in the active electrodes' mass due to dehydration [129]. Electrically conductive polymers, including polypyrrole also have high thermal stability. It is worth mentioning that the electrodes' thermal stability is determined by the employed materials as well as the binders. This is due to the fact that electrode materials and binder are usually in direct contact. The following section focuses on the thermal stabilization of binder.

4.2.3.2. Binder. Electrode thermal characteristics in supercapacitors are significantly affected by binder thermal stability. Carbon black and activated carbon may be used at high temperatures without experiencing any problems. Binders (usually PVDF), which are highly inert and pure fluoropolymers, have a relatively low melting point of 450 K. As a result, the operating temperature range of the electrodes can be limited by the melting temperatures of the binders. By carbonating the electrodes/binders at a higher temperature, greater than 873 K, under an inert atmosphere, the electrochemical performance of the electrodes may be improved [241]. This may be due to the constriction provided at the entrance of the porous lattice owing to the decomposition of binder and enhanced electrical conductivity [241]. Further, the binder materials also affect the thermal conductivity of the electrode. As an example, the polymer binders, used for coating of carbon nanotube networks, form one or multiple conductive substrates with thickness in nanometer level that can improve the thermal conductivity of electrodes [183].

4.2.3.3. Current collectors. Current collector materials are generally metal foils or carbon materials. Current collectors have high thermal conductivity and stability, so their use in low or high temperature supercapacitors is not a problem [309]. Carbon current collectors with high conductivity and contiguous growth of petals over carbon fibers boost the transfer of charge [29]. For a wide range of temperatures,

these freestanding carbon electrodes are excellent options for use in flexible supercapacitors as active materials and current collectors.

4.2.3.4. Lignin. Lignin can be used as the electrode material in supercapacitors [339]. In general, the plentiful oxygen atoms in lignin are advantageous to increase electrolyte ions adsorption and produce redox reactions for supercapacitors. Many oxygen atoms in lignin can be lost during the pyrolysis at large values of temperatures. As a result, the optimum carbonization and activation processes should be developed that can provide lignin derived electrodes with high degrees of carbonization and proper amount of oxygen atoms [339]. Lignin can be also thermally degraded as the carbonization temperature is increased that leads to a decrease in yield [339].

4.2.4. Effect of temperature on self-discharge

The supercapacitors charged to a specified value of voltage and held under the open-circuit conditions exhibit tendencies to experience loss of voltage, or the so called 'self-discharge'. The Gibbs free energy in charged supercapacitors is higher than that in discharged ones. This sets a thermodynamic force for discharging the open-circuit conditions [210]. The rate of self-discharge is usually maximum at the early stages and then deteriorates gradually to reach the steady-state values. The shelf life of supercapacitors is dominated by the self-discharge rates. Self-discharge rates are also indicative of the health condition of supercapacitors. Compared to the new ones, aged supercapacitors show considerably higher self-discharge rates. As a result, self-discharge is usually employed as a factor for quantifying aging in supercapacitors [73]. Operating temperatures of supercapacitors have considerable effects on the rates of self-discharging. At high temperatures, the ions mobility is enhanced which intensifies of the current leakage and self-discharge rates [22].

4.3. Supercapacitors aging mechanisms in operation at high temperatures

- **Pressure evolution:** Operation of supercapacitors at high temperatures lead to thermal decomposition and electrochemical degradation of the electrolyte. This leads to the evolution of decomposition gases, including hydrogen, carbon monoxide, and other organic byproducts. Pressure builds up because the gases are accumulated at the top of the electrolyte. Pressure rise is a critical safety issue that should be addressed through appropriate cell design [117]. Failure of the safety valves due to the rise of internal pressure is quite common in supercapacitors [42]. Further, diffusion of toxic gases into the atmosphere is an environmental concern. As an example, toxic gas evolution has been reported with aqueous electrolyte in excess of 2 V [43].
- **Increase in pore resistance:** Operation of supercapacitors at high temperatures speeds up the decomposition reactions on the interface between the electrolyte and electrode. The solid particles produced by reduction/oxidation of the carbon electrodes and electrolytes are deposited over the electrodes surfaces and block the pores. Hence, the effective surfaces in the electrodes decline which can cause capacitance reduction. Bittner et al. [32] carried out porosimetry investigations on the aged electrode and found that obstruction of the pores that have sizes analogous to those of the solvated ions could lead to the reduction in capacitance.
- **Increase in ESR and Joule heating:** Stronger Joule heating causes elevated temperatures that further accelerates the aging process [35]. As a result, this could be considered a cyclic process.
- **Appearance of oxides:** Oxidization in the current collector occurs at elevated temperatures that cause large contact resistances between the current collector and electrode. This, in turn, intensifies ESR as confirmed by EIS measurements [160].
- **Evaporation in electrolytes:** The electrolyte may evaporate at high temperatures, while the evaporation rate can be detected through

detecting the weight loss. As an example, a 25% weight loss was reported in the supercapacitors operating at 3 V and 343 K for 12,000 s [160].

- **Overvoltage:** In power cycling with constant current, if the capacitance declines because of aging at higher temperatures while charging is unchanged, the voltage increases rapidly causing further aging [36].

4.4. Extreme-temperature performances

There exists an increasing need for the design of power storage devices that can operate at extreme temperatures with very limited or even no thermal management. The applications include space avionics modules, electric and unmanned aircrafts, electric and hybrid vehicles. Extreme-temperature performances, in particular ESR and capacitance, are important for the use of supercapacitor in these applications.

4.4.1. Extreme low-temperature performance

At low-temperatures, energy storage modules with large powers are highly demanded for electronic systems, cold-cranking internal combustion engines, and hybrid vehicle. For some special applications, such as space-related electronics, these systems should operate well at 218 K or even lower. In these applications, the low-temperature energy storage modules should be compact and have a simple thermal management system [172, 337].

4.4.2. Performance at extreme high-temperatures

For specific applications, such as space, military and petroleum industry, performance of power supplies at high-temperatures is of significance. For example, the operating temperature of downhole drilling is larger than 393 K). The limiting factor for the high-temperature operation of supercapacitors is the stability of the electrolyte [178]. Organic electrolyte employed in a commercial supercapacitor is not suitable at high temperatures as it is flammable and the evolution of toxic gases is also possible. Even in hybrid vehicles in which the working temperature exceeds 333 K, the supercapacitors with organic electrolyte struggle due to lower electrochemical stability of organic solvents. In addition, the high vapor pressure of acetonitrile based electrolyte requires an accurate and costly thermal management module. Ionic liquids can be usually employed in applications with higher temperatures due to their higher thermal stability and lower vapor pressure [19]. This causes thermal reliability by intercepting thermal runaway and pressure build-up when the system operates at higher temperatures. Packaging is made easier by neat ionic liquid electrolytes due to the absence of any solvent at higher temperature. Ionic liquid electrolytes can be further enhanced by adding inorganic fillers, including clay, due to their superior thermal stability, sorption capacity, active surface area, and permeability [37]. The worst-case problem in a supercapacitor can be overcharging. Upon overcharging, the system usually builds up a pressure until it is finally vented, leaking gases and electrolyte [131]. In this situation, the system should not supply current as the continuous current supply after venting turns the capacitor into a large resistor that can generate a large amount of heat. Thermal runaways are not observed in a supercapacitor due to the lack of self-propagating chain reactions [131]. The high temperature supercapacitors, with operating temperature in the range of 233 K to 358 K, high voltage of 5.5 V, and good reliability have been already commercialized [226].

4.5. Thermal management of supercapacitors

4.5.1. Heat generation mechanism in supercapacitors

Fig. 43 shows the equivalent circuit corresponding to heat transport in supercapacitors. In general, convection, conduction and radiation heat transfer can be observed in a supercapacitor. Heat generated in the supercapacitor is transferred through conduction from the center of the supercapacitor towards the external wall and it is transferred by

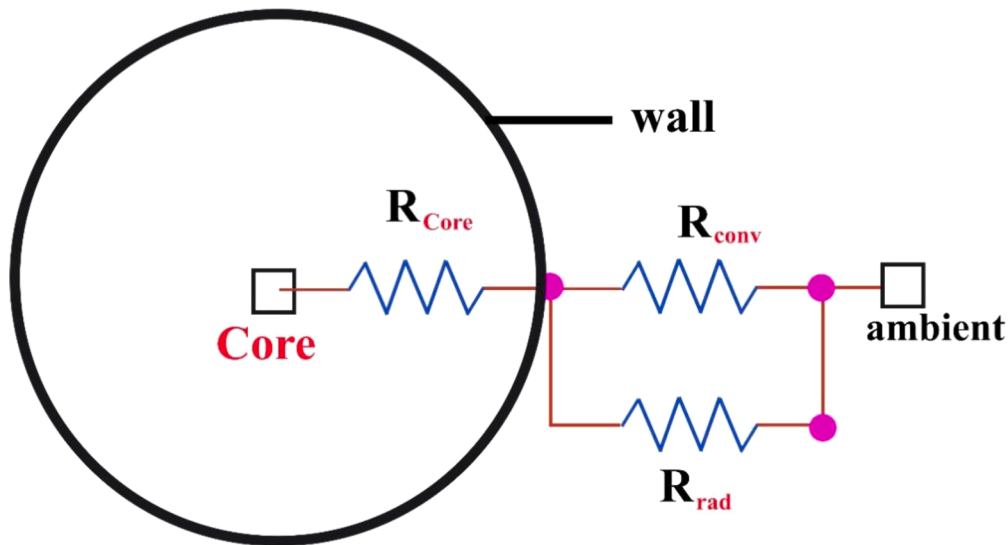


Fig. 43. The supercapacitor equivalent circuit for heat transport [309].

radiation and convection from the external wall to the surrounding environment.

Generation of heat in supercapacitors occurs through two mechanisms: an irreversible resistive (Joule) heating and a reversible heat variation. The irreversible Joule heating, q_{Joule} , in supercapacitors can be expressed by [309]:

$$\frac{dq_{Joule}}{dt} = I^2 R_s \quad (16)$$

In Eq. (17), R_s and I are the equivalent series resistance and charging current, respectively. There are different resistances in supercapacitors, including interfacial resistance between the current collectors and electrode, that of electrode material, diffusion and resistance of ions as they pass through the pores of electrode, the resistances of electrolyte and ions migrating throughout the separator [308].

In supercapacitors, the reversible generation of heat provided by the entropic effect can occur in the course of discharge/charge process. Unlike irreversible heat generation, the reversible generation of heat is positive in the charging process, while it is negative during the discharge process. In general, the reversible heat can become important when the thermal mass of the supercapacitors is reduced, and the duration of discharge/charging is increased. Reversible generation of heat is dominated by the ion's behavior [250]. During charging process, ions migrate to the electrodes to compensate for the positive and negative charge on the electrodes. In the charging process, the ions are in the state of maximum order and minimum entropy. This makes the ions release heat to the contacts, causing an increase in the temperature of those surfaces. However, in the discharging process, the ions are dispersed into the electrolyte and reach the maximum entropy. In this process, heat is absorbed by the ions from the contacting surfaces and accordingly cool these. As a result, the contacts alternately are heated up during charging and cooled during discharging [309].

Usually, a supercapacitor supports a current of about 400 A or more based on the cells capacitance and employed technologies. Although the equivalent series resistance in supercapacitors is in the range of $m\Omega$, the repeating charging and discharging cycles in the supercapacitors lead to a considerable heat generation [13]. The influence of irreversible heat is more important in the supercapacitors in which the charge and discharge processes are exothermic and endothermic, respectively [111]. An electric model could be used to calculate the Joule thermal losses in the supercapacitors. Conduction of heat takes place inside the capacitor, while there are convection and thermal radiation between the capacitor wall and the surroundings. The ambient temperature has

considerable effects especially at the extremes and, a safe operating temperature in the range of 233 K to 343 K is usually recommended by the supercapacitor manufacturers. The heat dissipated on the walls of supercapacitors should be maximized for preventing the cells from being overheated. The thermal dissipation improves as the surface-to-volume ratio increases [309].

The temperature distribution in supercapacitors is governed by the following energy equation [111]:

$$\rho C \frac{dT}{dt} = \nabla \cdot (k \nabla T) + \frac{Q(t)}{V_{Cell}}, \quad (17)$$

wherein ρ , C , and k are density, specific heat, and thermal conductivity, respectively. T and t are the temperature and time respectively, Q is the amount of heat generated inside the cell and V_{Cell} is the cell volume.

To work out the reversible temperature distribution in supercapacitors, the entropy change should be calculated. The variation of entropy in the supercapacitors is given by [111]:

$$\Delta S = \frac{2k_B}{e} C \Delta U \ln \left(\frac{V_H}{V_e} \right), \quad (18)$$

in which, ΔS and k_B are the entropy of the system and the Boltzmann constant, respectively. e and ΔU are the electron charge and the voltage variation of the supercapacitor, respectively. C indicates the supercapacitor capacitance. V_H and V_e are the volume of the Helmholtz layer and the total electrolyte volume, respectively.

4.5.2. Purpose of the thermal management of supercapacitors

An even increase in the temperature is considered being favorable as the electrolyte conductivity is enhanced. Electrolytes are usually manufactured by an organic solution in which the solvent evaporates at 293 K. From this viewpoint, a loss of solvent can occur by increasing the electrolyte temperature [281]. Further, the lifespan of supercapacitors decreases down to half by addition of every 10 K at temperatures above 298 K [250]. Hence, it is necessary to keep the maximum temperature below 323 K and the temperature difference inside the module less than 5 K for a full lifetime [332]. Supercapacitor resistances lead to heat production during the charge process and cause overheating [159], showing the significance of thermal management. This is particularly the case in supercapacitor modules where the cells are packed close to each other to keep the temperature distribution uniform or nearly uniform. Packed arrangement may also add extra mass, volume, and cost, and reduce the energy densities of the systems [309]. As a result, a

cooling module is often added to supercapacitors when there is a possibility of exceeding 338 K, as the maximum allowable operating temperature [13]. Conversely, supercapacitors feature an excellent low-temperature efficiency, even at temperatures below 233 K [309], while no heating system is needed.

4.5.3. Different techniques used for thermal management of supercapacitors

The cooling modules of supercapacitors are broadly categorized into two groups, of active and passive [309]. Usually, active cooling modules in supercapacitors use forced convection by air. These simple active cooling modules have compact structures with cost-effective features [142]. The supercapacitors employed in these modules are usually cylindrical in shape. A flow of air over the cylindrical objects in a perpendicular direction can effectively manage their temperatures [47, 115, 116].

In passive cooling modules for supercapacitors, phase change materials are often used to dissipate the heat produced inside the cells by conduction. Ideally, the phase change materials used for cooling should have a melting point between 303 K to 333 K, large values of latent heat, and narrow melting temperature ranges. Among different phase change materials, paraffin wax is mostly used as it is cheap and has good chemical stability. Xia et al. [307] designed a cooling air duct of a supercapacitor package (see Fig. 44) and showed that it could maintain the maximum temperature difference within the supercapacitor group at 5 K. Such system was able to meet the cooling needs of hybrid electric vehicles.

Voicu et al. [289] used forced air-cooling to manage the temperature distribution in a supercapacitor stack. They considered a staggered configuration for the supercapacitors and found that the arrangement with the lowest spacing could provide the highest cooling efficiency. Zhang et al. [332] optimized the air-cooling system used in a supercapacitor module compartment designed for an electric bus. In their design, cooling air flows through the supercapacitor from the passenger cabin, and exits from the air outlets placed on the hull side of the bus. It was found that the maximum temperature of the supercapacitor increased in the range of 300 K to 321 K in the optimized compartment. Yet, it was still lower than the maximum allowable temperature of 323 K.

As shown in Fig. 45, Voicu et al. [290] investigated the thermal management of a staggered supercapacitor stack by using air-cooling modules. They reported that among all rows of supercapacitors, the best cooling could be achieved in the second row, despite the central location of this row. However, the poorest cooling performance was reported for the first row. Further, there was no considerable temperature difference between the first and last rows of the supercapacitor. The lower temperature of the second row was attributed to the induced flow fluctuations as the air passes the first row. This leads to enhancement of heat transfer in the second row and therefore reduces the temperature. In the third row, there are no major influences of the flow fluctuations and the local heat transfer coefficient on the temperature distribution of the supercapacitor remains unaffected. This appears due to the increase in air temperature as it flows through the first and second rows, which reduces the heat transfer potentials. The cooling of the third row is also less effective as compared with the second one. As a result, the highest surface temperature is likely to appear in the last row of the supercapacitor because in the last row the local heat transfer rate is reduced by a downstream recirculating flow.

A problem associated with the cooling methods discussed so far, is that they require the capacitors to be held by external casings. This leads to obstruction of the major section of the supercapacitor for effective cooling process. The issue can be resolved by perforating the bottom plate to permit cooling fluid to flow throughout the system. The cells employed in the packs of supercapacitors are often designed as cylinders with terminals located at the end of the cell. Hence, the major portion of heat created in the discharge/charge process is transferred to the surrounding environment by the ends of the cells. A forced flow air through the cylindrical body of each cell can effectively decrease the temperature of the cells with cylindrical shape. In another design, a two-phase system was employed in which the coolant was pumped through a closed loop [200]. In the modified version of this design [316], the capacitors were pressed against the cold plates by using a spring plate. This flexible plate facilitates the movement of cold plates for engaging objects of different heights. The pipe's serpentine shape also permits flexibility, to position the cold plates. It is also possible to employ a temperature sensor instead of a thermal management module, which will reduce the charging current upon recognition of overheating conditions [303]. In general, a smaller cooling system is required for the supercapacitors as compared

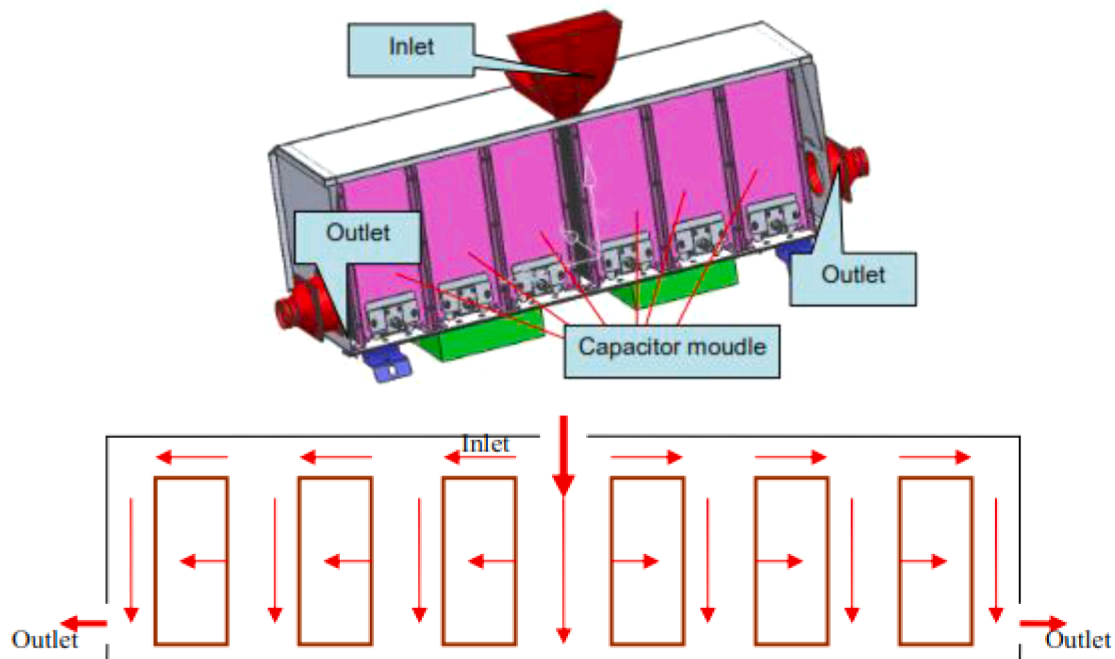


Fig. 44. Cooling air duct of supercapacitor package considered by Xia et al. [307].

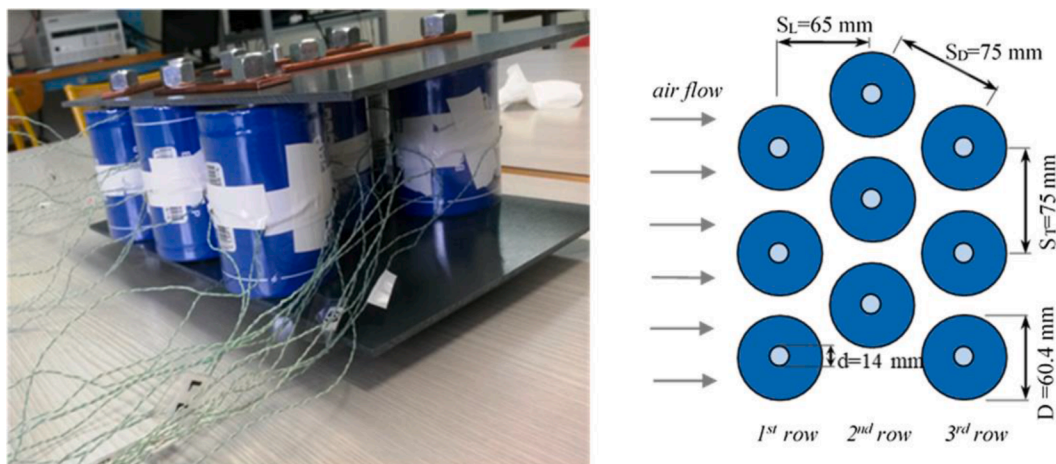


Fig. 45. The supercapacitors considered by Voicu et al. [290], a) supercapacitors module, b) configuration characteristics.

with batteries [195]. Further to active cooling methods, passive techniques employing PCMs are also in use to prevent sharp increases in the module temperature. The heat stored by PCM can warm the supercapacitors during the charging process or in cold weather. The PCMs used for cooling supercapacitors must have the melting point matched with the operating temperatures of supercapacitors, good latent heat, and narrow range of melting temperature. As an attractive option, paraffin waxes feature low costs and high chemical stability, while other options include combination of bromobenzene and chlorobenzene [193] and stearic acid [123]. PCMs are also suitable for preventing thermal runaways in a single cell, which may lead to failures [151].

4.5.4. Thermal management of cellulose nanofibril-based supercapacitors

A double electric layer is created on the solid/liquid interface due to the electronic and ionic conductivities of the electrodes and electrolyte. Internal resistances exist at the interface between the electrodes and the electrolyte and the generated heat is accumulated around the electrodes. This matter further necessitates heat diffusion from the electrodes. To avoid heat generation, the ripple current in supercapacitors should be reduced during the charge and discharge processes [4]. Improving the structures and materials of the electrodes is also of importance. The porous electrodes and current collectors are useful to extend the contact surface between electrodes and electrolyte [321]. This leads to enhancement of the power densities of the supercapacitors and provides an efficient diffusion channel. Cellulose nanofibril-based electrode materials are employed, as pseudo capacitor electrode materials, in supercapacitors to achieve higher capacitances and energy densities as compared with the double layer capacitor [231]. Combining cellulose nanofibrils and other conductive materials in the form of a composite material leads to higher compatibility. Electric charge can be transferred on the surface and inside of the cellulose nanofibrils-based electrodes, producing a capacitance [333]. In comparison with the costly metal oxide pseudo-capacitor electrodes, cellulose nanofibrils materials offer lower costs and controllable microstructures. The composite of cellulose nanofibrils enhances the ion and charge transferring rates, which in turn increase the power density and provide an efficient means of heat evacuation [333, 338].

4.5.5. Improving heat dissipation ability of supercapacitors

Large amount of heat are produced during the supercapacitors charging and discharging, particularly at high current densities. This could considerably accelerate the capacity fading, lead to human discomfort and ultimately to serious safety issues including explosion of the unit. Zhao et al. [334] used electrodes based on graphene-MnO₂ film with high thermal conductivity for the supercapacitor. These electrodes have much larger thermal conductivity ($613.5 \text{ W.m}^{-1}.\text{K}^{-1}$) compared

to that of the traditional MnO₂ slurry electrodes ($1.1 \text{ W.m}^{-1}.\text{K}^{-1}$). Zhao et al. concluded that the use of these electrodes significantly enhances the heat dissipation during charging and discharging processes. They also featured good cycling performance and great rate capacity for specific capacities up to 218.8 F.g^{-1} and a large current density of 10 A.g^{-1} .

4.5.6. Thermal management of lithium ion capacitors

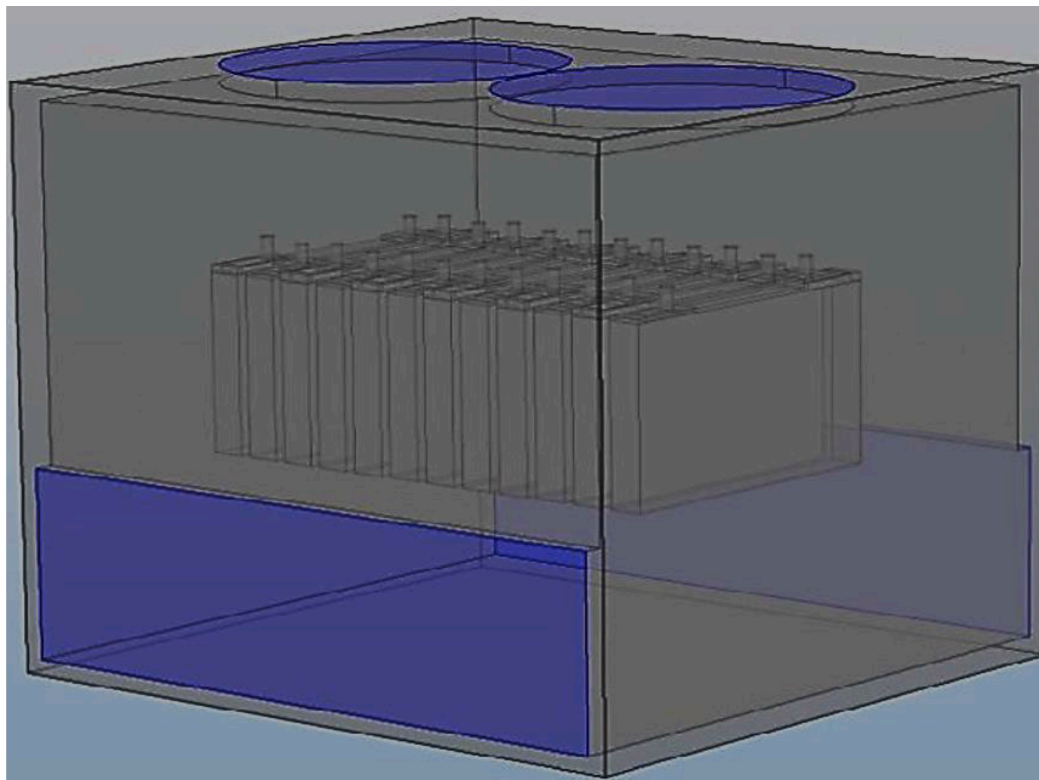
Lithium ion capacitors are hybrid energy storage systems in which energy storage mechanism of lithium ion batteries and the electrical double-layer capacitors are combined. In such systems, some advantages of both lithium ion batteries and capacitors are offered while some of their disadvantages are eliminated. They offer good power density, higher voltage operation than supercapacitors, and high durability (over 2 million cycles) [265]. Even with these advantages, lithium ion capacitors are prone to overheating due to excessive heat generation during high current applications [264]. As a result, it is necessary to develop suitable thermal management systems for this technology. Both active and passive cooling topologies are employed for lithium ion capacitors. In active techniques, external power is consumed for heating/cooling and the coolants include air and liquids [280] while, passive approaches are diverse [179] and involve the use of PCMs [23]. These techniques are discussed in the followings.

Air cooling

The air cooling based thermal management systems are one amongst the popular methods for lithium ion capacitors due to its low manufacturing costs, simple layout needs and high reliabilities. Soltani et al. [265] designed an air cooling system for the integration into a commercial lithium ion capacitor, consisting 12 cells. They observed that without using the cooling system, the temperature increased very rapidly. Their thermal management method was implemented in a modular hardware-case design and revealing that the cooling capacity of the thermal management system is highly related to the flow behaviors, fan locations, gap spaces and the air flow velocity in the system. For the evaluation of the effects of air direction on the cooling capacity, four inlet and outlet locations were considered (See Fig. 46). Side-cooling with two fans with the velocity of 5 m/s with the space of 5 mm was identified as the best design.

Liquid cooling

It has been demonstrated that liquid cooling is the most efficient thermal management technique to eliminate excessive heat with lower flow rate for lithium ion capacitors. Even by addition of extra components including piping, pump, and heat exchanger, liquid cooling is still amenable to compact designs, but they usually add more weight as compared with their air-based peers. Moreover, addition of liquid coolants in direct proximity to high-voltage components of lithium ion



Fans on top and outlet on both sides of module

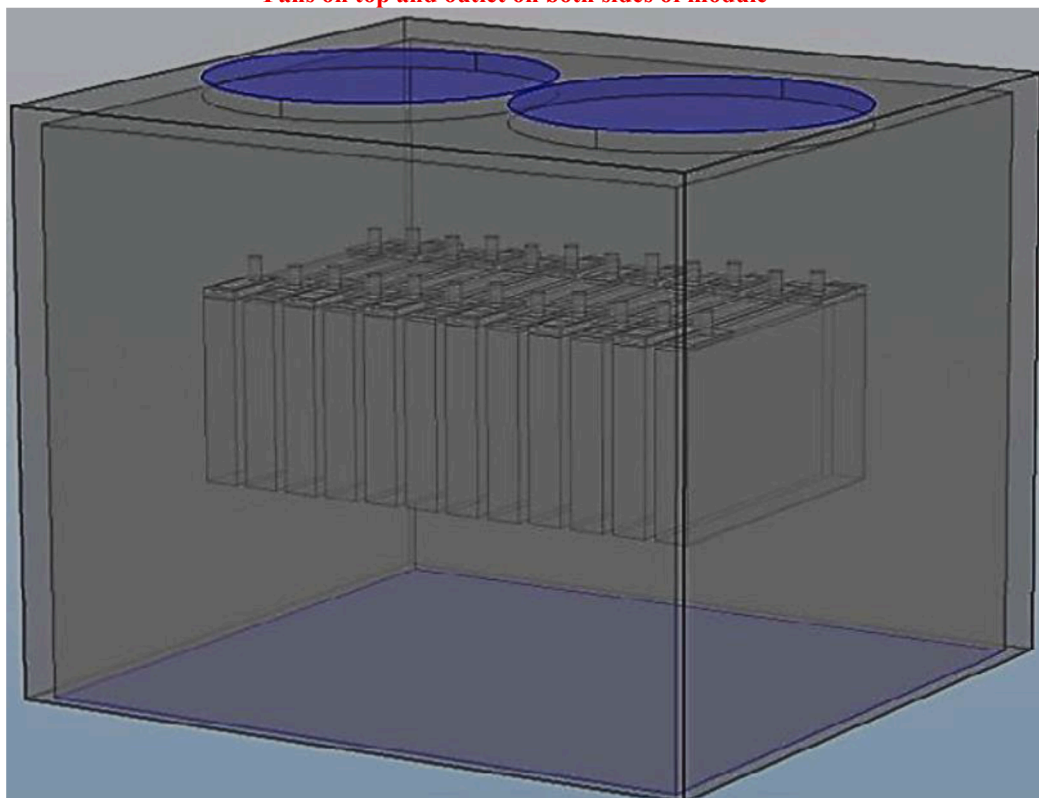


Fig. 46. Four air cooling topologies for lithium-ion capacitor proposed by Soltani et al. [265].

capacitors leads to some challenges. For all operation and crash scenarios, a safe insulation between coolant and live connectors should be guaranteed, while during production, operation and maintenance, continuous leakage sensing is necessary. Jaguemont et al. [135]

developed a three-dimensional thermal model integrated with the liquid cooling plates for thermal management of the lithium ion capacitor. They considered three domains, including battery, cooling-plate, and module domains. Within the battery domain, the energy balance

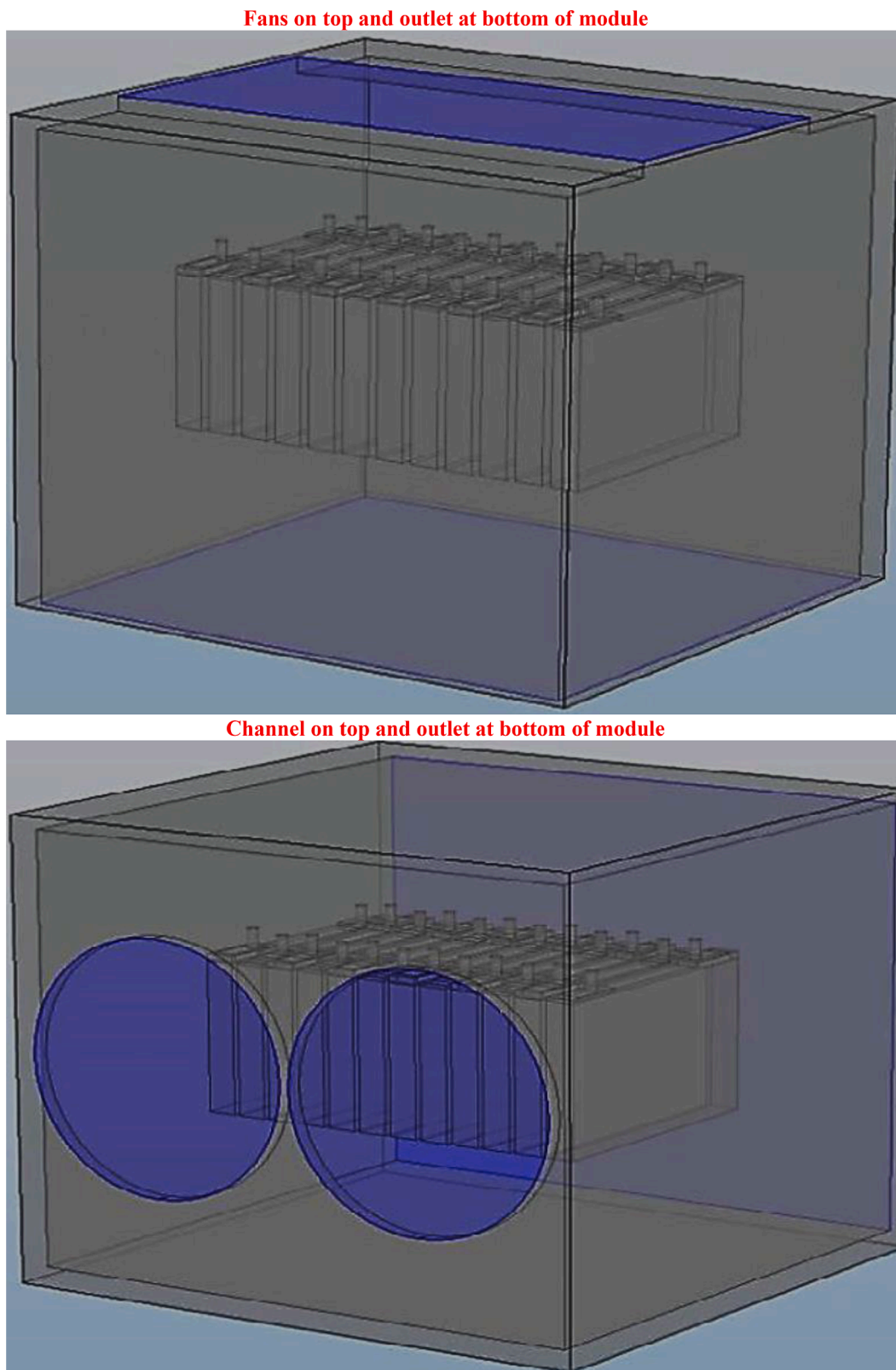
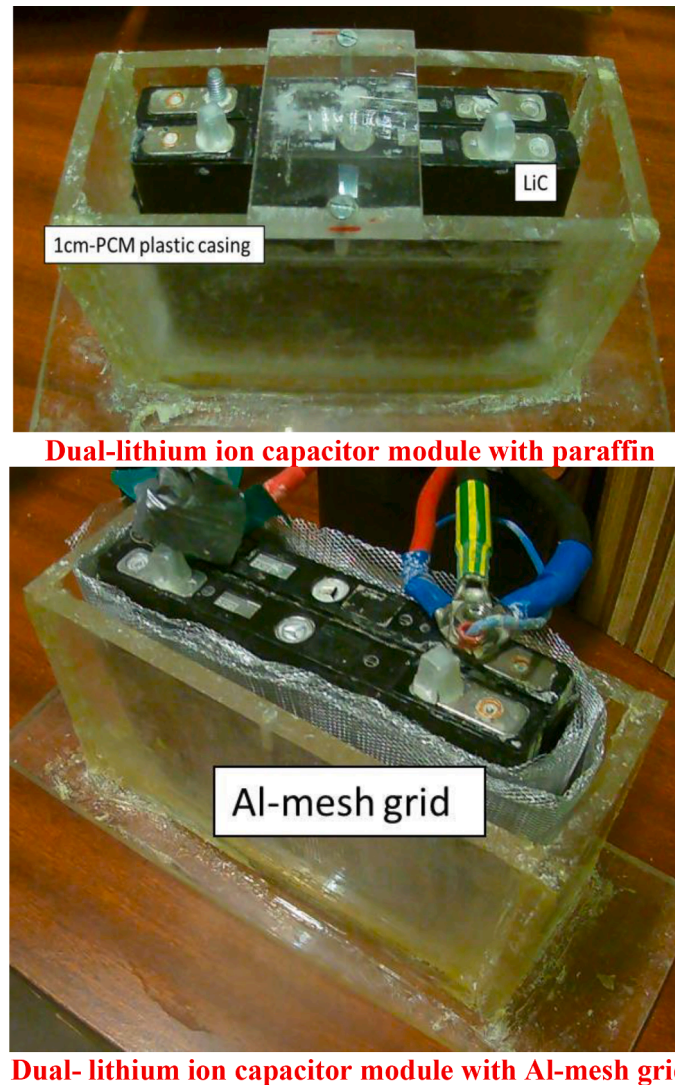


Fig. 46. (continued).

equation of the cell is employed for the description of the unsteady thermal distribution in the lithium ion capacitor, where the amount of produced heat should be stored in the cell or transferred from the cell to its surrounding. The heat produced by the battery is transferred to the cooling plates, and evacuated throughout the cooling ducts. They also

considered the stack of 12 cells spaced by the length of the cooling plate as the module. Their results showed that this liquid cooling strategy can successfully control the maximum temperature and decrease the temperature gradient owing to the high surface connection between the cooling duct and plates. This results in a more uniform temperature



Dual-lithium ion capacitor module with paraffin

Dual- lithium ion capacitor module with Al-mesh grid

Fig. 47. The lithium ion capacitor cell designed by Jaguemont et al. [136].

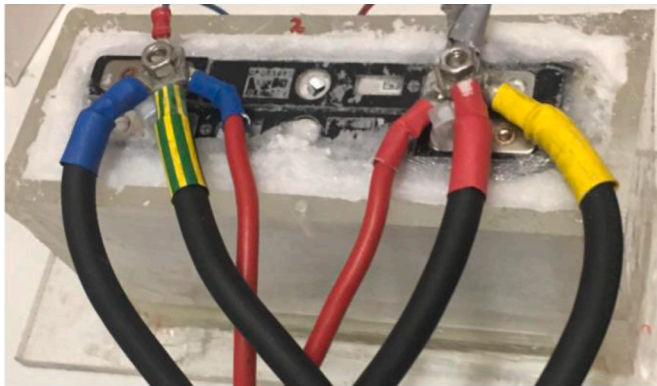


Fig. 48. The thermal management strategy used by Karimi et al. [148].

distribution of the cells in the pack.

Usage of phase change materials

Jaguemont et al. [136] employed paraffin as PCM for thermal management of small lithium ion capacitor with two cells (See Fig. 47). To enhance the thermal conductivity of paraffin, they added an aluminum mesh to the paraffin (See Fig. 48) which reduced the module

temperature for about 5 °C compared to when only paraffin was used. However, an extra active system, including liquid-cooled plates, should be combined with this cooling system for regeneration of PCMs, while such combination is yet to be studied. Karimi et al. [148] employed a similar methodology for the dual cell lithium ion capacitor module. They optimized the thickness of PCM and combined two PCMs with distinct phase change temperatures. These authors compared the performance of this combination with that of pure PCM showing that the maximum surface temperature of the module dropped over 2 °C.

5. Conclusions

Thermal management can heavily influence the performance of electrochemical energy technologies and is, therefore, of high significance. Understanding the fundamentals of heat generation and transport in electrochemical processes is central to achieving an effective control of temperature in electrochemical devices. There are also a large number of techniques for cooling of different electrochemical energy technologies. This review attempted to provide an in-depth coverage of the state-of-the-art in these fields with an emphasis on fuel cells, electrolyzers and supercapacitors. The main findings of this review are summarized as follows.

- The rate of heat generation in PEMFCs increases as the current density rises or the cell voltage drops. Consequently, at larger current densities, the rates of heat generation in PEMFCs exceed those of electricity generation. This poses major challenges on the thermal management of stacks, particularly for automotive applications that need to operate at high current densities.
- Working temperatures higher than 373 K makes the thermal management with heat spreaders practical for PEMFCs with larger active areas.
- The SOFC temperature range is mainly dominated by the oxygen ion conductivity across the electrolyte material. Currently, there exist research activities on new electrolyte materials operating at lower temperatures to lower the cost of the cell without jeopardizing performance.
- Liquid cooling is suitable for PEMFCs with high powers that can be implemented in electric vehicles, while air cooling can be used for PEMFCs with low powers employed in portable devices.
- De-ionizing filters are necessary when employing water or mixture of water/ethylene glycol as coolants in fuel cells. Deionization, however, features high capital and operational costs. Using nanofluid in the cooling loop can eliminate the need for de-ionizing filters.
- To avoid high temperature gradients across the active area of fuel cells; the thermal conductivities of the cooling plates should be very large. Because of their large thermal conductivity and small density, graphite based materials such as pyrolytic and expanded graphite are quite popular for the usage as the heat spreader in PEMFCs.
- Despite the low qualities of the heat captured from PEMFCs, the amount of heat in the coolant stream is suitable to be recovered and used in a number of applications. These include CHP, cooling in CCHP/CCP and power generation systems as well as preheating the inlet reactants and thermal management of metal hydride canister.
- New materials are being developed to reduce the operating temperature of SOFCs, while maintaining the efficiency close to those operating at higher temperatures. This requires improving ionic conductivities of the electrolytes at lower temperatures. Different approaches have been taken to improve the ionic conductivity of ceria-based electrolytes for intermediate temperature-SOFCs. These include manipulating ionic defects by doping or co-doping with aliovalent cations, nanocomposites, and tailoring the strain of the hetero-structure interface in the electrolyte thin film, while improving the electrodes' performance.
- In direct methanol fuel cells, a virtual increase in temperature enhances both anode and cathode kinetic parameters, however, the lack of the suitable dissipation of heat considerably increases the potential of thermal runaway.
- Two main strategies to limit thermal gradients in order to thermal management in the endothermic mode of SOECs were (i) heating through the recovery of heat stored in the exothermic mode and (ii) heating by hot fluids flowing inside the stack.
- Operating at or near the thermo-neutral voltage can simplify the thermal management of the stack of RSOC as no considerable excess flow of gas is needed and thermal stress in the components is minimized.
- PCMs used in the cooling process of supercapacitors must have a narrow range of melting temperature matching the operating temperatures of supercapacitors and, feature good latent heat. Paraffin waxes are attractive options due to their low costs and high chemical stabilities.
- Cellulose nanofibril materials in supercapacitors offer lower costs and controllable microstructures for thermal management, compared to the costly metal oxide pseudo-capacitor electrodes. The composite of cellulose nanofibrils enhances the ion and charge transferring rates, which in turn increase the power density and provide an efficient means of heat evacuation.
- Operating temperatures of supercapacitors leave considerable effects on the rate of self-discharging in supercapacitors. Ion mobility

enhances at higher temperatures, causing strong leakage currents and therefore faster self-discharging.

6. Future needs

Finally, the following future directions of research are proposed.

- Most of the existing strategies for thermal management of PEMFCs have been developed for steady operation. However, in practice, PEMFCs usually face a variety of complex operating conditions, and experience the transient loads. For example, the operation of vehicles includes starting, idling, accelerating, and shutting down processes. As a result, the temperature trends should be detected under the transient conditions and thermal management strategies of PEMFCs should be developed for such unsteady loads.
- Water-cooling particularly employing the phase change of saturated water has never been used for SOFCs stack design. High thermal conductivity and large latent heat of water enable thermal management and therefore, water-cooling of SOFCs sounds promising. The reason for not using SOFCs is not exactly known. However, it might be due to the significant temperature difference between SOFCs and the low saturation temperature of water at working pressure of SOFCs. SOFC stack can operate under the pressure of 5 to 10 atmosphere for the high power density. Hence, the challenge in water-cooling of SOFC would be to remove heat without overcooling. Further experimental studies are required to detect and address the challenges associated with water-cooling in the SOFCs.
- Heat recovery options from fuel cells have been studied extensively. However, comparatively less attention has been paid to the economic assessment of these systems. Performing exergy analysis for these systems helps understanding the thermo-economic performance of fuel cells heat recovery systems. In addition, utilizing the waste heat of fuel cells for desalination purposes deserves further studies.
- The existing thermal management techniques applied to SOFCs are highly focused on enhancing the overall heat transfer performance instead of efficient cooling for places with large heat generation. Further investigations on the local heat transfer improvement are recommended to control the temperature gradients in the SOFCs stacks.
- The long start-up time and heavy stainless steel envelop of heat pipes are two main challenges for their integration with fuel cells. Addressing these issues will significantly accelerate adoption of heat pipes in fuel cells used for mobile applications.
- There are only few studies on managing the electrical and thermal energies of SOFCs simultaneously for attaining both safety and high thermal performance.
- Durability issues regarding thermal management require more attention. Currently, the physics behind the detected degradation related to thermal management are not fully understood. Nonetheless, the correlations between material attributes and thermally related degradation are most useful for designing more durable fuel cell materials.
- Micro-supercapacitors have high potentials for the usage in future electronic systems. This type of supercapacitors is still in the initial steps of development. Further studies on the thermal management of micro-supercapacitors are required. In particular, new models should be developed to further understand thermal transport in such small-scale structures.
- Currently, there is no a comprehensive physics-based model for understanding thermal behavior of supercapacitors. Such a model should consider thermophysical attributes of all employed materials and the heat generated from all sources. This can facilitate development of new effective cooling strategies to avoid overheating and to diminish the associated problems including aging and performance decay.

- More studies should be conducted on the aging and degradation rates at different operating conditions of electrolyzers. In electrolyzers, high temperature usually helps improving electrochemical efficiency, while it may also accelerate the degradation rates. Information about the aging and degradation rate is useful for finding the optimal operating points under different situations.
- The surplus heat generated by electrolyzers can be potentially utilized. Combining the cooling systems of electrolyzers with higher temperature heat sources might be a viable option to increase the quality of surplus heat from electrolyzers.
- The PCMs seem to be attractive for absorption of the heat generated in lithium ion capacitors. However, when the tests are changed from cells to packs, PCMs cannot receive all the waste heat. As a result, an innovative hybrid cooling system composed of PCMs and active cooling technique (air cooling or liquid cooling) would be quite effective. Future studies can investigate such systems for vehicle applications.
- Supercapacitors, as high-performance electrochemical energy storage equipment, are designed to combine the benefits of rechargeable batteries with the benefits of supercapacitors [318]. Future studies can investigate the thermal management of these equipment.

Declaration of Competing Interest

On behalf of all co-authors, I wish to confirm that there are no known conflicts of interest associated with this publication and there has been no significant financial support for this work that could have influenced its outcome.

I confirm that the manuscript has been read and approved by all named authors and that there are no other persons who satisfied the criteria for authorship but are not listed. I further confirm that the order of authors listed in the manuscript has been approved by all co-authors.

Acknowledgment

N. Karimi acknowledges the financial support by the Engineering and Physical Science Research Council (EPSRC) through the grant number EP/V036777/1. Kyung Chun Kim acknowledges the financial support by the National Research Foundation of Korea (NRF) grant, funded by the Korean government (MSIT) (no. 2020R1A5A8018822). Bengt Sundén acknowledges financial support from the Scientific Council of Sweden (VR).

References

- [1] Abdelaziz EA, Saidur R, Mekhilef S. A review on energy saving strategies in industrial sector. *R Sustain Energy Rev* 2011;15:150–68.
- [2] Abderezak B. Heat transfer phenomena. introduction to transfer phenomena in PEM. *Fuel Cell* 2018;125–53.
- [3] Abdollahipour A, Sayyaadi H. Thermal energy recovery of molten carbonate fuel cells by thermally regenerative electrochemical cycles. *Energy* 2021;227:120489.
- [4] Abeywardana DBW, Hredzak B, Agelidis VG. Battery-supercapacitor hybrid energy storage system with reduced low frequency input current ripple. In: International Conference on Renewable Energy Research and Applications. (ICRERA); 2015.
- [5] Acharya PR. An advanced fuel cell simulator [thesis]. Houston-Dallas-Austin, TX: Texas A&M University; 2004.
- [6] Addo PK, Molero-Sanchez B, Chen M, Paulson S, Birss V. CO/CO₂ study of high performance La_{0.3}Sr_{0.7}Fe_{0.7}Cr_{0.3}O_{3-δ} reversible SOFC electrodes. *Fuel Cells* 2015;15:689–96.
- [7] Ajith Kumar S, Kuppusami P. Enhancing the ionic conductivity in the ceria-based electrolytes for intermediate temperature solid oxide fuel cells, chapter 5 in book of electrolytes, electrodes and interconnects. Elsevier; 2020. p. 113–63.
- [8] Akbari M, Tamayol A, Bahrami M. Thermal assessment of convective heat transfer in air-cooled PEMFC stacks: an experimental study. *Energy Procedia* 2012;29:1–11.
- [9] Akilu S, Baheta AT, Sharma KV. Evaluation on thermo-electrical characteristics of SiO₂ nanofluids for fuel cell cooling application in automobiles. *Int J Eng Technol* 2018;7:137–40.
- [10] Alizadeh R, Mohebbi Najm Abad J, Fattahi A, Alhajri ES, Karimi N. Application of machine learning to investigation of heat and mass transfer over a cylinder

- surrounded by porous media-The radial basic function network. *J Energy Resour Technol* 2020;142:112109.
- [11] Alizadeh R, Mohebbi Najm Abad J, Fattahi A, Mohebbi MR, Doranehgard MH, Li LKB, et al. A machine learning approach to predicting the heat convection and thermodynamics of an external flow of hybrid nanofluid. *ASME J Energy Resour Technol* 2021. In press.
 - [12] Al-Masri A, Peksen M, Blum L, Stolten D. A 3D CFD model for predicting the temperature distribution in a full scale APU SOFC short stack under transient operating conditions. *Appl Energy* 2014;135:539–47.
 - [13] Al Sakka M, Gualous H, Mierlo JV, Culcu H. Thermal modeling and heat management of supercapacitor modules for vehicle applications. *J Power Source* 2009;194:581–7.
 - [14] Al-Zareer M, Dincer I, Rosen MA. A review of novel thermal management systems for batteries. *Int J Energy Res* 2018;42:3182–205.
 - [15] An Z, Jia L, Ding Y, Dang C, Li X. A review on lithium-ion power battery thermal management technologies and thermal safety. *J Therm Sci* 2017;26:391–412.
 - [16] Andreasen SJ, Ashworth L, Remn IN, Rasmussen PL, Nielsen MP. Modeling and Implementation of a 1 kW, air cooled HTPEM fuel cell in a hybrid electrical vehicle. *ECS Trans* 2008;12:639–50.
 - [17] APEC. Water Deionization Process Explained. Available at: <http://www.freedrinkingwater.com/water-education/2/49-water-di-process.htm>, 2014.
 - [18] Ariyanfar L, Ghadamian H, Baghban Yousefkhani M, Ozgoli HA. A double pipe heat exchanger design and optimization for cooling an alkaline fuel cell system. *Iran J Hydrog Fuel Cell* 2014;4:223–31.
 - [19] Armand M, Endres F, MacFarlane DR, Ohno H, Scrosati B. Ionic-liquid materials for the electrochemical challenges of the future. *Nat Mater* 2009;8:621–9.
 - [20] Atan R, Najmi WM WA. Temperature profiles of an air-cooled pem fuel cell stack under active and passive cooling operation. *Procedia Eng* 2012;41:1735–42.
 - [21] Atreya S, Mata ME, Balan C. Thermal management of a high temperature fuel cell electrolyzer. Patent 2010. US8231774.
 - [22] Ayadi M, Eddahech A, Briat O, Vinassa JM. Voltage and temperature impacts on leakage current in calendar ageing of supercapacitors. In: 4th international conference on power engineering Istanbul; 2013. p. 1466–70.
 - [23] Bahiraie F, Fartaj A, Nazri GA. Electrochemical-thermal modeling to evaluate active thermal management of a lithium-ion battery module. *Electrochim Acta* 2017;254:59–71.
 - [24] Barbir F. PEM fuel cells: theory and practice. Amsterdam: Elsevier Academic Press; 2005.
 - [25] Bard AJ, Faulkner LR. *Electrochemical methods fundamentals and applications*. 2nd ed. New York: John Wiley & Sons; 2001.
 - [26] Baroutaji A, Wilberforce T, Ramadan M, Olabi AG. Comprehensive investigation on hydrogen and fuel cell technology in the aviation and aerospace sectors. *Renew Sustain Energy Rev* 2019;106:31–40.
 - [27] Barsukov IV, Johnson CS, Doninger JE, Barsukov VZ. New carbon based materials for electrochemical energy storage systems: batteries, supercapacitors and fuel cells. Dordrecht: Springer Netherlands; 2006.
 - [28] Berning T, Lu DM, Djiali N. Three-dimensional computation analysis of transport phenomena in a PEM fuel cell. *J Power Source* 2002;106:284–94.
 - [29] Bhuvana T, Kumar A, Sood A, Gerzeski RH, Hu J, Bhadram VS, Narayana C, Fisher TS. Contiguous petal-like carbon nanosheet outgrowths from graphite fibers by plasma CVD. *ACS Appl Mater Inter* 2010;2:644–8.
 - [30] Bierschenk DM, Wilson JR, Barnett SA. High efficiency electrical energy storage using a methane-oxygen solid oxide cell. *Energy Environ Sci* 2011;4:944–51.
 - [31] Bird RB, Stewart WE, Lightfoot EN. *Transport phenomena*. 2nd ed. New York: John Wiley & Sons; 2007.
 - [32] Bittner AM, Zhu M, Yang Y, Waibel HF, Konuma M, Starke U, et al. Ageing of electrochemical double layer capacitors. *J Power Source* 2012;203:262–73.
 - [33] Bockris JOM, Conway BE, Yeager E, White RE. *Comprehensive treatise of electrochemistry*. New York: Plenum Press; 1981.
 - [34] Hansen JB. Solid oxide electrolysis—a key enabling technology for sustainable energy scenarios. *Faraday Discuss* 2015;182:9–48.
 - [35] Bohlen O, Kowal J, Sauer DU. Ageing behaviour of electrochemical double layer capacitors Part I. Experimental study and ageing model. *J Power Source* 2007;172:468–75. a.
 - [36] Bohlen O, Kowal J, Uwe SD. Ageing behaviour of electrochemical double layer capacitors Part II. Lifetime simulation model for dynamic applications. *J Power Source* 2007;173:626–32. b.
 - [37] Borges RS, Reddy ALM, Rodrigues MTF, Gullapalli H, Balakrishnan K, Silva GG, Ajayan PM. Supercapacitor operating at 200 °C. *Sci Rep-Uk* 2013;3. <https://doi.org/10.1038/srep02572>.
 - [38] Boroumandjazi G, Rismanchi B, Saidur R. A review on energy analysis of industrial sector. *Renew Sustain Energy Rev* 2013;27:198–203.
 - [39] Bosio B, Marra D, Arato E. Thermal management of the molten carbonate fuel cell plane. *J Power Source* 2010;195:4826–34.
 - [40] Brandon NP, Matian M, Marquis AJ, Adjimar CS. Thermal management issues in fuel cell technology. In: Proceedings of the 14th International Heat Transfer Conference IHTC14; August 8-13, 2010.
 - [41] J. E. O'Brien, Thermodynamic Considerations for Thermal Water Splitting Processes and High Temperature Electrolysis, Proceedings of the 2008 International Mechanical Engineering Congress and Exposition, IMECE2008, October 31 – November 6, 2008, Boston, Massachusetts, USA.
 - [42] El Brouji H, Briat O, Vinassa J-M, Henry H, Woigard E. Analysis of the dynamic behavior changes of supercapacitors during calendar life test under several voltages and temperatures conditions. *Microelectron Reliab* 2009;49:1391–7.
 - [43] Brousse T, Toupin M, Bélanger D. A hybrid activated carbon-manganese dioxide capacitor using a mild aqueous electrolyte. *J Electrochem Soc* 2004;151:A614.

- [44] Burheim OS, Pharoah JG, Lampert H, Vie PJS, Kjelstrup S. Through-plane thermal conductivity of PEMFC porous transport layers. *J Fuel Cell Sci Technol* 2011;8: 021013.
- [45] Cai Q, Brandon NP, Adjiman CS. Modelling the dynamic response of a solid oxide steam electrolyser to transient inputs during renewable hydrogen production. *Front Energy* 2010;4:211–22.
- [46] Caney N, Marechal A, Marty P. Study of a new geometry for fuel cells cooling. *Mecanique Ind* 2007;8:545–9.
- [47] Gengel YA, Ghajar AJ. Heat and mass transfer fundamentals and applications. fourth ed. New York, USA: McGraw Hill Inc.; 2011.
- [48] Chan SH, Ho HK, Tian Y. Modelling of simple hybrid solid oxide fuel cell and gas turbine power plant. *J Power Source* 2002;109:111–20.
- [49] Chang HC, Gustave W, Yuan ZF, Xiao Y, Chen Z. One-step fabrication of binder-free air cathode for microbial fuel cells by using balsa wood biochar. *Environ Technol Innov* 2020;18:100615.
- [50] Chen M, Sun Q, Li Y, Wu K, Liu B, Peng P, Wang Q. A thermal runaway simulation on a lithium titanate battery and the battery module. *Energies* 2015;8:490–500.
- [51] Chen J, Kang S, E J, Huang Z, Wei K, Zhang B, et al. Effects of different phase change material thermal management strategies on the cooling performance of the power lithium ion batteries: a review. *J Power Source* 2019;442:227228.
- [52] Chi J, Yu H. Water electrolysis based on renewable energy for hydrogen production. *Chin J Catal* 2018;39:390–4.
- [53] Chinda P, Brault P. The hybrid solid oxide fuel cell (SOFC) and gas turbine (GT) systems steady state modeling. *Int J Hydrog Energy* 2012;37:9237–48.
- [54] Chippar P, Ko J, Ju H. A global transient, one-dimensional, two-phase model for direct methanol fuel cells (DMFCs) - Part II: analysis of the time-dependent thermal behavior of DMFCs. *Energy* 2010;35:2301–8.
- [55] Chnani M, Péra MC, Glises R, Kauffmann JM, Hissel D. Transient thermal behaviour of a solid oxide fuel cell. In: *The Fifth International Conference on Fuel Cell Science, Engineering and Technology*; Jun 2007. p. 28. hal-00582364.
- [56] Choi SU, Eastman J. Enhancing thermal conductivity of fluids with nanoparticles. IL (United States): Argonne National Lab; 1995.
- [57] Choi EJ, Park JY, Kim MS. Two-phase cooling using HFE-7100 for polymer electrolyte membrane fuel cell application. *Appl Therm Eng* 2019;148:868–77.
- [58] Choudhari VG, Dhoble AS, Sathe TM. A review on effect of heat generation and various thermal management systems for lithium ion battery used for electric vehicle. *J Energy Storage* 2020;32:101729.
- [59] Christopher P, Wendel H, Kazempoor P, Braun RJ. A thermodynamic approach for selecting operating conditions in the design of reversible solid oxide cell energy systems. *J Power Source* 2016;301:93–104.
- [60] Clement J, Wang X. Experimental investigation of pulsating heat pipe performance with regard to fuel cell cooling application. *Appl Therm Eng* 2013; 50:268–74.
- [61] Cocco D, Tola V. Externally reformed solid oxide fuel cell–micro-gas turbine (SOFC–MGT) hybrid systems fueled by methanol and di-methyl-ether (DME). *Energy* 2009;34:2124–30.
- [62] Colombo P. Solid oxide electrolysis system: Dynamic modelling and microgrid integration. Master's degree thesis in Energy and Nuclear Engineering. Polytechnic University of Turin; 2018.
- [63] Edited by Corre GPG, Irvine JTS. High temperature fuel cell technology. In: Stolten D, editor. *Hydrogen and fuel cells: fundamentals, technologies and applications*. Wenham: Wiley-VCH Verlag; 2010. p. 61–88.
- [64] Costamagna P, Magistri L, Massardo AF. Design and part-load performance of a hybrid system based on a solid oxide fuel cell reactor and a micro gas turbine. *J Power Source* 2001;96:352–68.
- [65] Cuevas FG, Montes JM, Cintas J, Urban P. Electrical conductivity and porosity relationship in metal foams. *J Porous Mater* 2009;16:675–81.
- [66] Dai W, Wang H, Yuan X-Z, Martin JJ, Yang D, Qiao J, et al. A review on water balance in the membrane electrode assembly of proton exchange membrane fuel cells. *Int J Hydrog Energy* 2009;34:9461–78.
- [67] Damm DL, Fedorov AG. Radiation heat transfer in SOFC materials and components. *J Power Source* 2005;143:158–65.
- [68] Da Silva LM, Cesar R, Moreira CMR, Santos JHM, De Souza LG, Pires BM, et al. Reviewing the fundamentals of supercapacitors and the difficulties involving the analysis of the electrochemical findings obtained for porous electrode materials. *Energy Storage Mater* 2020;27:555–90.
- [69] Das V, Padmanaban S, Venkitesamy K, Selvamuthukumar R, Blaabjerg F, Siano P. Recent advances and challenges of fuel cell based power system architectures and control – a review. *Renew Sustain Energy Rev* 2017;73:10–8.
- [70] De las Heras A, Vivas FJ, Segura F, Redondo MJ, Andújar JM. Air-Cooled fuel cells: keys to design and build the oxidant/cooling system. *Renew Energy* 2018; 125:1–20.
- [71] Deyab MA, Mele G. Stainless steel bipolar plate coated with polyaniline/Zn-Porphyrin composites coatings for proton exchange membrane fuel cell. *Sci Rep* 2020;10:3277.
- [72] Di Giorgio P, Desideri U. Potential of reversible solid oxide cells as electricity storage system. *Energies* 2016;9:662.
- [73] Diab Y, Venet P, Gualous H, Rojat G. Self-discharge characterization and modeling of electrochemical capacitor used for power electronics applications. *IEEE Trans Power Electron* 2009;24:510–7.
- [74] Dicks AL, Fellows RG, Mescal CM, Seymour C. A study of SOFC-PEM hybrid systems. *J Power Source* 2000;86:501–6.
- [75] Dillig M, Karl J. Thermal management of high temperature solid oxide electrolyser cell/fuel cell systems. *Energy Procedia* 2012;28:37–47.
- [76] Dillig M, Leimert J, Karl J. Planar high temperature heat pipes for SOFC/SOEC stack applications. *Fuel Cells* 2014;14:479–88.
- [77] Dillig M. Thermal management of solid oxide cell systems with integrated planar heat pipes, a thesis submitted to the faculty of engineering. University of Erlangen-Nuremberg; 2016.
- [78] Ding H. Nanostructured electrodes for high-performing solid oxide fuel cells. book: nanostructured materials for next-generation energy storage and conversion. 2018.
- [79] DoE. Program Plans, Roadmaps, and Vision Documents: the Department of Energy Hydrogen and Fuel Cells Program Plan. Available at: http://www.hydrogen.energy.gov/pdfs/program_plan2011.pdf, 2011.
- [80] Dohle H, Mergel J, Stolten D. Heat and power management of a direct-methanol-fuel-cell (DMFC) system. *J Power Source* 2002;111:268–82.
- [81] Dong W, Cao GY, Zhu XJ. Nonlinear modelling and adaptive fuzzy control of PEMFC. *Engineering Modelling* 2003;16:13–21.
- [82] M.C. Dos Santos, L.S. Parreira, F. DeMoura Seuzá, J. Camarge Junior, T. Gentil, Fuel Cells: hydrogen and Ethanol Technologies. In: S. Hashmi, Editor, *Reference module in materials science and materials engineering*. Oxford: Elsevier; 2017. p. 1–21. DOI:10.1016/B978-0-12-803581-8.09263-8.
- [83] Dos Santos AL, Cebola MJ, Santos DMF. Towards the hydrogen economy – A review of the parameters that influence the efficiency of alkaline water electrolyzers. *Energies* 2021;14.
- [84] Dziurdzia B, Magonski Z, Jankowski H. Commercialisation of solid oxide fuel cells-opportunities and forecasts. *Mater Sci Eng* 2016;104:012020.
- [85] Elder R, Cumming D, Bjerg Mogensen M. High temperature electrolysis, carbon dioxide utilisation. *Closing Carbon Cycle* 2015;35:183–209.
- [86] Evolvey V, Gebreegziabher T. A review of projected power-to-gas deployment scenarios. *Energies* 2018;11:1824.
- [87] European Hydrogen and Fuel Cell Technology Platform, *Strategic Research Agenda*. Available online: https://www.fch.europa.eu/sites/default/files/documents/hfp-sra004_v9-2004_sra-report-final_22jul2005.pdf (accessed on 23 July 2019).
- [88] Fallah Vostakola M, Horri BA. Progress in material development for low-temperature solid oxide fuel cells: a review. *Energies* 2021;14:1280.
- [89] Faghri A, Guo Z. Challenges and opportunities of thermal management issues related to fuel cell technology and modeling. *Int J Heat Mass Transf* 2005;48: 3891–920.
- [90] Faghri A, Guo Z. Integration of heat pipe into fuel cell technology. *Heat Transf Eng* 2008;29:232–8.
- [91] Falcão DS, Pires JCM, Pinho C, Pinto AMFR, Martins FG. Artificial neural network model applied to a PEM fuel cell. In: *IJCCI 2009 - Proceedings of the International Joint Conference on Computational Intelligence*; 2009. October 5–7.
- [92] Fardadi M, McLarty DF, Jabbari F. Investigation of thermal control for different SOFC flow geometries. *Appl Energy* 2016;178:43–55.
- [93] Felseghi RA, Carcadea E, Simona Raboaca M, Trufin CN, Filote C. Hydrogen fuel cell technology for the sustainable future of stationary applications. *Energies* 2019;12:4593.
- [94] Fergus JW. Materials challenges for solid-oxide fuel cells. *JOM* 2007;59:56–62.
- [95] Fly A. Thermal and water management of evaporatively cooled fuel cell vehicles, a doctoral thesis submitted in partial fulfilment of the requirements for the award of. Degree of Doctor of Philosophy of Loughborough University; 2015.
- [96] Fly A, Thring RH. Temperature regulation in an evaporatively cooled proton exchange membrane fuel cell stack. *Int J Hydrog Energy* 2015;40:11976–82.
- [97] Fly A, Thring RH. A comparison of evaporative and liquid cooling methods for fuel cell vehicles. *Int J Hydrog Energy* 2016;41:14217–29.
- [98] Foteini Sapountzi M, Jose Gracia M, (Kees-Jan) Weststrate CJ, Hans, Fredriksson OA, (Hans) Niemantsverdriet JW. Electrocatalysts for the generation of hydrogen, oxygen and synthesis gas. *Prog Energy Combust Sci* 2017;58:1–35.
- [99] Franco A. Optimization of separate air flow cooling system for Polymer Electrolyte Membrane (PEM) Fuel Cells. In: *27th UIT Heat Transfer Conferene, Reggio Emilia*; 2009.
- [100] Fuel Cells 2000. Fuel cell vehicles (from auto manufacturers), <http://www.fuelcells.org/info/charts/carchart.pdf>; 2011.
- [101] Frano B. PEM fuel cells: theory and practice. Academic, Burlington Google Scholar; 2005.
- [102] Fronk MH, Wetter DL, Masten DA, Bosco A. PEM fuel cell system solutions for transportation. *SAE Int J Fuel Lubr* 2000;109:212–9.
- [103] Galland N, Romanowicz K, Züttel A. An analytical model for the electrolyser performance derived from materials parameters. *J Power Energy Eng* 2017;5: 34–49.
- [104] Gao X, Andreasen SJ, Kær SK, Rosendahl LA. Optimization of a thermoelectric generator subsystem for high temperature PEM fuel cell exhaust heat recovery. *Int J Hydrog Energy* 2014;39:6637–45.
- [105] Gao Z, Mogni LV, Miller EC, Railsback JG, Barnett SA. A perspective on low-temperature solid oxide fuel cells. *Energy Environ Sci* 2016;9:1602–44.
- [106] Garg A, Vijayaraghavan V, Mahapatra SS, Tai K, Wong CH. Performance evaluation of microbial fuel cell by artificial intelligence methods. *Expert Syst Appl* 2014;41:1389–99.
- [107] Garrity PT, Klausner JF, Mei R. A flow boiling microchannel evaporator plate for fuel cell thermal management. *Heat Transf Eng* 2007;28:877–84.
- [108] Goebel SG. Evaporative cooled fuel cell. Google Patents; 2005.
- [109] Gómez SY, Hotza D. Current developments in reversible solid oxide fuel cells. *Renew Sustain Energy Rev* 2016;61:155–74.
- [110] González A, Goikolea E, Barrena JA, Mysyk R. Review on supercapacitors: technologies and materials. *Renew Sustain Energy Rev* 2016;58:1189–206.
- [111] Gualous H, Louahlia H, Gallay R. Supercapacitor characterization and thermal modelling with reversible and irreversible heat effect. *IEEE Trans Power Electron* 2011;26:3402–9.

- [112] Gualous H, Gallay R. Supercapacitor module sizing and heat management under electric, thermal, and aging constraints. Wiley. KGaA 2013.
- [113] Guk E, Venkatesan V, Babar S, Jackson L, Kim JS. Parameters and their impacts on the temperature distribution and thermal gradient of solid oxide fuel cell. *Appl Energy* 2019;241:164–73.
- [114] Guthrie DG, Torabi M, Karimi N. Combined heat and mass transfer analyses in catalytic microreactors partially filled with porous material-The influences of nanofluid and different porous-fluid interface models. *Int J Therm Sci* 2019;140:96–113.
- [115] Habib R, Karimi N, Yadollahi B, Doranehgard MH, Li LKB. A pore-scale assessment of the dynamic response of forced convection in porous media to inlet flow modulations. *Int J Heat Mass Transf* 2020;153:119657. a.
- [116] Habib R, Yadollahi B, Karimi N, Doranehgard MH. On the unsteady forced convection in porous media subject to inlet flow disturbances-A pore-scale analysis. *Int Commun Heat Mass Transf* 2020;116:104639. b.
- [117] Hahn M, Kötzer R, Gallay R, Siggel A. Pressure evolution in propylene carbonate based electrochemical double layer capacitors. *Electrochim Acta* 2006;52:1709–12.
- [118] Han J, Yu S. Ram air compensation analysis of fuel cell vehicle cooling system under driving modes. *Appl Therm Eng* 2018;142:530–42.
- [119] Hasanuzzaman M, Rahim NA, Hosenuzzaman M, Saidur R, Mahbubul IM, Rashid MM. Energy savings in the combustion based process heating in industrial sector. *Renew Sustain Energy Rev* 2012;16:4527–36.
- [120] Hashmi SMH. Cooling strategies for pem fc stacks, thesis. Universität der Bundeswehr Hamburg; 2010.
- [121] Hasani M, Rahbar N. Application of thermoelectric cooler as a power generator in waste heat recovery from a PEM fuel cell—an experimental study. *Int J Hydrog Energy* 2015;40:15040–51.
- [122] Hauge HH, Presser V, Burheim O. In-situ and ex-situ measurements of thermal conductivity of supercapacitors. *Energy* 2014;75:373–83.
- [123] Hawes DW, Feldman D. Absorption of phase change materials in concrete. *Sol Energy Mater Sol Cells* 1992;27:91–101.
- [124] Haynes C, Wepfer WJ. Characterizing heat transfer within a commercial-grade tubular solid oxide fuel cell for enhanced thermal management. *Int J Hydrog Energy* 2001;26:369–79.
- [125] Hedayat N, Du Y, Ilkhani H. Pyrolyzable pore-formers for the porous-electrode formation in solid oxide fuel cells: a review. *Ceram Int* 2018;44:4561–76.
- [126] Hemmat Esfe M, Afrand M. A review on fuel cell types and the application of nanofluid in their cooling. *J Therm Anal Calorim* 2020;140:1633–54.
- [127] Hermann A, Chaudhuri T, Spagnol P. Bipolar plates for PEM fuel cells: a review. *Int J Hydrog Energy* 2005;30:1297–302.
- [128] Hsing I, Futerko P. Two-dimensional simulation of water transport in polymer electrolyte fuel cells. *Chem Eng Sci* 2000;55:4209–18.
- [129] Hu CC, Chen WC, Chang KH. How to achieve maximum utilization of hydrous ruthenium oxide for supercapacitors. *J Electrochem Soc* 2004;151:A281–90.
- [130] Huang Y-H, Dass RI, King Z-L, Goodenough JB. Double perovskites as anode materials for solid-oxide fuel cells. *Science* 2006;312:254–7.
- [131] Huang S, Zhu X, Sarkar S, Zhao Y. Challenges and opportunities for supercapacitors. *APL Mater* 2019;7:100901.
- [132] Hwang JJ, Zou ML, Chang WR, Su A, Weng FB, Wu W. Implementation of a heat recovery unit in a proton exchange membrane fuel cell system. *Int J Hydrog Energy* 2010;35:8644–53.
- [133] Ishizawa M, Okada S, Yamashita T. Highly efficient heat recovery system for phosphoric acid fuel cells used for cooling telecommunication equipment. *J Power Source* 2000;86:294–7.
- [134] Islam MR, Shabani B, Rosengarten G, Andrews J. The potential of using nanofluids in PEM fuel cell cooling systems: a review. *Renew Sustain Energy Rev* 2015;48:523–39.
- [135] Jaguemont J, Ghamraoui A-M, Omar N, Hergazy O, Ronsmans J, Soltani M, Van Den Bossche P, Van Mierlo J. Liquid thermal management of a lithium-ion capacitor module. In: *EVS 2017 - 30th Int. Electr. Veh. Symp. Exhib.*; 2017.
- [136] Jaguemont J, Karimi D, Van Mierlo J. Investigation of a passive thermal management system for lithium-ion capacitors. *IEEE Trans Veh Technol* 2019;68:10518–24.
- [137] Jensen SH, Larsen PH, Mogensen M. Hydrogen and synthetic fuel production from renewable energy sources. *Int J Hydrog Energy* 2007;32:3253–7.
- [138] Jensen SH, Graves C, Mogensen M, Wendel C, Braun R, Hughes G, Gao Z, Barnett SA. Large-scale electricity storage utilizing reversible solid oxide cells combined with underground storage of CO₂ and CH₄. *Energy Environ Sci* 2015;8:2471–9.
- [139] Jiang K, Liao G, Jiaqiang E, Zhang F, Chen J, Leng E. Thermal management technology of power lithium-ion batteries based on the phase transition of materials: a review. *J Energy Storage* 2020;32:101816.
- [140] Jiao K, Li X. Water transport in polymer electrolyte membrane fuel cells. *Prog Energy Combust Sci* 2011;37:221–91.
- [141] Jiao K, Ni M. Challenges and opportunities in modelling of proton exchange membrane fuel cells (PEMFC). *Int J Energy Res* 2017;41:1793–7.
- [142] Jilte RD, Kumar R. Numerical investigation on cooling performance of Li-ion battery thermal management system at high galvanostatic discharge, *Engineering Science and Technology. Int J* 2018;21:957–69.
- [143] Ju H, Meng H, Wang C-Y. A single-phase, non-isothermal model for PEM fuel cells. *Int J Heat Mass Transf* 2005;48:1303–15.
- [144] Kadier A, Simayi Y, Abdeshahian P, Farhana Azman N, Chandrasekhar K, Kalil MdS. A comprehensive review of microbial electrolysis cells (MEC) reactor designs and configurations for sustainable hydrogen gas production. *Alex Eng J* 2016;55:427–43.
- [145] Kai J, Saito R, Terabaru K, Li H, Nakajima H, Ito K. Effect of temperature on the performance of polymer electrolyte membrane water electrolysis: numerical analysis of electrolysis voltage considering gas/liquid two-phase flow. *J Electrochem Soc* 2019;166:F246–54.
- [146] Kandlikar SG, Lu Z. Fundamental research needs in combined water and thermal management within a proton exchange membrane fuel cell stack under normal and cold-start conditions. *J Fuel Cell Sci Technol* 2009;6:044001.
- [147] Kandlikar SG, Lu Z. Thermal management issues in a PEMFC stack—A brief review of current status. *Appl Therm Eng* 2009;29:1276–80.
- [148] Karimi D, Behi H, Jaguemont J, Sokkeh MA, Kalogiannis T, Hosen MS, et al. Thermal performance enhancement of phase change material using aluminum-mesh grid foil for lithium-capacitor modules. *J Energy Storage* 2020;30:101508.
- [149] Kazemipoor P, Braun R. Model validation and performance analysis of regenerative solid oxide cells: electrolytic operation. *Int J Hydrog Energy* 2014;39:2669–84.
- [150] Kharel S, Shabani B. Hydrogen as a long-term large-scale energy storage solution to support renewables. *Energies* 2018;11:2825.
- [151] Khateeb SA, Farid MM, Selman JR, Al-Hallaj S. Design and simulation of a lithium-ion battery with a phase change material thermal management system for an electric scooter. *J Power Source* 2004;128:292–307.
- [152] Khotseng L. *Fuel Cell Thermodynamics*. IntechOpen 2019. <https://doi.org/10.5772/intechopen.90141>.
- [153] Kim DH, Kim BJ, Lim HC, Lee CG. Numerical studies of a separator for stack temperature control in a molten carbonate fuel cell. *Int J Hydrog Energy* 2011;36:8499–507.
- [154] Kim IH, Kim KB. Electrochemical characterization of hydrous ruthenium oxide thin-film electrodes for electrochemical capacitor applications. *J Electrochem Soc* 2006;153:A383–9.
- [155] Kim J, Oh J, Lee H. Review on battery thermal management system for electric vehicles. *Appl Therm Eng* 2019;149:192–212.
- [156] Ko R, Carlen M. Principles and applications of electrochemical capacitors. *Electrochim Acta* 2000;45:2483–98.
- [157] Kone1 JP, Zhang X, Yan Y, Hu G, Ahmadi G. Three-dimensional multiphase flow computational fluid dynamics models for proton exchange membrane fuel cell: a theoretical development. *J Comput Multiph Flow* 2017;9:3–25.
- [158] Kordi M, Jabari Moghadam A, Afshari E. Effects of cooling passages and nanofluid coolant on thermal performance of polymer electrolyte membrane fuel cells. *J Electrochem Energy Convers Storage* 2019;16:031001.
- [159] Kötzer R, Hahn M, Gallay R. Temperature behavior and impedance fundamentals of supercapacitors. *J Power Source* 2006;154:550–5.
- [160] Kotz R, Ruch PW, Cericola D. Aging and failure mode of electrochemical double layer capacitors during accelerated constant load tests. *J Power Source* 2010;195:923–8.
- [161] Kuar G. *Intermediate temperature solid oxide fuel cells electrolytes, electrodes and interconnects*. Book: published by Elsevier; 2020. <https://doi.org/10.1016/C2018-0-00575-7>.
- [162] Kumar P, Chaudhary D, Varshney P, Varshney U, Yahya SM, Rafat Y. Critical review on battery thermal management and role of nanomaterial in heat transfer enhancement for electrical vehicle application. *J Energy Storage* 2020;32:102003.
- [163] Larminie J, Dicks A. *Fuel cell systems explained*. 2 editor. Chichester, West Sussex: John Wiley & Sons; 2003.
- [164] Larminie J, Dicks A. *Fuel cell systems explained*. 2nd ed. Wiley; 2006.
- [165] Laurencin J, Kane D, Delette G, Deseure J, Lefebvre-Joud F. Modelling of solid oxide steam electrolyser: impact of the operating conditions on hydrogen production. *J Power Source* 2011;196:2080–93.
- [166] Laurencin J, Delette G, Reyter M. High-temperature or fuel-cell electrochemical system having improved thermal management. Patent, 2013. WO2013/060869.
- [167] S.K. Lee, Y.H. Han, W. Lee, W. Ryu, Cooperation Foundation, US Patent, 2015. <http://patentimages.storage.googleapis.com/09/a3/33/a880d4ce5b18a4/US9644277.pdf>.
- [168] Lewandowska-Bernata A, Desideri U. Opportunities of power-to-gas technology. *Energy Procedia* 2017;105:4569–74.
- [169] Li J, Liu W, Qi W. Hydrogen production technology by electrolysis of water and its application in renewable energy consumption. In: *E3S Web of Conferences*. 236; 2021. p. 02001.
- [170] Li PW, Chyu MK. Electrochemical and transport phenomena in solid oxide fuel cells. *J Heat Transf* 2005;127:1344–62.
- [171] Li X. *Principles of fuel cells*. New York: Taylor & Francis; 2006.
- [172] Li X, Liu L, Wang X, Sik Ok Y, Elliott JAW, Chang SX, Chung HJ. Flexible and self-healing aqueous supercapacitors for low temperature applications: polyampholyte gel electrolytes with biochar electrodes. *Sci Rep* 2017;7:1685.
- [173] Li Y, Wang H, Dai Z. Using artificial neural network to control the temperature of fuel cell. In: *International Conference on Communications, Circuits and Systems*; 2006.
- [174] W. Lin, *Waste heat recovery system for fuel cell system*, Project Report 2009 TRRF05 Fuel Cell Technology, 2009, Lund, Sweden.
- [175] Liang J, Wu Z. Simulation and optimization of air-cooled PEMFC stack for lightweight hybrid vehicle application. *Math Probl Eng* 2015;2015:1–12.
- [176] Lin C, Yan X, Wei G, Ke C, Shen S, Zhang J. Optimization of configurations and cathode operating parameters on liquid cooled proton exchange membrane fuel cell stacks by orthogonal method. *Appl Energy* 2019;253:113496.
- [177] Lin-Kwong-Chon C, Grondin-Pérez B, Amangoua Kadjo JJ, Damour C, Benne M. A review of adaptive neural control applied to proton exchange membrane fuel cell systems. *Annu Rev Control* 2019;47:133–54.

- [178] Lin R, Taberna PL, Fantini S, Presser V, Pérez CR, Malbosc F, et al. Capacitive energy storage from -50 to 100 °C using an ionic liquid electrolyte. *J Phys Chem Lett* 2011;2:2396–401.
- [179] Liu H, Wei Z, He W, Zhao J. Thermal issues about Li-ion batteries and recent progress in battery thermal management systems: a review. *Energy Convers Manage* 2017;150:304–30.
- [180] Liu W, Wen F, Xue Y. Power-to-gas technology in energy systems: current status and prospects of potential operation strategies. *J Mod Power Syst Clean Energy* 2017;5:439–50.
- [181] Long R, Li B, Liu Z, Liu W. A hybrid system using a regenerative electrochemical cycle to harvest waste heat from the proton exchange membrane fuel cell. *Energy* 2015;93:2079–86.
- [182] Lu J, Yin S, Shen PK. Carbon-encapsulated electrocatalysts for the hydrogen evolution reaction. *Electrochem Energy Rev* 2019;2:105–27.
- [183] Luo J, Glatkowski P, Wallis P. Polymer binders for flexible and transparent conductive coatings containing carbon nanotubes. United States; 2005.
- [184] Luo L, Huang B, Bai X, Cheng Z, Jian Q. Temperature uniformity improvement of a proton exchange membrane fuel cell stack with ultra-thin vapor chambers. *Appl Energy* 2020;270:115192.
- [185] MacKinnon SM, Paone MP, Kingma RJ, Montie GJ. Reactant flow channels for electrolyzer applications. US Patent; 2017.
- [186] Mansilla C, Sigurvinsson J, Bontemps A, Marechal A, Werkoff F. Heat management for hydrogen production by high temperature steam electrolysis. *Energy* 2007;32:423–30.
- [187] Mastropasqua L, Campanari S, Brouwer J. Solid oxide fuel cell short stack performance testing - Part A: experimental analysis and μ -combined heat and power unit comparison. *J Power Source* 2017;371:225–37. a.
- [188] Mastropasqua L, Campanari S, Brouwer J. Solid oxide fuel cell short stack performance testing - part B: operation in carbon capture applications and degradation issues. *J Power Source* 2017;371:238–48. b.
- [189] May GJ, Davidson A, Monahov B. Lead batteries for utility energy storage: a review. *J Energy Storage* 2018;15:145–57.
- [190] Mermelstein J, Posdziech O. Development and demonstration of a novel reversible SOFC system for utility and micro grid energy storage. *Fuel Cells* 2016; 306:59–70.
- [191] Mench MM, Wang ZH, Bhatia K, Wang CY. Design of a micro direct methanol fuel cell (μ DMFC). In: Proceedings of the IMECE'01, International Mechanical Engineering Congress and Exposition (IMECE); 2001. November 11–16.
- [192] Mench MM. Fuel cell engines. Hoboken: John Wiley & Sons; 2008.
- [193] Michaud F, Mondieig D, Soubzmaigne V, Negrier P, Haget Y, Tauler E. A system with a less than 2 degree melting window in the range within -31 °C and -45 °C chlorobenzene-bromobenzene. *Mater Res Bull* 1996;31:943–50.
- [194] Milewski J, Kupecki J, Szcześniak A, Uzunow N. Hydrogen production in solid oxide electrolyzers coupled with nuclear reactors. *Int J Hydrog Energy* 2020. <https://doi.org/10.1016/j.ijhydene.2020.11.217>.
- [195] Miller JR, Burke AF. Electrochemical capacitors: challenges and opportunities for real-world applications, 17. *Electrochemical Society Interface*; 2008. p. 53–7.
- [196] Mohebbi Najm Abad J, Alizadeh R, Fattahi A, Doranehgard MH, Alhajri E, Karimi N. Analysis of transport processes in a reacting flow of hybrid nanofluid around a bluff-body embedded in porous media using artificial neural network and particle swarm optimization. *J Mol Liq* 2020;313:113492.
- [197] Mottaghizadeh P, Santhanam S, Heddrich MP, Andreas Friedrich K, Rinaldi F. Process modeling of a reversible solid oxide cell (r-SOC) energy storage system utilizing commercially available SOC reactor. *Energy Convers Manage* 2017;142: 477–93.
- [198] Mottaghizadeh P, Fardadi M, Jabbari F, Brouwer J. Thermal management of a reversible solid oxide system for long-term renewable energy storage. *ASME Int Mech Eng Congr Expo* 2020. November 16–19Virtual, Online.
- [199] Motylinski K, Wierzbicki M, Jagielski S, Kupecki J. Investigation of off-design characteristics of solid oxide electrolyser (SOE) operated in endothermic conditions. In: E3S Web of Conferences. 137; 2019. p. 01029.
- [200] N.P. Myers, T.C. Trent, Cooling system and method, (2013), Google Patents.
- [201] Nagata S, Momma A, Kato T, Kasuga Y. Numerical analysis of output characteristics of tubular SOFC with internal reformer. *J Power Source* 2001;101: 60–71.
- [202] Nakajo A, Stiller C, Härkegård G, Bolland O. Modeling of thermal stresses and probability of survival of tubular SOFC. *J Power Source* 2006;158:287–94.
- [203] Neto DM, Oliveira MC, Alves JL, Menezes LF. Numerical study on the formability of metallic bipolar plates for Proton Exchange Membrane (PEM) Fuel Cells. *Metals (Basel)* 2019;9:810.
- [204] News Green Hydrogen. Apex starts up green hydrogen plant with McPhy electrolyser. *Fuel Cells Bull* 2020;2020:11.
- [205] Nguyen HQ, Aris AM, Shabani B. PEM fuel cell heat recovery for preheating inlet air in standalone solar-hydrogen systems for telecommunication applications: an energy analysis. *Int J Hydrog Energy* 2016;41:2987–3003.
- [206] Nguyen HQ, Shabani B. Proton exchange membrane fuel cells heat recovery opportunities for combined heating/cooling and power applications. *Energy Convers Manage* 2020;204:112328.
- [207] Ni M. Modeling of solid oxide fuel cells. *Sci Bull* 2016;61:1311–2.
- [208] Ni M, Leung MKH, Leung DYC. Technological development of hydrogen production by solid oxide electrolyzer cell (SOEC). *Int J Hydrog Energy* 2008;33: 2337–54.
- [209] Nikolic VM, Tasic GS, Maksic AD, Saponjic DP, Miulovic SM, Marceta Kaninski MP. Raising efficiency of hydrogen generation from alkaline water electrolysis – Energy saving. *Int J Hydrog Energy* 2010;35:12369–73.
- [210] Niu J, Conway BE, Pell WG. Comparative studies of self-discharge by potential decay and float-current measurements at C double-layer capacitor and battery electrodes. *J Power Source* 2004;135:332–43.
- [211] J.E. O'Brien, C.M. Stoots, J.S. Herring, M.G. McKellar, E.A. Harvego, M.S. Sohal, K.G. Condie, High temperature electrolysis for hydrogen production from nuclear energy—technology summary, A report prepared for the U.S. Department of Energy Office of Nuclear Energy Under DOE Idaho Operations Office Contract DE-AC07-05ID14517, (2010).
- [212] O'Brien J, McKellar M. High-temperature electrolysis for large-scale hydrogen and syngas production from nuclear energy - system simulation and economic analyses. *Hydrog Energy* 2010;35:4808–19.
- [213] Odabae M, Hooman K. Metal foam heat exchangers for thermal management of fuel cell systems. In: Porous Media and Its Applications in Science, Engineering, and Industry, AIP Conf. Proc. 1453; 2012. p. 237–42.
- [214] Odabae M, Mancin S, Hooman K. Metal foam heat exchangers for thermal management of fuel cell systems – An experimental study. *Exp Therm Fluid Sci* 2013;51:214–9.
- [215] Oldham KB, Myland JC. Fundamentals of electrochemical science. 1nd ed. San Diego: Academic Press; 1993.
- [216] Ormerod RM. Solid oxide fuel cells. *Chem Soc Rev* 2003;32:17–28.
- [217] Owejan JP, Owejan JE, Gu W, Trabold TA, Tighe TW, Mathias MF. Water transport mechanisms in PEMFC gas diffusion layers. *J Electrochem Soc* 2010; 157:B1456–64.
- [218] Owusu PA, Asumadu-Sarkodie S. A review of renewable energy sources, sustainability issues and climate change mitigation, 3. *Cogent Engineering*; 2016. p. 1–14.
- [219] Park H. Numerical assessment of liquid cooling system for power electronics in fuel cell electric vehicles. *Int J Heat Mass Transf* 2014;73:511–20.
- [220] V. Pasquale, Curie Temperature, In: Gupta H.K. (eds) Encyclopedia of solid earth geophysics, encyclopedia of earth sciences series. Springer, Dordrecht. https://doi.org/10.1007/978-90-481-8702-7_109.
- [221] C. Perret, High temperature water electrolysis device with improved performance, Patent, ES2477520T3, (2010).
- [222] F. Petipas, A. Brisse, C. Bouallou, Control of a high-temperature electrolyzer, Patent, WO2015059404A1, (2015).
- [223] Petipas F, Brisse A, Bouallou C. Thermal management of solid oxide electrolysis cell systems through air flow regulation. *Chem Eng Trans* 2017;61:1069–74.
- [224] Promsen M, Komatsu Y, Sciazko A, Kaneko S, Shikazono N. Feasibility study on saturated water cooled solid oxide fuel cell stack. *Appl Energy* 2020;279:115803.
- [225] Qin B, Han Y, Ren Y, Sui D, Zhou Y, Zhang M, et al. A ceramic-based separator for high-temperature supercapacitors. *Energy Technol* 2017;6:1–7.
- [226] Nichicon Corporation. 2021. https://www.nichicon.co.jp/english/products/alm_chip/index.html.
- [227] Qiu D, Yi P, Peng L, Lai X. Study on shape error effect of metallic bipolar plate on the GDL contact pressure distribution in proton exchange membrane fuel cell. *Int J Hydrog Energy* 2013;38:6762–72.
- [228] Qiu D, Peng L, Tang J, Lai X. Numerical analysis of air-cooled proton exchange membrane fuel cells with various cathode flow channels. *Energy* 2020;198: 117334.
- [229] Ragupathy P, Park DH, Campet G, Vasani HN, Hwang SJ, Choy JH. N. Munichandriah Remarkable capacity retention of nanostructured manganese oxide upon cycling as an electrode material for supercapacitor. *J Phys Chem C* 2009;113:6303–9.
- [230] Rajput RK. Engineering thermodynamics. 3rd ed. New Delhi: Laxmi; 2007. p. 922.
- [231] Rakhi RB, Chen W, Cha D, Alshareef HN. Substrate dependent self-organization of mesoporous cobalt oxide nanowires with remarkable pseudocapacitance. *Nano Lett* 2012;12:2559–67.
- [232] Ramousse J, Lottin O, Didierjean S, Maillat D. Heat sources in proton exchange membrane (PEM) fuel cells. *J Power Source* 2009;192:435–41.
- [233] Rashidi R. A Thesis Submitted in Partial Fulfillment of the Requirements for the Degree of Master of Applied Science in The Faculty of Engineering and Applied Science. Mechanical Engineering Program, University of Ontario Institute of Technology; December 2008.
- [234] Rashidi S, Mahian O, Languri EM. Applications of nanofluids in condensing and evaporating systems. *J Therm Anal Calorim* 2018;131:2027–39.
- [235] Rashidi S, Hormozi F, Sarafraz MM. Fundamental and subphenomena of boiling heat transfer. *J Therm Anal Calorim* 2020. <https://doi.org/10.1007/s10973-020-09468-3>. a.
- [236] Rashidi S, Hormozi F, Sarafraz MM. Potentials of boiling heat transfer in advanced thermal energy systems. *J Therm Anal Calorim* 2020. <https://doi.org/10.1007/s10973-020-09511-3>. b.
- [237] Razbani O, Wærnhus I, Assadi M. Experimental investigation of temperature distribution over a planar solid oxide fuel cell. *Appl Energy* 2013;105:155–60.
- [238] Ren P, Pei P, Li Y, Wu Z, Chen D, Huang S. Degradation mechanisms of proton exchange membrane fuel cell under typical automotive operating conditions. *Prog Energy Combust Sci* 2020;80:100859.
- [239] Rezaei M, Mostafaeipour A, Qolipour M, Momeni M. Energy supply for water electrolysis systems using wind and solar energy to produce hydrogen: a case study of Iran. *Front Energy* 2019;13:539–50.
- [240] Rodatz P, Buchi F, Onder C, Guzzella L. Operational aspects of a large PEFC stack under practical conditions. *J Power Source* 2004;128:208–17.
- [241] Ruiz V, Blanco C, Granda M, Menéndez R, Santamaría R. Effect of the thermal treatment of carbon-based electrodes on the electrochemical performance of supercapacitors. *J Electroanal Chem* 2008;618:17–23.

- [242] Rulliere R, Lefevre F, Lallemand M. Prediction of the maximum heat transfer capability of two-phase heat spreaders - Experimental validation. *Int J Heat Mass Transf* 2007;50:1255–62.
- [243] Saeedan M, Ziaei-Rad M, Afshari E. Numerical thermal analysis of nanofluid flow through the cooling channels of a polymer electrolyte membrane fuel cell filled with metal foam. *Int J Energy Res* 2020. <https://doi.org/10.1002/er.5332>.
- [244] Saidura R, Leong KY, Mohammad HA. A review on applications and challenges of nanofluids. *Renew Sustain Energy Rev* 2011;15:1646–68.
- [245] Sánchez D, Muñoz A, Sánchez T. An assessment on convective and radiative heat transfer modelling in tubular solid oxide fuel cells. *J Power Source* 2007;169:25–34.
- [246] Santhanam S, Heddrich MP, Riedel M, Friedrich KA. Theoretical and experimental study of Reversible Solid Oxide Cell (r-SOC) systems for energy storage. *Energy* 2017;141:202–14.
- [247] Sasmito AP, Birgersson E, Mujumdar AS. Numerical evaluation of various thermal management strategies for polymer electrolyte fuel cell stacks. *Int J Hydrog Energy* 2011;36:12991–3007.
- [248] Sasmito AP, Shamim T, Birgersson E, Mujumdar AS. Computational study of edge cooling for open-cathode polymer electrolyte fuel cell stacks. *J Fuel Cell Sci Technol* 2012;9:061008.
- [249] Sasmito AP, Shamim T, Mujumdar AS. Passive thermal management for PEM fuel cell stack under cold weather condition using phase change materials (PCM). *Appl Therm Eng* 2013;58:615–25.
- [250] Schiffer J, Linzen D, Sauer DU. Heat generation in double layer capacitors. *J Power Source* 2006;160:765–72.
- [251] Scholta J, Zhang W, Jorissen L, Lehert W. Conceptual design for an externally cooled HT-PEMFC stack. *ECS Trans* 2008;12:113–8.
- [252] Scott K. Introduction to Electrolysis, Electrolysers and Hydrogen Production. *Electrochemical methods for hydrogen production*. Book Series: Energy and Environment Series; 2019. p. 1–27.
- [253] Shahjalal M, Shams T, Islam MdE, Alam W, Modak M, Bin Hossain S, et al. A review of thermal management for Li-ion batteries: prospects, challenges, and issues. *J Energy Storage* 2021;39:102518.
- [254] Shah RK. Heat exchangers for fuel cell systems. In: *The 4th International conference on Compact Heat Exchangers and Enhancement Technology for the Process Industries*; 2003.
- [255] Shahsavari S. Thermal analysis of air-cooled pem fuel cells, a master thesis. Simon Fraser University; 2011.
- [256] Shanmuga Priya M, Divya P, Rajalakshmi R. A review status on characterization and electrochemical behaviour of biomass derived carbon materials for energy storage supercapacitors. *Sustain Chem Pharm* 2020;16:100243.
- [257] Sharma P, Bhatti T. A review on electrochemical double-layer capacitors. *Energy Convers Manage* 2010;51:2901–12.
- [258] Shen ZG, Chen S, Liu X, Chen B. A review on thermal management performance enhancement of phase change materials for vehicle lithium-ion batteries. *Renew Sustain Energy Rev* 2021;148:111301.
- [259] Shibata M, Murakami N, Akbay T, Eto H, Hosoi K, Nakajima H, Kano J, Nishiwaki F, Inagaki T, Yamasaki S. Development of intermediate-temperature SOFC modules and systems. *ECS Trans* 2007;7:77–83.
- [260] Sigurvinsson J, Mansilla C, Arnason B, Bontemps A, Maréchal A, Sigfusson TI, et al. Heat transfer problems for the production of hydrogen from geothermal energy. *Energy Convers Manage* 2006;47:3543–51.
- [261] Simon P, Gogotsi Y. Materials for electrochemical capacitors. *Nat Mater* 2008;7:845–54.
- [262] Simon P, Brousse T, Favier F. Supercapacitors based on carbon or pseudocapacitive materials. Wiley-ISTE; 2017.
- [263] Singh D, Toutbort J, Chen G, et al. Heavy vehicle systems optimization merit review and peer evaluation. Argonne National Laboratory; 2006.
- [264] Soltani M, Ronsmans J, Kakihara S, Jaguemont J, Van den Bossche P, van Mierlo J, et al. Hybrid battery/lithium-ion capacitor energy storage system for a pure electric bus for an urban transportation application. *Appl Sci* 2018;8:1176.
- [265] Soltani M, Berkmans G, Jaguemont J, Ronsmans J, Kakihara S, Hegazy O, Van Mierlo J, Omar N. Three dimensional thermal model development and validation for lithium-ion capacitor module including air-cooling system. *Appl Therm Eng* 2019;153:264–74.
- [266] Song TW, Choi KH, Kim JR, Yi JS. Pumpless thermal management of water-cooled high-temperature proton exchange membrane fuel cells. *J Power Source* 2011;196:4671–9.
- [267] Soupremanien U, Person SL, Favre-Marinet M, Bultel Y. Tools for designing the cooling system of a proton exchange membrane fuel cell. *Appl Therm Eng* 2012;40:161–73.
- [268] Staffell I, Scamman D, Velazquez Abad A, Balcombe P, Dodds PE, Ekins P, Shahd N, Ward KR. The role of hydrogen and fuel cells in the global energy system. *Energy Environ Sci* 2019;12:463–91.
- [269] Stojic DL, Marceta MP, Sovilj SP, Miljanic SS. Hydrogen generation from water electrolysis—Possibilities of energy saving. *J Power Source* 2003;118:315–9.
- [270] Sui PC, Zhu X, Djilali N. Modeling of PEM fuel cell catalyst layers: status and outlook. *Electrochem Energy Rev* 2019;2:428–66.
- [271] Sundén B. *Hydrogen, batteries and fuel cells*. Academic Press; 2019. <https://doi.org/10.1016/C2018-0-01247-5>.
- [272] Takashiba T, Yagawa S. Development of fuel cell coolant. *Honda R&D Techn Rev* 2009;21:58–62.
- [273] Syu-Fang L, Chu HS, Yuan P. Effect of inlet flow maldistribution on the thermal and electrical performance of a molten carbonate fuel cell unit. *J Power Source* 2006;161:1030–40.
- [274] Tan WC, Iwai H, Kishimoto M, Yoshida H. Quasi-three-dimensional numerical simulation of a solid oxide fuel cell short stack: effects of flow configurations including air-flow alternation. *J Power Source* 2018;400:135–46.
- [275] Tao S, Si-jia Y, Guang-yi C, Xin-jian Z. Modelling and control PEMFC using fuzzy neural networks. *J Zhejiang Univ-SCIENCEA* 2005;6:1084–9.
- [276] Tete PR, Gupta MM, Joshi SS. Developments in battery thermal management systems for electric vehicles: a technical review. *J Energy Storage* 2021;35:102255.
- [277] Thomas JM, Edwards PP, Dobson PJ, Owen GP. Decarbonising energy: the developing international activity in hydrogen technologies and fuel cells. *J Energy Chem* 2020;51:405–15.
- [278] Tiktak WJ. Heat management of pem electrolysis, a study on the potential of excess heat from medium- to large-scale PEM electrolysis and the performance analysis of a dedicated cooling system. Delft University of Technology; 2019. A master thesis at the.
- [279] Tolj I, Penga Z, Vukićević D, Barbir F. Thermal management of edge-cooled 1 kW portable proton exchange membrane fuel cell stack. *Appl Energy* 2020;257:114038.
- [280] Tong W, Somasundaram K, Birgersson E, Mujumdar AS, Yap C. Numerical investigation of water cooling for a lithium-ion bipolar battery pack. *Int J Therm Sci* 2015;94:259–69.
- [281] Torregrossa D, Paolone M. Modelling of current and temperature effects on supercapacitors ageing. Part II: state-of-Health assessment. *J Energy Storage* 2016;5:95–101.
- [282] Tucker MC, Cheng L. Integrated thermal management strategy and materials for solid oxide fuel cells. *J Power Source* 2011;196:10074–8.
- [283] Udagawa J, Aguiar P, Brandon NP. Hydrogen production through steam electrolysis: model-based steady state performance of a cathode-supported intermediate temperature solid oxide electrolysis cell. *J Power Source* 2007;166:127.
- [284] Vasiliev LL, Vasiliev Jr LL. Heat pipes to increase the efficiency of fuel cells. *Int J Low-Carbon Technol* 2009;4:96–103.
- [285] Venkataraman V. Thermal modelling and coupling of a heat pipe integrated desorber with a Solid Oxide Fuel Cell. *Appl Therm Eng* 2019;147:943–61.
- [286] Villagra A, Millet P. An analysis of PEM water electrolysis cells operating at elevated current densities. *Int J Hydrog Energy* 2019;44:9708–17.
- [287] Vincipio Oro M, Bazzo E. Flat heat pipes for potential application in fuel cell cooling. *Appl Therm Eng* 2015;90:848–57.
- [288] Viswanath RP. A patent for generation of electrolytic hydrogen by a cost effective and cheaper route. *Int J Hydrog Energy* 2004;29:1191–4.
- [289] Voicu I, Louahlia H, Gualous H, Gallay R. Thermal management and forced air-cooling of supercapacitors stack. *Appl Therm Eng* 2015;85:89–99.
- [290] Voicu I, Rizk R, Louahlia H, Bode F, Gualous H. Experimental and numerical study of supercapacitors module with air-cooling. *Appl Therm Eng* 2019;159:113903.
- [291] Wachsmann ED, Lee KT. Lowering the temperature of solid oxide fuel cells. *Science* 2011;334:935–9.
- [292] Wang L-S, Li C-X, Li G-R, Yang G-J, Zhang S-L, Li C-J. Enhanced sintering behavior of LSGM electrolyte and its performance for solid oxide fuel cells deposited by vacuum cold spray. *J Eur Ceram Soc* 2017;37:4751–61.
- [293] Wang S, Jiang SP. Prospects of fuel cell technologies. *Natl Sci Rev* 2017;4:163–6.
- [294] Wei M, Smith SJ, Sohn MD. Experience curve development and cost reduction disaggregation for fuel cell markets in Japan and the US. *Appl Energy* 2017;191:346–57.
- [295] Weinstein L, Dash R. Capacitive deionization: challenges and opportunities. *Desalination Water Reuse* 2013:34–7.
- [296] Wen CY, Huang GW. Application of a thermally conductive pyrolytic graphite sheet to thermal management of a PEM fuel cell. *J Power Source* 2008;178:132–40.
- [297] Wen CY, Lin YS, Lu CH. Performance of a proton exchange membrane fuel cell stack with thermally conductive pyrolytic graphite sheets for thermal management. *J Power Source* 2009;189:1100–5.
- [298] Wen CY, Lin YS, Lu CH, Luo TW. Thermal management of a proton exchange membrane fuel cell stack with pyrolytic graphite sheets and fans combined. *Int J Hydrog Energy* 2011;36:6082–9.
- [299] Wendel CH. Design and analysis of reversible solid oxide cell systems for electrical energy storage. Ph.D.Thesis. USA: Colorado School of Mines, Arthur Lakes Library, Golden, CO; 2015.
- [300] Wendel CH, Kazempoor P, Braun RJ. A thermodynamic approach for selecting operating conditions in the design of reversible solid oxide cell energy systems. *J Power Source* 2016;301:93–104.
- [301] Weng FB, Dlamini MM, Jung G, Lian CX. Analyses of reversible solid oxide cells porosity effects on temperature reduction. *Int J Hydrog Energy* 2020;45:12170–84.
- [302] Widiyanto A, Sulistyono, Tony Suryo Utomo MSK. Analysis of the effect of anode porosity on temperature distribution on planar radial type SOFC. In: *E3S Web of Conferences*. 73; 2018. p. 01010. ICENIS 2018.
- [303] Wilk MD, Stone KT, Quintana NAV. High-power ultracapacitor energy storage pack and method of use. patent citation, ise corporation. Poway CA, United States; 2009.
- [304] Winter M, Brodd RJ. What are batteries, fuel cells, and supercapacitors? *Chem Rev* 2004;104:4245–70.
- [305] Wu M, Zhang H, Zhao J, Wang F, Yuan J. Performance analyses of an integrated phosphoric acid fuel cell and thermoelectric device system for power and cooling cogeneration. *Int J Refrig* 2018;89:61–9.

- [306] Wu Q, Li H, Yuan W, Luo Z, Wang F, Sun H, Zhao X, Fu H. Performance evaluation of an air-breathing high-temperature proton exchange membrane fuel cell. *Appl Energy* 2015;160:146–52.
- [307] Xia Z, Zhou C, Shen D, Ni H, Yuan Y, Ping L. Study on the cooling system of supercapacitors for hybrid electric vehicle. *Appl Mech Mater* 2014;492:37–42.
- [308] Xiong GP, Meng CZ, Reifemberger RG, Irazoqui PP, Fisher TS. A review of graphene-based electrochemical microsupercapacitors. *Electroanalysis* 2014;26:30–51.
- [309] G. Xiong, A. Kundu, T.S. Fisher, *Thermal effects in supercapacitors*, 2015, First edition, Published by Springer International Publishing. doi: http://doi.org/10.1007/978-3-319-20242-6_1.
- [310] Xu M, Li TS, Yang M, Andersson M, Fransson I, Larsson T, et al. Modeling of an anode supported solid oxide fuel cell focusing on thermal stresses. *Int J Hydrog Energy* 2016;41:14927–40.
- [311] Xu W, Scott K, Basu S. Performance of a high temperature polymer electrolyte membrane water electrolyser. *J Power Source* 2011;196:8918–24.
- [312] Yan D, Zhang C, Liang L, Li K, Jia L, Pu J, Jian L, Li X, Zhang T. Degradation analysis and durability improvement for SOFC 1-cell stack. *Appl Energy* 2016;175:414–20.
- [313] Yan WM, Lee CY, Li CH, Li WK, Rashidi S. Study on heat and mass transfer of a planar membrane humidifier for PEM fuel cell. *Int J Heat Mass Transf* 2020;152:119538. a.
- [314] Yao L, Yang B, Cui H, Zhuang J, Ye J, Xue J. Challenges and progresses of energy storage technology and its application in power systems. *J Mod Power Syst Clean Energy* 2016;4:519–28.
- [315] Yassine M, Fabris D. Performance of commercially available supercapacitors. *Energies* 2017;10:1340.
- [316] A.I. Yatskov, J. Marsala, *Cooling system and method*, (2011), Google Patents.
- [317] Yoshida H, Iwai H. Thermal management in solid oxide fuel cell systems. In: *Proceedings of Fifth International Conference on Enhanced, Compact and Ultra-Compact Heat Exchangers: Science, Engineering and Technology*. Engineering Conferences International; September 2005. editors R.K. Shah, M. Ishizuka, T.M. Rudy, and V.V. Wadekar.
- [318] Yu L, Chen GZ. Supercapacitors as high-performance electrochemical energy storage devices. *Electrochem Energy Rev* 2020;3:271–85.
- [319] Yuan J, Faghri M, Sundén B. On heat and mass transfer phenomena in PEMFC and SOFC and modeling approaches. In: Sundén B, Faghri M, editors. Chapter 4 in transport phenomena in fuel cells. WIT Press; 2005. p. 133–74 (eds).
- [320] Yuan J, Sundén B. On continuum models for heat transfer in micro/nano-scale porous structures relevant for fuel cells. *Int J Heat Mass Transf* 2013;58:441–56.
- [321] Yuan J, Sundén B. On mechanisms and models of multi-component gas diffusion in porous structures of fuel cell electrodes. *Int J Heat Mass Transf* 2014;69:358–74.
- [322] Yuan WL, Yang X, He L, Xue Y, Qin S, Tao GH. Viscosity, conductivity, and electrochemical property of dicyanamide ionic liquids. *Front Chem* 2018;6:1–12.
- [323] Yuan Z, Chuai W, Guo Z, Tu Z, Kong F. Investigation of self-adaptive thermal control design in passive direct methanol fuel cell. *Energy Storage* 2019;1:e64.
- [324] Zakaria IA, Michael Z, Mamat AMI, Mohamed WANW. Thermal and electrical experimental characterization of Ethylene Glycol and water mixture nanofluids for a 400 w Proton Exchange Membrane Fuel Cell. In: *2014 IEEE International Conference on Control System, Computing and Engineering (ICCSCE 2014)*; 2014.
- [325] Zeng K, Zhang D. Recent progress in alkaline water electrolysis for hydrogen production and applications. *Prog Energy Combust Sci* 2010;36:307–26.
- [326] Zeng H, Wang Y, Shi Y, Cai N, Yuan D. Highly thermal integrated heat pipe-solid oxide fuel cell. *Appl Energy* 2018;216:613–9.
- [327] Zhan R, Wang Y, Ni M, Zhang G, Du Q, Jiao K. Three-dimensional simulation of solid oxide fuel cell with metal foam as cathode flow distributor. *Int J Hydrog Energy* 2020;45:6897–911.
- [328] Zhang J, Xie Z, Zhang J, Tang Y, Song C, Navessin T, et al. High temperature PEM fuel cells. *J Power Source* 2006;160:872–91.
- [329] Zhang G, Kandlikar SG. A critical review of cooling techniques in proton exchange membrane fuel cell stacks. *Int J Hydrog Energy* 2012;37:2412–29.
- [330] Zhang H, Chen B, Xu H, Ni M. Thermodynamic assessment of an integrated molten carbonate fuel cell and absorption refrigerator hybrid system for combined power and cooling applications. *Int J Refrig* 2016;70:1–12.
- [331] Zhang X, Chan SH, Ho HK, Tan SC, Li M, Li G, et al. Towards a smart energy network: the roles of fuel/electrolysis cells and technological perspectives. *Int J Hydrog Energy* 2015;40:6866–919.
- [332] Zhang X, Wang W, He H, Hua L, Heng J. Optimization of the air-cooled supercapacitor module compartment for an electric bus. *Appl Therm Eng* 2017;112:1297–304.
- [333] Zhang Y, Hao N, Lin X, Nie S. Emerging challenges in the thermal management of cellulose nanofibril-based supercapacitors, lithium-ion batteries and solar cells: a review. *Carbohydr Polym* 2020;234:115888.
- [334] Zhao B, Fu XZ, Sun R, Wong CP. Highly thermal conductive graphene-based electrodes for supercapacitors with excellent heat dissipation ability. *Sustain Energy Fuel* 2017;10:1–12.
- [335] Zhao G, Wang X, Negnevitsky M, Zhang H. A review of air-cooling battery thermal management systems for electric and hybrid electric vehicles. *J Power Source* 2021;501:230001.
- [336] Zhao P, Wang J, Gao L, Dai Y. Parametric analysis of a hybrid power system using organic Rankine cycle to recover waste heat from proton exchange membrane fuel cell. *Int J Hydrog Energy* 2012;37:3382–91.
- [337] Zhou Y, Ghaffari M, Lin M, Xu H, Xie H, Kood CM, Zhang QM. High performance supercapacitor under extremely low environmental temperature. *RSC Adv* 2015;5:71699–703.
- [338] Zhe G, Zhu H, Gillette E, Han X, Sang BL. Natural cellulose fiber as substrate for supercapacitor. *ACS Nano* 2013;7:6037–46.
- [339] Zhu J, Yan C, Zhang X, Yang C, Jiang M, Zhang X. A sustainable platform of lignin: from bioresources to materials and their applications in rechargeable batteries and supercapacitors. *Prog Energy Combust Sci* 2020;76:100788.
- [340] Zichen W, Changqing D. A comprehensive review on thermal management systems for power lithium-ion batteries. *Renew Sustain Energy Rev* 2021;139:110685.
- [341] Hakeem Akinlabi AA, Solyali D. Configuration, design, and optimization of air-cooled battery thermal management system for electric vehicles: A review. *Renewable and Sustainable Energy Reviews* 2020;125:109815.



Dr Rashidi received his BA and MS degrees in Mechanical Engineering at Semnan University, Iran in 2010 and 2013, respectively. He received PhD degree in Mechanical Engineering, Energy Conversion Field, at Ferdowsi University of Mashhad, Iran in 2016. He is currently the assistant professor of the Department of the Energy in Semnan University. His-research interests are about the thermal energy systems, investigation of different techniques used for efficiency improvement of various thermal systems, entropy generation analysis, transport phenomena, solar thermal energy systems. He has published about 100 refereed journal papers in Domestic and International Journals.



Dr Karimi is currently a Reader (Associate Professor) in Mechanical Engineering at the School of Engineering and Materials Science, Queen Mary University of London where his research is in the broad area of thermofluids. Prior to this, he received his PhD from University of Melbourne, Australia (2009) and, completed two post-doctoral works at Darmstadt University of Technology in Germany (2011) and University of Cambridge, UK (2013) and further served as an assistant professor at James Watt School of Engineering, University of Glasgow. His-research experiences and interests include Experimental and Theoretical Studies on Chemically Reacting Flows, Heat and Mass Transfer and, Energy Conversion and

Storage. Dr Karimi has authored/co-authored three book chapters and over 140 articles in the leading international scientific journals and conferences. He has also delivered invited seminars in the key research institutes around the world including GE Global Research in NY, United States and Technical University of Munich, Germany.



Bengt Sundén received his M.Sc. in 1973, Ph.D. in 1979 and became Docent in 1980, all from Chalmers University of Technology, Gothenburg, Sweden. He was appointed Professor of Heat Transfer at Lund University, Lund, Sweden in 1992 and served as Head of the Department of Energy Sciences, Lund University for 21 years, 1995–2016. He has served as Professor Emeritus and Senior Professor since 2016. The research activities mainly include various heat transfer enhancement techniques, gas turbine heat transfer, computational modeling and analysis of multiphysics and multiscale transport phenomena for fuel cells, nano-and microscale heat transfer, boiling and condensation, aerospace heat transfer, thermal management of

batteries. He has supervised 51 Ph.D. students and many post docs as well hosted many visiting scholars and Ph.D. students. He serves as Guest or Honorary Professor of several prestigious universities. He is a Fellow of ASME, a regional editor for *Journal of Enhanced Heat Transfer* since 2007, an associate editor of *Heat Transfer Research* since 2011, ASME J. Thermal Science, Engineering and Applications in 2010–2016 and ASME J. Electrochemical Energy Conversion and Storage 2017–2023. He was a recipient of the ASME Heat Transfer Memorial Award 2011 and Donald Q. Kern Award 2016. He received the ASME HTD 75th Anniversary Medal 2013. He has edited 30+ books and authored three major textbooks. He has published more than 500 papers in well-established and highly ranked journals. The h-index is 49 and the number of citations is more than 12000.



Prof Kim received his BA degree at Pusan National University, Korea in 1979. He received MS and PhD degrees at KAIST, Korea in 1981 and 1987 respectively. Since 1983, he was hired as a faculty member in Pusan National University (PNU), Korea. He was invited as a visiting professor from Ottawa University in Canada for 1989–1990. He joined at the department of theoretical and applied mechanics in University of Illinois, Urbana-Champaign, USA as an invited professor for 1996–1997. Prof Kim was selected as a PNU Distinguished Professor in 2018. During 37 years at PNU, he has published about 640 refereed journal papers in Domestic and International Journals and supervised 206 MS and PhD

students. His-research interests include Fuel Cell, Two-Phase Flows, Flow Visualization, PIV, LIF, PSP, TSP, CFD, Heat Transfer, Thermal System Simulation and Optimization, Multi-scale Multi-Physics Analysis and Measurement Techniques, and Artificial Intelligence.



Prof Olabi is Chair and Head of Sustainable and Renewable Energy Engineering Department “SREE” at the University of Sharjah “UOS”. Before joining UOS, he was the director and founding member of the Institute of Engineering and Energy Technologies at the University of the West of Scotland. Prof Olabi received his M.Eng and Ph.D. from Dublin City University, since 1984 he worked at different national and international institutes such as; National Research Centre-Italy “CNR”, Research Centre of FIAT-Italy “CRF”, Dublin City University “DCU” and Institute of Engineering and Energy Technologies “IET” at UWS.

Prof Olabi is an Academic Expert Reviewer, he acted as

member and chairman for several accreditation panels.

Prof Olabi has supervised postgraduate research students (38 PhD) to successful completion. Prof Olabi has edited more than 30 proceedings and has published more than 400 papers in peer-reviewed international journals and international conferences, in addition to more than 45 book chapters. In the last 4 years Prof Olabi has patented 2 innovative projects. Prof Olabi is the founder of the International Conference on Sustainable Energy and Environmental Protection SEEP, www.seepconference.com and the International Conference on Materials Science and Smart Materials. He is the Subject Editor of the Elsevier Energy Journal, Editor in Chief of the Encyclopedia of Smart Materials (Elsevier), Editor of the Reference Module of Materials Science and Engineering (Elsevier), Editor in Chief of Renewable Energy section of Energies and board member of a few other journals. Prof Olabi has coordinated different National, EU and International Projects. He has produced different reports to the Irish Gov. regarding: Hydrogen and Fuel Cells and Solar Energy.



Prof Mahian is a professor and doctoral supervisor at School of Chemical Engineering, Xi’an Jiaotong University. His-research interests are Renewable Energies, Modeling of Thermal Equipment for Temperature Management, and Nanotechnology (Especially Nanofluids). He is currently a member of the editorial board of Energy and Renewable Energy journals published by Elsevier. He is also a senior associate editor of Journal of Thermal Analysis and Calorimetry, and an associate editor in Alexandria Engineering Journal (Elsevier) and Journal of Thermal Science (Springer). To date, he has published more than 160 SCI papers, with an H-index (H-index) of 49, and the article has been cited more than 8000 times. He was

selected as a highly cited scientist for three consecutive years since 2018